Issue 3 2019 | Volume 15

The Journal on Advanced Studies in Theoretical and Experimental Physics, including Related Themes from Mathematics

PROGRESS IN PHYSICS

"All scientists shall have the right to present their scientific research results, in whole or in part, at relevant scientific conferences, and to publish the same in printed scientific journals, electronic archives, and any other media." — Declaration of Academic Freedom, Article 8

ISSN 1555-5534

The Journal on Advanced Studies in Theoretical and Experimental Physics, including Related Themes from Mathematics

PROGRESS IN PHYSICS

A quarterly issue scientific journal, registered with the Library of Congress (DC, USA). This journal is peer reviewed and included in the abstracting and indexing coverage of: Mathematical Reviews and MathSciNet (AMS, USA), DOAJ of Lund University (Sweden), Scientific Commons of the University of St. Gallen (Switzerland), Open-J-Gate (India), Referativnyi Zhurnal VINITI (Russia), etc.

Electronic version of this journal:
http://www.ptep-online.com

Postal Address

Department of Mathematics and Science,
University of New Mexico,
705 Gurley Ave., Gallup, NM 87301, USA

ISSN: 1555-5534 (print)
ISSN: 1555-5615 (online)

Standard Address Number: 297-5092
Printed in the United States of America

October 2019 **Vol. 15, Issue 3**

CONTENTS

Information for Authors

Progress in Physics has been created for rapid publications on advanced studies in theoretical and experimental physics, including related themes from mathematics and astronomy. All submitted papers should be professional, in good English, containing a brief review of a problem and obtained results.

All submissions should be designed in LaTeX format using *Progress in Physics* template. This template can be downloaded from *Progress in Physics* home page http://www.ptep-online.com

Preliminary, authors may submit papers in PDF format. If the paper is accepted, authors can manage LaTeXtyping. Do not send MS Word documents, please: we do not use this software, so unable to read this file format. Incorrectly formatted papers (i.e. not LaTeXwith the template) will not be accepted for publication. Those authors who are unable to prepare their submissions in LaTeXformat can apply to a third-party payable service for LaTeX typing. Our personnel work voluntarily. Authors must assist by conforming to this policy, to make the publication process as easy and fast as possible.

Abstract and the necessary information about author(s) should be included into the papers. To submit a paper, mail the file(s) to the Editor-in-Chief.

All submitted papers should be as brief as possible. Short articles are preferable. Large papers can also be considered. Letters related to the publications in the journal or to the events among the science community can be applied to the section *Letters to Progress in Physics*.

All that has been accepted for the online issue of *Progress in Physics* is printed in the paper version of the journal. To order printed issues, contact the Editors.

Authors retain their rights to use their papers published in *Progress in Physics* as a whole or any part of it in any other publications and in any way they see fit. This copyright agreement shall remain valid even if the authors transfer copyright of their published papers to another party.

Electronic copies of all papers published in *Progress in Physics* are available for free download, copying, and re-distribution, according to the copyright agreement printed on the titlepage of each issue of the journal. This copyright agreement follows the *Budapest Open Initiative* and the *Creative Commons Attribution-Noncommercial-No Derivative Works 2.5 License* declaring that electronic copies of such books and journals should always be accessed for reading, download, and copying for any person, and free of charge.

Consideration and review process does not require any payment from the side of the submitters. Nevertheless the authors of accepted papers are requested to pay the page charges. *Progress in Physics* is a non-profit/academic journal: money collected from the authors cover the cost of printing and distribution of the annual volumes of the journal along the major academic/university libraries of the world. (Look for the current author fee in the online version of *Progress in Physics*.)

From the Geometry of the FLRW to the Gravitational Dynamics

Alexander Kritov
E-mail: alex@kritov.ru

The approach when the scale factor that describes the expansion of space, being its pure geometrical property, is derived from the dynamical (the Friedman) equations is questioned. The opposite path when the geometry determines the dynamics is more consistent, but not vice versa. Starting from the FLRW, the equivalent form of the metric in static coordinates is proposed. Based of few models for $a(t)$ the corresponding static metrics are derived. Further dynamics and the analogue of the Friedman equations can be obtained as consequence. The embedding of the FLRW geometry into the higher-dimensional Minkowski space as the hypersurface can be considered as the base for the model. The deceleration parameter for the Schwarzschild-de Sitter (SdS) case is reviewed based on such approach.

1 Introduction

In recent author's work [5] the hydrodynamic model of spherically symmetric gravitational field was reviewed. As it was shown the gravitational metrics can be modelled by expanding parcels of the fluid based on the respective functions of the volume change with time in co-moving frame. As it has explicit similarity with the space expansion, the present attempt is to use the geometrical approach to describe spherically symmetric gravitational filed starting from the FLRW metric.

2 The FLRW metric

Let's consider the static pseudo-Minkowski coordinates with the observer M at rest in the center. The static spherical coordinates are to be denoted as t, r, θ, ϕ, where r is coordinate distance to the observer P who is at rest, but is attached to the point of expanding space. The co-moving coordinates are given as T, R, θ, ϕ, where R is co-moving distance (from M to P). Respectively, time T is measured by the observer P. If space expands, the point P, attached to it, moves in the static coordinate system, so as observed by M, the motion of P represents the function of coordinate distance $r(t)$. The correspondence between the static coordinate and the co-moving distance is given by

$$r = Ra \tag{1}$$

where $a(T)$ is the scale factor. Then the proper velocity measured by the observed P,*

$$v = \frac{dr}{dT} = \frac{dR}{dT}\, a + R\, \frac{da}{dT} \tag{2}$$

and point P is at rest in its reference frame, so the first term is identically zero therefore

$$v = R\dot{a}\,. \tag{3}$$

*This is not coordinate velocity. This velocity is ratio of coordinate distance change to time measured in co-moving observer's clock.

Using (1) then

$$v = \frac{dr}{dT} = r(T)\, \frac{\dot{a}}{a}\,. \tag{4}$$

This expression provides the velocity of the space motion due to its expansion or the velocity of the reference frame attached to point P in the static coordinate system where r is the coordinate distance.

The Friedmann–Lemaître–Robertson–Walker (FLRW) metric in the spatially flat case ($k = 0$) is given by

$$ds^2 = -c^2 dT^2 + a(T)^2 \left(dR^2 + R^2 d\Omega^2 \right) \tag{5}$$

where $d\Omega^2 = \sin^2\theta d\phi^2 + d\theta^2$ and $a(T)$ is the scale factor. The metric is written explicitly in comoving coordinates, attached to the point of expanding space. Using (1) we may write

$$dr = \dot{a}R dT + a dR$$

from which

$$dR = \frac{dr}{a} - v\, \frac{dT}{a}\,.$$

Substituting it into the FLRW metric (5) leads to

$$ds^2 = -c^2 \left(1 - \frac{v^2}{c^2} \right) dT^2 - 2v dT dr + dr^2 + r^2 d\Omega^2 \tag{6}$$

which is the Gullstrand-Painlevé form of the metric which is spatially flat and describes co-moving observer in its free float with velocity v. The transformation of time coordinate T from co-moving to fixed frame of reference t is given by

$$dT = dt - \frac{v}{c^2} \left(1 - \frac{v^2}{c^2} \right)^{-1} dr\,. \tag{7}$$

The substitution of this expression into (6) leads to the respective static metric

$$ds^2 = -c^2 \left(1 - \frac{v^2}{c^2} \right) dt^2 + \left(1 - \frac{v^2}{c^2} \right)^{-1} dr^2 + r^2 d\Omega^2 \tag{8}$$

where velocity v is to be determined from (4). The velocity v is called the river velocity in [2, 4] and the shift in ADM formalism. Importantly, the metric (8) is equivalent to the FLRW, but written in the static coordinate systems of the observer M. Such form of the metric is known, starting from Lenz and Sommerfeld [11] and used in the river model of black holes and similar analogous models [3,4] for the spherically symmetric gravitational field.

The proposed approach starts from a certain function for the scale factor $a(T)$, and then the solution of the equation (4) provides the velocity $v(r)$ resulting in the corresponding metric in static coordinate system based on (8).

As it was stressed in the author's previous work [5], the sign of the velocity v does not play a role, as it comes to the metric as squared value. In the present approach the value of the velocity as given in (4) is obviously positive ($\dot{a} > 0$) and as coordinate center is placed in the center point of M the velocity is radial and directed outwards.

3 The case of the de Sitter metric

The easiest case to demonstrate the proposed approach is the de Sitter metric. The starting point is $a(T) = e^{H_0 T}$, or equivalently, the constancy of the Hubble constant with time

$$H_0 = \frac{\dot{a}}{a}\,. \tag{9}$$

Then using (4) gives

$$v = rH_0\,. \tag{10}$$

And substitution into (8) leads to

$$ds^2 = -\left(1 - \frac{H_0^2 r^2}{c^2}\right)c^2dt^2 + \left(1 - \frac{H_0^2 r^2}{c^2}\right)^{-1} dr^2 + r^2 d\Omega^2 \tag{11}$$

which is the de Sitter metric as expected.

4 The case of the Schwarzschild metric

Let's now assume that

$$a(T) \propto T^{2/3}\,. \tag{12}$$

Then, using (4), it follows that

$$v(r) = \frac{c_1}{r^{1/2}} \tag{13}$$

where c_1 - is an integration constant. Then the substitution into (8) leads to the form the Schwarzschild metric with precision by constant c_1. In order to determine the meaning of the integration constant, it is required to normalize (12), for example in such way that $a(0) = 1$

$$a = (\omega T + 1)^{2/3} \tag{14}$$

where ω is some constant. Then it would imply

$$r = r_0\,(\omega T + 1)^{2/3} \tag{15}$$

where r_0 is the initial coordinate distance at time $T = 0$. Then the velocity

$$v = \frac{2}{3}\left(\frac{\omega^2 r_0^3}{r}\right)^{1/2}\,. \tag{16}$$

The equation shows that the integration constant in (13) should have correspondence to the initial volume and therefore to the central mass, if one introduces a density in the equation. Proposed boundary conditions allow to put the scale factor function in direct relation with the particle mass and to remove the initial singularity.

Interestingly from (13) and (1) the scale factor in terms of the coordinate distance is simply $r = r_0 a$. From that, using (1), the co-moving distance is $R = r_0$. As expected, the scale factor a changes with time instead of the co-moving distance R which remains constant and always equals to its initial value in the static coordinates.

5 The Schwarzschild-de Sitter (SdS) metric

As suggested in [10] the scale factor that describes current Universe expansion within the frame of standard model of the cosmology has following form

$$a(T) = \sinh\left(\frac{3}{2}H_0 T\right)^{2/3}\,. \tag{17}$$

This corresponds (differing by factor of 2) to proposed in the hyperbolic model [5]*

$$a\,(T) = (\cosh(3H_0 T) - 1)^{1/3}\,. \tag{18}$$

Then using (4)

$$v = \frac{dr}{dT} = r_0\,\frac{H_0 \sinh\,(3H_0 T)}{(\cosh(3H_0 T) - 1)^{2/3}} \tag{19}$$

from which

$$r(T) = r_0\,(\cosh\,(3H_0 T) - 1)^{1/3} \tag{20}$$

where r_0 is integration constant with dimension of length. Expressing hyperbolic sine from this and substitution into (19) leads to

$$v = \left(H_0^2 r^2 + \frac{2r_0^3 H_0^2}{r}\right)^{1/2}\,. \tag{21}$$

Exact determination of the constant r_0 for the volume can be found in [5]. It was suggested that such volume can be associated with the mass via the fluid density. The substitution into (8) leads to the SdS metric

$$\begin{aligned} ds^2 = &-\left(1 - \frac{2Gm}{c^2 r} - \frac{H_0^2 r^2}{c^2}\right)c^2dt^2 + \\ &+ \left(1 - \frac{2Gm}{c^2 r} - \frac{H_0^2 r^2}{c^2}\right)^{-1} dr^2 + r^2 d\Omega^2\,. \end{aligned} \tag{22}$$

*Obviously the presented approach has direct correspondence to the cited author's fluid model via $\dot{V} \propto a^2\dot{a}$ and $V(t) \propto a^3$.

6 The embedding the FLRW geometry

The embedding of the de Sitter geometry in the pseudo-Euclidian five-dimensional space is well known and was obtained by Robertson [7, 8]. This corresponds to embedding of the spatially flat FLRW metric with $a(t) = e^{H_0 t}$. However, as demonstrated in [9] and reviewed in [1] the generalization of the FLRW metric ($k = 0$) embedding is possible via reconstruction of the respective curve and the Minkowski five-dimensional metric is

$$t' = \frac{1}{2}\int \frac{\dot{a}^2 - 1}{\dot{a}}\, dT\,, \quad r' = \frac{1}{2}\int \frac{\dot{a}^2 + 1}{\dot{a}}\, dT\,, \quad \text{and } x' = x \quad y' = y \quad x' = z\,. \tag{23}$$

The embedding of the FLRW metric with the hyperbolic function as (17) was reviewed in [6], however it was concluded that the integral has no analytical expression.

7 On the deceleration parameter for the SdS metric

Presented approach provides a simple way to determine the deceleration parameter

$$q_0 = -\frac{\ddot{a}a}{\dot{a}^2}\,. \tag{24}$$

And as

$$\alpha = \ddot{a}R \quad v = \dot{a}R \quad r = Ra \tag{25}$$

then for the SdS metric using the deceleration parameter can be expressed via coordinate distance as

$$q_0 = \frac{Gm - H_0^2 r^3}{2Gm + H_0^2 r^3}\,. \tag{26}$$

In case of mass m is uniformly distributed within a sphere and if the density is expressed in terms of $\Omega_M = \rho/\rho_{crit}$ then the deceleration parameter is

$$q_0 = \frac{1}{2}\frac{\Omega_M - 2}{\Omega_M + 1}\,. \tag{27}$$

In case of $\Omega_M = 0.27$ it gives the deceleration parameter $q_0 = -0.68$ which is close to the observed value. As example the equation results in $q_0 = -1$ for empty the de Sitter Universe, and $q_0 = -0.4$ in case of $\Omega_M = 1$.

8 The Friedman equations

In the frame of present approach the dynamical Friedman equations appear as a result of the original scale factor function. In general case, as the resulting metric provides us with the values for acceleration $\alpha(r)$ and the velocity $v(r)$ and with use of (25) the Friedman equations are derived. In case of the SdS metric, the first Friedman equation can be directly obtained from the result (21)

$$\left(\frac{\dot{a}}{a}\right)^2 = H_0^2\left[1 + \frac{2}{a^3}\right]. \tag{28}$$

In the reverse way it obviously would reproduce (17). In case of uniformly distributed matter it has following form

$$\left(\frac{\dot{a}}{a}\right)^2 = H_0^2\,(1 + 2\Omega_M)\,. \tag{29}$$

The second Friedman equation is from (21)

$$\frac{\ddot{a}}{a} = H_0^2\left[1 - \frac{1}{a^3}\right] \tag{30}$$

or for uniformly distributed matter in terms of Ω_M

$$\frac{\ddot{a}}{a} = H_0^2\left[-\frac{1}{2}\Omega_M + 1\right]. \tag{31}$$

Another types of functions $a(t)$ can be proposed and in that way would originate different dynamical equations that could be analysed for its compliance with the cosmological observations.

9 Conclusions

The spatial expansion phenomena is considered as the space flow. The curvature of space-time in the static four-dimensional coordinate systems emerges as the consequence of such motion. Then the dynamics and the physical forces are derived from the resulting metric. The scale factor being the primary property of space should have the fundamental significance (instead of being secondary consequence of the dynamical equations). Because of the reviewed boundary conditions the scale factor may originate on the elementary particle level and can be a key for understanding the origin of gravity. The function for $a(t)$ that results in the SdS metric was reviewed, the deceleration parameter is determined (27) and the result is close to the observed value.

Received on July 1, 2019

References

1. Akbar M. M. Embedding FLRW Geometries in Pseudo-Euclidian abd Anti-de Sitter Spaces. arXiv: gr-qc/1702.00987v2.
2. Braeck S., Gron O. A river model of space. arXiv: gr-qc/1204.0419.
3. Czerniawski J. The possibility of a simple derivation of the Schwarzschild metric. arXiv: gr-qc/0611104.
4. Hamilton A. J. S., Lisle J. P. The river model of black holes. *American Journal of Physics*, 2008, v. 76, 519–532. arXiv: gr-qc/0411060.
5. Kritov A. On the Fluid Model of the Spherically Symmetric Gravitational Field. *Progress in Physics*, 2019, v. 15 (2), 101–105.
6. Lachiéze-Rey M. The Friedman-Lemaître models in perspective. *Astronomy ans Astrophysics*, 2000, v. 364, 894–900.
7. Robertson H. P. On Relativistic Cosmology. *Phylosophy Magazin*, 1928, v. 5, 835–848.
8. Robertson H. P. Relativistic Cosmology. *Review of Modern Physics*, 1933, v. 5, 62–90.
9. Rosen J. Embedding of Various Relativistic Riemannian Spaces in Pseudo-Euclidean Spaces. *Review of Modern Physics*, 1965, v. 37, 204–214.
10. Sazhin M. V., Sazhina O. S., Chadayammuri U. The Scale Factor in the Universe with Dark Energy. arXiv: astro-ph/1109.2258v1.
11. Sommerfeld A. Electrodynamics. Lectures on Theoretical Physics, Vol. III. Academic Press, New York, 1952.

The Physics of Transcendental Numbers

Hartmut Müller

E-mail: hm@interscalar.com

The difference between rational, irrational algebraic and transcendental numbers is not only a mathematical task, but appears to be a stability criterion in complex dynamic systems. This paper introduces an approach to study the physical consequences of arithmetic properties of real numbers being ratios of measured quantities. This approach allows reformulating and resolving some unsolved tasks in particle physics, astrophysics and cosmology.

Introduction

Natural systems are highly complex and at the same time they impress us with their lasting stability. For instance, the solar system hosts at least 800 thousand orbiting each other bodies. If numerous bodies are gravitationally bound to one another, classic models predict long-term highly unstable states [1, 2] that contradict the physical reality in the solar system. In the last century, advanced models [3–7] were developed, which explain basic features of the solar system formation. However, many metric characteristics of the solar system they do not predict. The problem is that Kepler's laws, the Newton law of gravitation and the Einstein field equations allow for an infinite diversity of orbits.

In reality, however, planets in the extrasolar systems Trappist 1, Kepler 20 and many others have nearly the same orbits as some moons of Jupiter, Saturn, Uranus and Neptune [8]. Why they prefer similar orbits if there are infinite possibilities? Up to now, there have not been sufficiently convincing explanations why the solar system has installed the orbital periods 87.97 days (Mercury), 224,70 days (Venus), 365.25 days (Earth), 686.97 days (Mars), 4.60 years (Ceres), 11.87 years (Jupiter), 29.46 years (Saturn), 84.02 years (Uranus), 164.80 years (Neptune) and 248.00 years (Pluto). In conventional models, they appear as to be accidental.

Furthermore, celestial mechanics does not know any law concerning the periods of planetary rotation. Though, if the periods of rotation are accidental, why then have the Moon and the Sun similar periods of rotation? Why have the Earth, Mars and the planetoid Eris similar periods of rotation? Why have Jupiter, Saturn and the planetoid Ceres similar periods of rotation?

Not only orbital and rotational periods, but also the Earth axial precession cycle (25,770 years), the obliquity variation cycle (41,000 years) as well as the apsidal precession cycle and the orbital eccentricity cycle (both 112,000 years) appear as to be accidental. And this isn't just a shortcoming of astrophysics only.

In particle physics, bosons are considered to have no rest mass, and there are no convincing explanations why the W/Z-bosons must be 90 times as massive as the proton. A rough shortcoming of the Higgs-mechanism of particle mass generation is that the origin of the Higgs-mass itself is not elaborated and this leads to a vicious circle.

Furthermore, there is no convincing explanation why the proton-to-electron mass ratio must be close to 1836 and why these fermions are stable.

Of course, in the standard model, the electron is stable because it is the least massive particle with non-zero electric charge. Its decay would violate charge conservation. Actually, this answer only readdresses the question: What causes then the stability of the elementary electric charge? In the same model, the proton is stable, because it is the lightest baryon and the baryon number is conserved. However, also this answer only readdresses the question: Why then is the proton the lightest baryon? To answer this question, the standard model introduces quarks which violate the conservation of the integer elementary electric charge.

Measurements of the cosmic microwave background radiation (CMBR) are critical to cosmology, since any proposed model of the universe must explain it. However, in Big Bang cosmology, its current average temperature of 2.725 K appears to be accidental, because CMBR is interpreted as a remnant from an early stage of the observable universe when stars and planets didn't exist yet, and the universe was denser and much hotter.

This paper introduces an approach that considers arithmetic properties of the measured ratios of physical quantities. This approach allows not only answering our questions above, but also reformulating and resolving some unsolved tasks in paticle physics, astrophysics and cosmology.

Methods

Measurement is the source of data that allow us developing and proofing theoretical models of the reality. The result of a measurement is the ratio of two physical quantities where one of them is the reference quantity called unit of measurement. In general, this ratio is a real value that can approximate a rational, irrational algebraic or transcendental number.

In [9] we have shown that the difference between rational, irrational algebraic and transcendental numbers is not only a mathematical task, but it is also an essential aspect of stability in complex systems. For instance, integer and rational

frequency ratios provide resonance interaction that can destabilize a system.

With reference to the solar system and its stability, we may therefore expect that the ratio of any two orbital periods should be not rational. However, it is not so simple to clarify the type of number a measured ratio approximates. In general, there is no possibility to know it for sure. For example, how can we find out if the Venus-to-Earth orbital period ratio approximates a rational, irrational algebraic or transcendental number?

From the first impression, the obtained value 0.615 seems to be a rational number, but higher resolution data [10] deliver more digits, for example 0.615198 years = 224.701 days = 224 days, 16 hours and 49 minutes. Indeed, also this value is an average. In reality, the sidereal orbital period of Venus is not constant, but varies between 224.695 days = 0.61518 years and 224.709 days = 0.61522 years. According to classic models, that is due to perturbations from other planets, mainly Jupiter and Earth. As well, the orbital period of the Earth is not constant, but shows cyclic variations in the duration up to 7 minutes [11]. However, several authors [12, 13] have suggested that the Venus-to-Earth orbital period ratio coincides with 8/13 approximating the golden section $\phi = (\sqrt{5}-1)/2 = 0.618\ldots$ that is an irrational algebraic number.

It is remarkable that approximation interconnects all types of real numbers – rational, irrational algebraic and transcendental. In 1950, the mathematician Khinchin [14] made an important discovery: He could demonstrate that continued fractions deliver biunique (one-to-one) representations of all real numbers, rational and irrational. Whereas infinite continued fractions represent irrational numbers, finite continued fractions represent always rational numbers. In this way, any irrational number can be approximated by finite continued fractions, which are the convergents and deliver always the nearest and quickest rational approximation.

It is notable that the nearest rational approximation of an irrational number by a finite continued fraction is not a task of computation, but only an act of termination of the fractal recursion. For example, the golden number $\phi = (\sqrt{5}+1)/2$ has a biunique representation as simple continued fraction:

$$\phi = 1 + \cfrac{1}{1 + \cfrac{1}{1 + \cfrac{1}{1 + \cdots}}}.$$

To save space, in the following we use square brackets to write down continued fractions, for example the golden number $\phi = [1; 1, 1, \ldots]$. So long as the sequence of denominators is considered as infinite, this continued fraction represents the irrational number ϕ. If we truncate the continued fraction, the sequence of denominators will be finite and we get a convergent that is always the nearest rational approximation of the irrational number ϕ.

Let's see how it works. Increasing always the length of the continued fraction, we obtain a sequence of rational approximations of ϕ, from the worst to always better and better ones (see Table 1).

Figure 1 demonstrates the process of step by step approximation. As we can see, the rational approximations oscillate around the eigenvalue ϕ of the continued fraction that is shown as dotted line. With every step the approximation comes closer and closer to ϕ, never reaching it and describing a damped asymptotic oscillation around ϕ.

In 1950 Gantmacher and Krein [15] have demonstrated that continued fractions are solutions of the Euler-Lagrange equation for low amplitude harmonic oscillations in simple chain systems. Terskich [16] generalized this method for the analysis of oscillations in branched chain systems. The continued fraction method can also be extended to the analysis of chain systems of harmonic quantum oscillators [17].

The rational approximations of the golden number ϕ are always ratios of neighboring Fibonacci numbers – the elements of the recursive sequence 1, 1, 2, 3, 5, 8, 13, 21, 34, 55, 89, ... where the sum of two neighbors always yields the following number [18].

As we can see, only the 10^{th} approximation gives the cor-

Table 1: Approximations of the irrational number ϕ.

$[1] = 1$
$[1; 1] = 2$
$[1; 1, 1] = 3/2 = 1.5$
$[1; 1, 1, 1] = 5/3 = 1.\overline{66}$
$[1; 1, 1, 1, 1] = 8/5 = 1.6$
$[1; 1, 1, 1, 1, 1] = 13/8 = 1.625$
$[1; 1, 1, 1, 1, 1, 1] = 21/13 = 1.\overline{615384}$
$[1; 1, 1, 1, 1, 1, 1, 1] = 34/21 = 1.\overline{619047}$
$[1; 1, 1, 1, 1, 1, 1, 1, 1] = 55/34 = 1.\overline{61764705882352941}$
$[1; 1, 1, 1, 1, 1, 1, 1, 1, 1] = 89/55 = 1.\overline{618}$

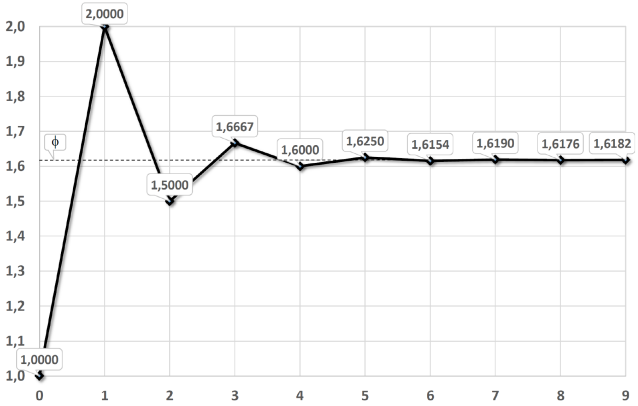

Fig. 1: The approximation steps 0 – 9 of the golden number $\phi = 1.618\ldots$ (dotted line) by continued fraction $[1; 1, 1, \ldots]$.

rect third decimal of ϕ. The approximation process is very slow because of the small denominators. In fact, the denominators in the continued fraction of ϕ are the smallest possible and consequently, the approximation speed is the lowest possible. The golden number ϕ is therefore treated as the "most irrational" number in the sense that a good approximation of ϕ by rational numbers cannot be given with small quotients.

On the contrary, transcendental numbers can be approximated exceptionally well by rational numbers, because their continued fractions contain large denominators and can be truncated with minimum loss of precision. For instance, the simple continued fraction of the number $\pi = 3.1415927\ldots = [3; 7, 15, 1, 292, \ldots]$ delivers the following sequence of rational approximations:

$[3] = 3$
$[3; 7] = 3.\overline{142857}$
$[3; 7, 15] = 3.\overline{14150943396226}$
$[3; 7, 15, 1] = 3.1415929\ldots$

We can see that the 2nd approximation delivers the first 2 decimals correctly, and the 4th approximation shows already 6 correct decimals.

Much like the continued fraction of the golden number ϕ contains only the number 1, a prominent continued fraction [19] of Euler's number contains all natural numbers as denominators and numerators, forming an infinite fractal sequence of harmonic intervals:

$$e = 2 + \cfrac{1}{1 + \cfrac{1}{2 + \cfrac{2}{3 + \cfrac{3}{4 + \cdots}}}}.$$

As Euler's number is transcendental, it can also be represented as a continued fraction with quickly increasing denominators:

$$e = 1 + \cfrac{2}{1 + \cfrac{1}{6 + \cfrac{1}{10 + \cfrac{1}{14 + \cdots}}}}.$$

In this way, already the 4th approximation delivers the first 3 decimals correctly and returns in fact the rounded Euler's number $e = 2.71828\ldots$ of 5 decimals' resolution:

1
3
$2.\overline{714285}$
$2.7183\ldots$

This special arithmetic property of continued fractions [20] of transcendental numbers has the consequence that transcendental numbers are distributed near by rational numbers of small quotients or close to integers, like $e^3 = 20.08\ldots$ or $e^{4.5} = 90.01\ldots$. This can create the impression that complex systems like the solar system provide ratios of physical quantities that approximate rational numbers. More likely, they approximate transcendental numbers, which are located close to rational numbers.

Namely, transcendental numbers define the preferred ratios of quantities which avoid destabilizing resonance interaction [9]. In this way, they sustain the lasting stability of periodic processes in complex dynamic systems. At the same time, a good rational approximation can be induced quickly, if the system temporarily requires local resonance interaction. Though, algebraic irrational numbers like $\sqrt{2}$ or the golden number ϕ do not compellingly prevent resonance, because they can be transformed into integer or rational numbers by multiplication.

Among all transcendental numbers, Euler's number $e = 2.71828\ldots$ is unique, because its real power function e^x coincides with its own derivatives. In the consequence, Euler's number allows inhibiting resonance interaction regarding any interacting periodic processes and their derivatives. Because of this unique property of Euler's number, complex dynamic systems tend to establish relations of quantities that coincide with values of the natural exponential function e^x for integer and rational exponents x.

Therefore, we expect that periodic processes in real systems prefer frequency ratios close to Euler's number and its rational powers. Consequently, the logarithms of the frequency ratios should be close to integer 1, 2, 3, 4, ... or rational values $\frac{1}{2}, \frac{1}{3}, \frac{1}{4}, \ldots$ In [21] we exemplified our hypothesis in particle physics, astrophysics, cosmology, geophysics, biophysics and engineering.

Thanks to Khinchin's [14] discovery, any real number has a biunique representation as a continued fraction. Now let's apply this to the real argument x of the natural exponential function e^x itself:

$$x = [n_0; n_1, n_2, \ldots, n_k]. \tag{1}$$

All denominators $n_1, n_2, \ldots, n_k$ of the continued fraction including the free link n_0 are integer numbers. All numerators equal 1. The length of the continued fraction is given by the number k of layers.

The canonical form (all numerators equal 1) does not limit our conclusions, because every continued fraction with partial numerators different from 1 can be transformed into a canonical continued fraction using the Euler equivalent transformation [22]. With the help of the Lagrange [23] transformation, every continued fraction with integer denominators can be represented as a continued fraction with natural denominators that is always convergent [24].

Now we are going to study the fractal distribution of the rational eigenvalues of the finite continued fractions (1). The

first layer is given by the truncated after n_1 continued fraction:

$$x = [n_0; n_1] = n_0 + \frac{1}{n_1}.$$

For the beginning we take $n_0 = 0$. The denominators n_1 follow the sequence of integer numbers ±1, ±2, ±3 etc. The second layer is given by the truncated after n_2 continued fraction:

$$x = [n_0; n_1, n_2] = n_0 + \cfrac{1}{n_1 + \cfrac{1}{n_2}}.$$

Figure 2 shows the first and the second layer in comparison. As we can see, reciprocal integers $\pm 1/2, \pm 1/3, \pm 1/4, \ldots$ are the attractor points of the distribution. In these points, the distribution density always reaches a local maximum. Whole numbers $0, \pm 1, \ldots$ are the main attractors of the distribution.

Now let's remember that we are observing the fractal distribution of rational values $x = [n_0; n_1, n_2, \ldots, n_k]$ of the real argument x of the natural exponential function e^x. What we see is the fractal distribution of transcendental numbers of the type $\exp([n_0; n_1, n_2, \ldots, n_k])$ on the natural logarithmic scale. Near integer exponents the distribution density of these transcendental numbers is maximum.

Consequently, for integer exponents x, the natural exponential function e^x defines attractor points of transcendental numbers and create islands of stability.

Figure 2 shows that these islands are not points, but ranges of stability. Integer exponents $0, \pm 1, \pm 2, \pm 3, \ldots$ are attractors which form the widest ranges of stability. Half exponents $\pm 1/2$ form smaller islands, one third exponents $\pm 1/3$ form the next smaller islands and one fourth exponents $\pm 1/4$ form even smaller islands of stability etc.
For rational exponents, the natural exponential function is always transcendental [25]. Increasing the length of the continued fraction (1), the density of the distribution of transcendental numbers of the type $\exp([n_0; n_1, n_2, \ldots, n_k])$ is increasing as well. Nevertheless, their distribution is not homogeneous, but fractal. Applying continued fractions and truncating them, we can represent the real exponents x of the natural exponential function e^x as rational numbers and make visible their fractal distribution.

Here I would like to underline that the application of continued fractions doesn't limit the universality of our conclusions, because continued fractions deliver biunique representations of all real numbers including transcendental. Therefore, the fractal distribution of transcendental eigenvalues of the natural exponential function e^x of the real argument x, represented as continued fraction, is an inherent characteristic of the number continuum. This characteristic we call the Fundamental Fractal [26].

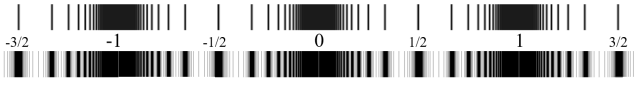

Fig. 2: The Fundamental Fractal – the fractal distribution of transcendental numbers of the type e^x with $x = [n_0; n_1, n_2, \ldots, n_k]$ on the natural logarithmic scale for $k = 1$ (first layer above) and for $k = 2$ (second layer below) in the range $-3/2 \leqslant x \leqslant 3/2$.

In physical applications, the natural exponential function e^x of the real argument x is the ratio of two physical quantities where one of them is the reference quantity called unit of measurement. Therefore, we can rewrite the equation (1):

$$\ln(\mathrm{X/Y}) = [n_0; n_1, n_2, \ldots, n_k], \tag{2}$$

where X is the measured physical quantity and Y the unit of measurement.

In this way, the natural exponential function e^x of the rational argument $x = [n_0; n_1, n_2, \ldots, n_k]$ generates the set of preferred ratios X/Y of quantities which avoid destabilizing resonance and in this way, provide the lasting stability of real systems regardless of their complexity. This is a very powerful conclusion, as we will see in the following.

Results

Now let's apply this result to our first example of the Venus-to-Earth orbital period ratio. In this case, X = 224.701 days and Y = 365.256363 days. Following (2) we calculate the natural logarithm ln (X/Y):

$$\ln\left(\frac{Venus\ orbital\ period}{Earth\ orbital\ period}\right) = \ln\left(\frac{224.701}{365.256363}\right) = -0.49.$$

We can see that this logarithm is close to $-1/2$. The deviation is only 0.01. In accordance with (2), $n_0 = 0$ and $n_1 = 2$. Consequently, the Venus-to-Earth orbital period ratio is close to an attractor point of the Fundamental Fractal, the center of a local island of stability.

In fact, the ratios of the orbital periods in the solar system approximate Euler's number and its rational powers [9]. Obviously, in this way, the solar system can ovoid destabilizing resonance of the orbital motions and reach lasting stability. For instance, Saturn's sidereal orbital period [27] equals 10759.22 days, that of Uranus is 30688.5 days. The natural logarithm of the ratio of their orbital periods is close to 1:

$$\ln\left(\frac{Uranus\ orbital\ period}{Saturn\ orbital\ period}\right) = \ln\left(\frac{30688.5}{10759.22}\right) = 1.05.$$

Jupiter's sidereal orbital period equals 4332.59 days, that of the planetoid Ceres is 1681.63 days. The natural logarithm of the ratio of their orbital periods is also close to 1:

$$\ln\left(\frac{Jupiter\ orbital\ period}{Ceres\ orbital\ period}\right) = \ln\left(\frac{4332.59}{1681.63}\right) = 0.95.$$

Not only neighboring orbits show Euler ratios, but far apart from each other orbits do this as well. Pluto's sidereal orbital

period is 90560 days, that of Venus is 224.701 days. The natural logarithm of the ratio of their orbital periods equals 6:

$$\ln\left(\frac{\textit{Pluto orbital period}}{\textit{Venus orbital period}}\right) = \ln\left(\frac{90560}{224.701}\right) = 6.00.$$

In [8] we have analyzed the orbital periods of the largest bodies in the solar system including the moon systems of Jupiter, Saturn, Uranus and Neptune, as well as the exoplanetary systems Trappist 1 and Kepler 20. In the result we can assume that the stability of all these orbital systems is given by the transcendence of Euler's number and its rational powers.

The most stable systems we know are of atomic scale. Because of their exceptional stability, proton and electron form stable atoms, the structural elements of matter. The lifespans of the proton and electron surpass everything that is measurable, exceeding 10^{30} years. The proton-to-electron ratio 1836.152674 is considered as fundamental physical constant [28] and it has the same value for their rest energies and rest masses, frequencies and wavelengths. The natural logarithm is close to seven and a half:

$$\ln(1836.152674) = 7.515427\ldots \simeq 6 + \frac{3}{2}.$$

This result suggests the assumption that the stability of the proton and electron comes from the number continuum, more specifically, from the transcendence of Euler's number and its rational powers. Already in the eighties the scaling exponent 3/2 was found in the distribution of particle masses by Valery Kolombet [29]. Applying hyperscaling [26] by Euler's number (tetration), we get the next approximation of the logarithm of the proton-to-electron ratio:

$$6 + \frac{e^e}{10} = 7.515426\ldots$$

We suppose that hyperscaling by Euler's number causes the exceptional stability of proton and electron.

In [17] we have analyzed the mass distribution of hadrons, mesons, leptons, the W/Z and Higgs bosons and proposed scaling by Euler's number and its roots as model of particle mass generation [30]. In this model, the $W^{\pm}$-boson mass 80385 MeV/c^2 and the Z^0-boson mass 91188 MeV/c^2 appear as the 12 times scaled up electron rest mass 0.511 MeV/c^2:

$$\ln\left(\frac{W^{\pm}}{electron}\right) = \ln\left(\frac{80385}{0.511}\right) = 11.97.$$

$$\ln\left(\frac{Z^0}{electron}\right) = \ln\left(\frac{91188}{0.511}\right) = 12.09.$$

Expected, the square root of Euler's number defines the next island of stability – in fact, the corresponding state of matter was discovered in 2012 and interpreted [31] as Higgs-boson H^0 with the rest mass 125.18 GeV/c^2:

$$\ln\left(\frac{H^0}{electron}\right) = \ln\left(\frac{125180}{0.511}\right) = 12.41.$$

Euler's number and its rational powers are universal scaling factors that inhibit resonance and in this way, stabilize periodic processes bound in a chain system. This approach we call Global Scaling [21]. The rest energy of the proton can be seen as the $6+\frac{3}{2}$ times scaled up rest energy of the electron. In the same way, Pluto's orbital period can be seen as the 6 times scaled up by Euler's number orbital period of Venus or as the 3 times scaled up by Euler's number orbital period of Jupiter. Here it is important to understand that only scaling by Euler's number and its rational powers inhibits resonance interaction and provides lasting stability of bound processes and allows for the formation of stable atoms or stable planetary systems, for instance.

Now we could ask the question: Starting with the electron oscillation period, if we continue to scale up always multiplying by Euler's number, will we meet the orbital period, for instance, of Jupiter?

Actually, it is so. If we multiply the electron oscillation period 66 times by Euler's number, we meet exactly the orbital period of Jupiter:

$$\ln\left(\frac{T_{Jupiter\ orb}}{\tau_{electron}}\right) = \ln\left(\frac{3.7434\cdot 10^8\ \mathrm{s}}{8.093\cdot 10^{-21}\ \mathrm{s}}\right) = 66.00.$$

Jupiter's orbital period $T_{Jupiter\ orb}$ = 4332.59 days = 3.7434×10^8 s. The oscillation period of the electron $\tau_{electron}$ derives from its rest energy $E_{electron}$ = 0.511 MeV:

$$\tau_{electron\ angular} = \hbar/E_{electron} = 1.288\times 10^{-21}\mathrm{s},$$

$$\tau_{electron} = 2\pi\cdot\tau_{electron\ angular} = 8.093\times 10^{-21}\mathrm{s}.$$

$\hbar$ is the reduced Planck constant. Data taken from [28]. Similarly, the oscillation period of the proton τ_{proton} derives from its rest energy E_{proton} = 938.272 MeV:

$$\tau_{proton\ angular} = \hbar/E_{proton} = 7.015\times 10^{-25}\mathrm{s},$$

$$\tau_{proton} = 2\pi\cdot\tau_{proton\ angular} = 4.408\times 10^{-24}\mathrm{s}.$$

Within our approach, electron and proton define two complementary classes of stability in the sense of the avoidance of destabilizing resonance. Here and in the following, we use the letter E for electron stability and the letter P for proton stability. In accordance with (2), we use rectangle brackets for continued fractions. For example, E[66] means the main attractor 66 of electron stability. In the solar system, this attractor stabilizes the orbital period of Jupiter.

The main attractor E[63] stabilizes the orbital period of Venus. The siderial orbital period of Venus $T_{Venus\ orb}$ equals 224.701 days = 1.9414×10^7 s:

$$\ln\left(\frac{T_{Venus\ orb}}{\tau_{electron}}\right) = \ln\left(\frac{1.9414\times 10^7\ \mathrm{s}}{8.093\times 10^{-21}\ \mathrm{s}}\right) = 63.04 = E[63].$$

Not only the orbits of planets and planetoids, but also the orbits of moons are stabilized by the Fundamental Fractal (2).

For example, the main attractor $E[61]$ stabilizes the orbital period $T_{Moon\ orb}$ = 27.321661 days = 2.36059×10^6 s of the Moon:

$$\ln\left(\frac{T_{Moon\ orb}}{\tau_{electron}}\right) = \ln\left(\frac{2.36059 \times 10^6\ \mathrm{s}}{8.093 \times 10^{-21}\ \mathrm{s}}\right) = 60.94 = E[61].$$

The attractor $E[62]$ stabilizes the orbital period of Saturn's moon Iapetus $T_{Iapetus\ orb}$ = 79.3215 days = 6.8534×10^6 s:

$$\ln\left(\frac{T_{Iapetus\ orb}}{\tau_{electron}}\right) = \ln\left(\frac{6.8534 \times 10^6\ \mathrm{s}}{8.093 \times 10^{-21}\ \mathrm{s}}\right) = 62.00 = E[62].$$

As well, it is not surprising that Ceres, the largest body of the main asteroid belt, orbits the Sun close to a main attractor. The orbital period of Ceres $T_{Ceres\ orb}$ equals 1681.63 days = 1.4529×10^8 s:

$$\ln\left(\frac{T_{Ceres\ orb}}{\tau_{electron}}\right) = \ln\left(\frac{1.4529 \times 10^8\ \mathrm{s}}{8.093 \times 10^{-21}\ \mathrm{s}}\right) = 65.05 = E[65].$$

Now let us analyze some rotational periods. Although the rotation of Venus is retrograde, its period $T_{Venus\ rot}$ = 5816.667 hours = 2.094×10^7 s is close to the main attractor $E[65]$:

$$\ln\left(\frac{T_{Venus\ rot}}{\tau_{electron\ angular}}\right) = \ln\left(\frac{2.094 \times 10^7\ \mathrm{s}}{1.288 \times 10^{-21}\ \mathrm{s}}\right) = 64.96 = E[65].$$

As well, the full rotational period of the Sun $T_{Sun\ rot}$ = 34.3 days = 2.9635×10^6 s fits with a main attractor:

$$\ln\left(\frac{T_{Sun\ rot}}{\tau_{electron\ angular}}\right) = \ln\left(\frac{2.9635 \times 10^6\ \mathrm{s}}{1.288 \times 10^{-21}\ \mathrm{s}}\right) = 63.00 = E[63].$$

As we have seen, the main attractor $E[63]$ stabilizes the rotational period of the Sun as well as the orbital period of Venus. From this, directly follows:

$$T_{Venus\ orb} = 2\pi \cdot T_{Sun\ rot}$$

Although π is transcendental, its real power function π^x does not coincide with its own derivatives. Therefore, π cannot inhibit resonance interaction regarding the derivatives of periodic processes, but it does not violate the transcendence [32] of Euler's number. Within our approach, 2π connects stable rotation with stable orbital motion.

In addition, the main attractor $E[65]$ stabilizes the orbital period of Ceres as well as the rotational period of Venus. From this, directly follows:

$$T_{Ceres\ orb} = 2\pi \cdot T_{Venus\ rot}$$

Obviously, preferred rotational periods are not accidental, but follow the Fundamental Fractal (2) and are connected by 2π with stable, avoiding resonance orbital periods.

Within our approach, the approximation level of an attractor of stability indicates evolutionary trends. For example, the orbital period of Venus must still decrease for reaching the center of $E[63]$. On the contrary, the orbital period of the Moon must still increase for reaching the center of $E[61]$. Actually, exactly this is observed [33].

While all the orbital and rotational periods we have analyzed are stabilized by main attractors of electron stability, the rotational period of Mars $T_{Mars\ rot}$ = 24.62278 hours = 88642 s approximates a main attractor of proton stability:

$$\ln\left(\frac{T_{Mars\ rot}}{\tau_{proton\ angular}}\right) = \ln\left(\frac{88642\ \mathrm{s}}{7.015 \times 10^{-25}\ \mathrm{s}}\right) = 67.01 = P[67].$$

The rotational period of the Earth $T_{Earth\ rot}$ = 23.934 hours = 86164 s approximates the same attractor $P[67]$:

$$\ln\left(\frac{T_{Earth\ rot}}{\tau_{proton\ angular}}\right) = \ln\left(\frac{86164\ \mathrm{s}}{7.015 \times 10^{-25}\ \mathrm{s}}\right) = 66.98 = P[67].$$

This means that the main attractor $P[67]$ stabilizes the rotational periods of Mars and Earth. Furthermore, the attractor $P[71]$ stabilizes the orbital period $T_{Earth\ orb}$ = 365.25636 days = 3.1558×10^7 s of the Earth:

$$\ln\left(\frac{T_{Earth\ orb}}{\tau_{proton}}\right) = \ln\left(\frac{3.1558 \times 10^7\ \mathrm{s}}{4.408 \times 10^{-24}\ \mathrm{s}}\right) = 71.05 = P[71].$$

Obviously, the Earth's orbital eccentricity variation cycle $T_{Earth\ orb\ ecc} \approx 112,600$ years = 3.5533×10^{12} s is stabilized by the main attractor $E[77]$:

$$\ln\left(\frac{T_{Earth\ orb\ ecc}}{\tau_{electron\ angular}}\right) = \ln\left(\frac{3.5533 \times 10^{12}\ \mathrm{s}}{1.288 \times 10^{-21}\ \mathrm{s}}\right) = 77.00 = E[77].$$

This attractor stabilizes also the Earth's apsidal precession cycle $\approx 112,000$ years. The Earth's orbital inclination variation cycle $T_{Earth\ orb\ inc} \approx 70,000$ years = $2.209 \cdot 10^{12}$ s is stabilized by the attractor $E[76;2]$:

$$\ln\left(\frac{T_{Earth\ orb\ inc}}{\tau_{electron\ angular}}\right) = \ln\left(\frac{2.209 \times 10^{12}\ \mathrm{s}}{1.288 \times 10^{-21}\ \mathrm{s}}\right) = 76.51 = E[76;2].$$

The obliquity variation cycle of the ecliptic $T_{Ecliptic\ obliquity} \approx 41,000$ years = 1.2938×10^{12} s is stabilized by the main attractor $E[76]$:

$$\ln\left(\frac{T_{Ecliptic\ obliquity}}{\tau_{electron\ angular}}\right) = \ln\left(\frac{1.2938 \times 10^{12}\ \mathrm{s}}{1.288 \times 10^{-21}\ \mathrm{s}}\right) = 75.99 = E[76].$$

The Earth's axial precession cycle $T_{Earth\ axial\ prec} \approx 25,770$ years = 8.1328×10^{11} s is stabilized by the attractor $E[75;2]$:

$$\ln\left(\frac{T_{Earth\ axial\ prec}}{\tau_{electron\ angular}}\right) = \ln\left(\frac{8.1328 \times 10^{11}\ \mathrm{s}}{1.288 \times 10^{-21}\ \mathrm{s}}\right) = 75.52 = E[75;2].$$

The Earth's axial nutation period $T_{Earth\ axial\ prec}$ = 18.6 years = 5.8696×10^8 s is stabilized by the main attractor $P[74]$:

$$\ln\left(\frac{T_{Earth\ axial\ prec}}{\tau_{proton}}\right) = \ln\left(\frac{5.8696 \times 10^8\ \mathrm{s}}{4.408 \times 10^{-24}\ \mathrm{s}}\right) = 73.97 = P[74].$$

The Chandler wobble of the Earth's axis $T_{Chandler\ wobble}$ = 433 days = 3.741×10^7 s is stabilized by the main attractor P[73]:

$$\ln\left(\frac{T_{Chandler\ wobble}}{\tau_{proton\ angular}}\right) = \ln\left(\frac{3.741 \times 10^7\ \mathrm{s}}{7.015 \times 10^{-25}\ \mathrm{s}}\right) = 73.05 = P[73].$$

As we have seen, within our approach, the current orbital and rotational periods in the solar system do not appear as to be accidental, but correspond with islands of stability defined by Euler's number and its rational powers that allow avoiding destabilizing resonance. This is valid not only for the solar system, but also for exoplanetary systems as we have shown in [8]. Furthermore, our approach explains the durations of the axial precession cycle including the nutation period and the Chandler wobble, the obliquity variation cycle, the orbital inclination variation cycle, the apsidal precession cycle and the orbital eccentricity cycle of the Earth.

In [21] we have shown that the divisibility of their integer logarithms interconnects all the main attractors of electron and proton stability and causes interscalar effects, which stabilize also biophysical periodical processes.

Concluding this overview, I would like to mention that, within our approach, the current average temperature $\mathrm{T}_{\mathrm{CMBR}}$ = 2.725 K [34] of the cosmic microwave background radiation (CMBR) does not appear to be accidental. On the contrary, obviously, this process is stable, because its average temperature is close to a main attractor of proton stability:

$$\ln\left(\frac{\mathrm{T}_{\mathrm{CMBR}}}{\mathrm{T}_{\mathrm{proton}}}\right) = \ln\left(\frac{2.725\ \mathrm{K}}{1.0888 \times 10^{13}\ \mathrm{K}}\right) = -29.01 = P[-29].$$

The proton blackbody temperature $\mathrm{T}_{\mathrm{proton}} = E_{proton}/k$ derives from the proton rest energy $E_{proton} = 938.272\,MeV$ and the Boltzmann [28] constant k.

Consequently, the current temperature of the CMBR is not accidental, and it is highly unlikely that this temperature will still decrease.

In [35] we have shown that integer powers of Euler's number define also the ratios of fundamental physical constants. In our approach, this means that the transcendence of Euler's number stabilizes energy-frequency and energy-mass conversions and makes possible the existence of fundamental physical constants. For instance, the 88^{th} power of Euler's number stabilizes the ratio of the speed of light c, the Planck constant $\hbar$, the proton rest mass m_p and the gravitational constant G:

$$\frac{\hbar \cdot c}{G \cdot m_p^2} = e^{88}. \tag{3}$$

Quantum mechanics only postulates, but does not derive the constancy of the Planck constant as well as general relativity postulates the constancy of the gravitational constant, but does not derive it. Also special relativity postulates, but does not derive the constancy of the speed of light. Up to now, there have not been sufficiently convincing explanations why the speed of light should be constant, why it should have the value 299792458 m/s and why it should be the maximum possible velocity in the universe.

Within our approach, we can derive the speed of light c from other fundamental physical constants stabilized by integer powers of Euler's number. Naturally, the proton is not the only stable particle. The electron is stable as well. Furthermore, the proton-to-electron ratio is stabilized by Euler's number and its rational powers. From this and (3), directly follows that 299792458 m/s is not the maximum speed. Indeed, rational powers of Euler's number define a logarithmically fractal set of stable velocities $c_{n,m}$ which are superluminal for $n > 0$:

$$c_{n,m} = c \cdot e^{\,n/m}$$

where n, m are integer numbers. In general, the rational exponents are finite continued fractions (1). In [35] we verified the fractal set $c_{n,m}$ of stable subluminal and superluminal velocities on experimental and astrophysical data.

Conclusion

In this paper, we discussed the physical significance of transcendental numbers approximated by ratios of physical quantities. In particular, the transcendence of Euler's number allows avoiding destabilizing resonance interaction in real systems and appears to be a universal criterion of stability.

For instance, Euler's number and its rational powers stabilize the orbital and rotational periods of planets, planetoids and moons in the solar system.

Our approach allows deriving the mass ratios of the fundamental elementary particles electron, proton, $W^{\pm}$, Z^0 and H^0-boson as well as the temperature 2.725 K of the cosmic microwave background from Euler's number and its rational powers. Integer powers of Euler's number stabilize also the ratios of the fundamental physical constants $\hbar$, c, G.

Acknowledgements

The author is grateful to Simon Shnoll, Viktor Panchelyuga, Valery Kolombet, Svetlana Zaichkina, Oleg Kalinin, Viktor Bart, Sergey Surin, Alexey Petrukhin, Erwin Müller, Michael Kauderer, Ulrike Granögger and Leili Khosravi for valuable discussions.

Submitted on August 16, 2019

References

1. Heggie D. C. The Classical Gravitational N-Body Problem. arXiv: astro-ph/0503600v2, 11 Aug 2005.
2. Hayes B. The 100-Billion-Body Problem. *American Scientist*, 2015, v. 103, no. 2.
3. Williams I. O., Cremin A.W. A survey of theories relating to the origin of the solar system. Qtly. Rev. RAS 9: 40-62, (1968), ads.abs.harvard.edu/abs.
4. Alfven H. Band Structure of the Solar System. // Dermot S. F. Origin of the Solar System. pp. 41-48. Wiley, (1978).

5. Woolfson M. M. The Solar System: Its Origin and Evolution. *Journal of the Royal Astronomical Society*, 1993, v. 34, 1–20.
6. Van Flandern T. Our Original Solar System-a 21st Century Perspective. MetaRes. Bull. 17: 2-26, (2008). D21, 475–491, 2000.
7. Woolfson M. M. Planet formation and the evolution of the Solar System. arXiv:1709.07294, (2017).
8. Müller H. Global Scaling of Planetary Systems. *Progress in Physics*, 2018, v. 14, 99–105.
9. Müller H. On the Cosmological Significance of Euler's Number. *Progress in Physics*, 2019, v. 15, 17–21.
10. Venus Fact Sheet. NASA Space Science Archive. www.nssdc.gsfc.nasa.gov.
11. Fedorov V. M. Interannual Variations in the Duration of the Tropical Year. Doklady Earth Sciences, 2013, Vol. 451, Part 1, pp. 750–753, (2013) // Doklady Akademii Nauk, 2013, Vol. 451, No. 1, pp. 95–97., (2013).
12. Pletser V. Orbital Period Ratios and Fibonacci Numbers in Solar Planetary and Satellite Systems and in Exoplanetary Systems. arXiv:1803.02828 (2018).
13. Butusov K. P. The Golden Ratio in the solar system. *Problems of Cosmological Research*, vol. 7, Moscow–Leningrad, 1978.
14. Khintchine A. Continued fractions. University of Chicago Press, Chicago, 1964.
15. Gantmacher F. R., Krein M. G. Oscillation matrixes, oscillation cores and low oscillations of mechanical systems. Leningrad, 1950.
16. Terskich V. P. The continued fraction method. Leningrad, 1955.
17. Müller H. Fractal Scaling Models of Natural Oscillations in Chain Systems and the Mass Distribution of Particles. *Progress in Physics*, 2010, v. 6, 61–66.
18. Devlin K. The Man of Numbers. Fibonacci's Arithmetic Revolution. Bloomsbury Publ., 2012.
19. Yiu P. The Elementary Mathematical Works of Leonhard Euler. Florida Atlantic University, 1999, pp. 77–78.
20. Perron O. Die Lehre von den Kettenbrüchen. 1950.
21. Müller H. Global Scaling. The Fundamentals of Interscalar Cosmology. *New Heritage Publishers*, Brooklyn, New York, USA, (2018).
22. Skorobogatko V. Ya. The Theory of Branched Continued Fractions and mathematical Applications. Moscow, Nauka, 1983.
23. Lagrange J. L. Additions aux elements d'algebre d'Euler. 1798.
24. Markov A. A. Selected work on the continued fraction theory and theory of functions which are minimum divergent from zero. Moscow–Leningrad, 1948.
25. Hilbert D. Über die Transcendenz der Zahlen e und π. *Mathematische Annalen*, Bd. 43, 216–219, 1893.
26. Müller H. Scale-Invariant Models of Natural Oscillations in Chain Systems and their Cosmological Significance. *Progress in Physics*, 2017, v. 13, 187–197.
27. Astrodynamic Constants. JPL Solar System Dynamics. ssd.jpl.nasa.gov (2018).
28. Tanabashi M. et al. (Particle Data Group), Phys. Rev. D 98, 030001 (2018), www.pdg.lbl.gov
29. Kolombet V. Macroscopic fluctuations, masses of particles and discrete space-time, *Biofizika*, 1992, v. 36, 492–499.
30. Müller H. Emergence of Particle Masses in Fractal Scaling Models of Matter. *Progress in Physics*, 2012, v. 8, 44–47.
31. Bezrukov F. et al. Higgs boson mass and new physics. arXiv:1205.2893v2 [hep-ph] 27 Sep 2012.
32. Bailey D. H. Numerical Results on the Transcendence of Constants Involving pi, e, and Euler's Constant. *Mathematics of Computation*, 1988, v. 50(181), 275–281.
33. Bills B. G., Ray R. D. Lunar Orbital Evolution: A Synthesis of Recent Results. *Geophysical Research Letters*, v. 26, Nr. 19, pp. 3045–3048, (1999)
34. Fixsen D. J. The Temperature of the Cosmic Microwave Background. *The Astrophysical Journal*, vol. 707 (2), 916–920. arXiv:0911.1955, 2009.
35. Müller H. The Cosmological Significance of Superluminality. *Progress in Physics*, 2019, v. 15, 26–30.

A New Understanding of the Matter-Antimatter Asymmetry

Linfan Mao

1. Chinese Academy of Mathematics and System Science, Beijing 100190, P.R. China
2. Academy of Mathematical Combinatorics & Applications(AMCA), Colorado, USA
E-mail: maolinfan@163.com

There are no theory on antimatter structure unless the mirror of its normal matter, with the same mass but opposite qualities such as electric charge, spin,$\cdots$, etc. to its matter counterparts holding with the Standard Model of Particle. In theory, a matter will be immediately annihilated if it meets with its antimatter, leaving nothing unless energy behind, and the amounts of matter with that of antimatter should be created equally in the Big Bang. So, none of us should exist in principle but we are indeed existing. A few physicists explain this puzzling thing by technical assuming there were extra matter particles for every billion matter-antimatter pairs, or asymmetry of matter and antimatter in the end. Certainly, this assumption comes into beings by a priori hypothesis that the matter and antimatter forming both complying with a same composition mechanism after the Big Bang, i.e., antimatter consists of antimolecules, antimolecule consists of antiatoms and antiatom consists of antielectrons, antiprotons and antineutrons without experimental evidences unless the antihydrogen, only one antimolecule. *Why only these antimatters are detected by experiments*? *Are there all antimatters in the universe*? In fact, if the behavior of gluon in antimatter, i.e., antigluon is not like the behavior but opposites to its matter counterparts or reverses gluon interaction $\mathcal{F}_{g^k}$ to $-\mathcal{F}_{g^k}$, $1 \leq k \leq 8$ complying with the Standard Model of Particle, then the residual strong interaction within hadrons is repulsion. We can establish a new mechanism of matter and antimatter without the asymmetry assumption but only by composition theory of matter, explain the asymmetry of matter-antimatter and why only these antimatters found, claim both the attractive and repulsive properties on gravitation. All of the conclusions are consistent with known experiments on matter and antimatter.

1 Introduction

Antimatter and dark energy are both physical reality in the universe. An antimatter is literally, a mirror image with the same mass but reversed electrical charges and spin as its correspondent normal matter such as those of positrons, antiprotons, antideuteron,$\cdots$ and antihydrogen. The most interesting phenomenon on antimatter $\overline{M}$ is that if it collides with its normal matter M will completely annihilate into energy E in global energy shortage today. For example,

$$e^- + e^+ \to \gamma + \gamma,$$

i.e., an electron e^- collides with a positron e^+ will completely transforms to 2 photons γ, an energy form.

Antimatter was first theoretically considered by Paul A.M.Dirac in 1928 for his equation $E = \pm mc^2$ which allowed for the negative energy existence, corespondent to anti-particles in the universe. And then, Carl Anderson discovered positron, the first evidence that antimatter existed in 1932. A few famous things signed the founding of antimatter $\overline{M}$ are listed following ([2],[3]):

(1) Positron by C. Anderson in 1932;

(2) Antiprotons by E. Segrè and O. Chamberlain et al at Bevatron of Berkeley in 1955;

(3) Antineutron by B. Cork et al at Bevatron of Berkeley in 1957;

(4) Antideuteron by Antonino Zichichi et al at CERN in 1965;

(5) Antihydrogen by W. Oelert et al at CERN in 1995.

In fact, modern physics convinces that there exists elementary antiparticle for every elementary particle ([4]), founded in its decay, scattering and radiation such as those known rulers following:

(1)(β-Decay) $n \to p + e^- + \overline{\nu}_e$, i.e., a neutron n can spontaneously decays to a proton p, a electron e^- and antineutrino $\overline{\nu}_e$;

(2)(Scattering) $\gamma + \gamma \to e^- + e^+$, i.e., a photon γ collides with another γ will scattering an electron e^- and a positron e^+;

(3)(Radiation) $e^- \to e^- + \gamma$, i.e., a high level electron e^- jumps to a low level e^- will radiating a proton γ.

For explaining the observation that the universe is expanding at an accelerating rate, the dark energy is suggested in the standard model of cosmology in 1998 ([15]). But, neither its detecting nor forming mechanism is hold by humans unless it contributes 68% energy to the total energy in the observable universe. *Where does*

it comes from and how is it formed? Certainly, the dark energy and antimatter are both related to Big Bang but we have no a theory for explaining their born and rulers in universe. The key point is holding on the forming of antimatter with action on matter.

Usually, antimatter is understood as the mirror of its normal matter with the same mass but opposite qualities such as electric charge, spin,$\cdots$, etc. to its matter counterparts, holds with the Standard Model of Particle, and a priori hypothesis that the matter and antimatter forming both comply with a same composition mechanism after the Big Bang by humans, i.e., a matter consists of molecules, a molecule consists of atoms, a atom consists of electrons, protons and neutrons,$\cdots$, and an antimatter also consists of antimolecules, an antimolecule also consists of antiatoms, an antiatom also consists of antielectrons, antiprotons and antineutrons, $\cdots$, respectively, a mirror composition theory on antimatter ([17]). However, there are no antimatter unless elementary antiparticles, and only one antimolecules, i.e., antihydrogen found by experimental evidence. Then, *why only these antimatters are detected and where are other antimatters hidden, or there are no other antimaters*? Furthermore, *could we claim the composition mechanism of antimatter is the same that of matter*? We can certainly not unless only by purely imagination. The central factor is the behavior of antigluon in antimatter. Clearly, gluon is an attraction in the composition of normal matter by the Standard Model of Particle. But, *is antigluon only an attraction, or its counterpart, a repulsion*? By its action property, antigluon should be a repulsion, not a mirror of a normal gluon complying with the Standard Model of Particle.

However, if the action of antigluon is a repulsion, we can easily explain why we exist, naturally abandoning the asymmetry assumption and understanding well the material constitution. We can therefore establish a new mechanism of matter and antimatter without the asymmetry assumption but only by composition theory of matter, explain the asymmetry of matter-antimatter and the scenery behind the Big Bang. We also discuss the property of gravitation between matters, antimatters, i.e., attraction and repulsion, the source of dark energy and clarify a few confused questions on applying antimatter in this paper.

2 Antimatter's Composition

2.1 Antimatter's Quark Structure

As is well known, atoms appear as a building block of all matters with a microcosmic structure, i.e., a nuclei consisting of electrons, protons and neutrons, $\cdots$, etc.. Notice that the action in QCD is an integral of Lagrangian density over space-time following

$$S_{QCD} = \frac{1}{4}\int d^4x F^k_{\mu\nu}F^{k\mu\nu} + \int d^4x\overline{q}\left(\gamma^\nu D_\nu + m_q\right)q$$

where, the first term is the gluon interaction described by the field strength tensor F^k_μ, where

$$\begin{aligned} F^k_{\mu\nu} &= \partial_\mu F^k_\nu - \partial_\nu F^k_\mu + g_s\lambda^k_{ij}F^i_\mu F^j_\nu, \\ D_\mu &= \partial_\mu + ig_sF^k_\mu\lambda_k \end{aligned}$$

and the second term is the quark action with quark mass m_q. In the Standard Model of Particle, baryons such as those of the proton and neutron are bound of 3 quarks q and antiquarks $\overline{q}$, and mesons including gluon, W and Z particles consist of a quark q and an antiquark $\overline{q}$, explains the strong and weak force well in an atom.

Notice that gluons are carrier of the strong interaction in the Standard Model of Particle, which is attraction of quarks in hadrons such as those shown in Fig.1

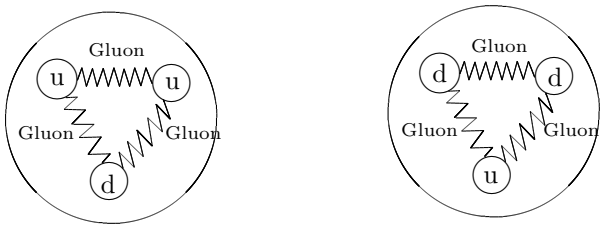

Fig. 1

and each quark or antiquark carries one of red r, green g, blue b or antired $\overline{r}$, antigreen $\overline{g}$, antiblue $\overline{b}$, i.e., color-charges resulting in 8 gluons listing following which characterizes strong interaction of quarks with exchanging gluons

$$\begin{aligned} &g^1 = r\overline{g},\ g^2 = r\overline{b}, \\ &g^3 = g\overline{b}, \\ &g^4 = \tfrac{1}{\sqrt{2}}\left(r\overline{r} - b\overline{b}\right), \\ &g^5 = g\overline{r},\ g^6 = b\overline{r},\ g^7 = b\overline{g}, \\ &g^8 = \sqrt{6}\left(r\overline{r} + b\overline{b} - 2g\overline{g}\right). \end{aligned} \tag{2.1}$$

Moreover, g^i is an attraction if $R_1 < r < R_2$, and a repulsion if $r < R_1$ for integers $1 \le i \le 8$ by experiments ([5]) such as those shown in Fig. 2

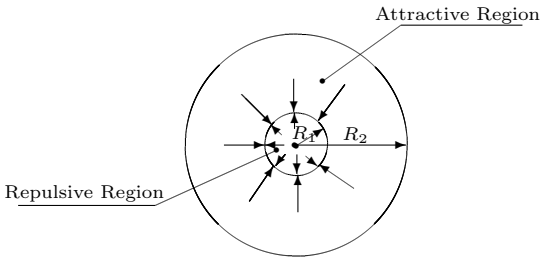

Fig. 2

where r is the distance of 2 quarks and $R_1 = 5\times10^{-14}$cm, $R_2 = 4\times10^{-12}$cm are respective the attractive, repulsive radius of quark.

Clearly, the composition theory of matter by quarks and gluons are essentially the new globally mathematical elements introduced in [14], i.e., continuity flows and discussed extensively on their mathematical characters in [9]-[13], or combinatorial geometry in [5]-[8].

Noticed that one Yin (Y^-) and one Yang (Y^+) constitute everything of universe in Chinese culture. We therefore know that there maybe 2 kind assumptions on the behavior of gluons hold with the Standard Model of Particle in the region $R_1 < R_2$ following:

Attraction Assumption. In this case, the composition of antimatters is the same as the ruler of matters, i.e., antimatter consists of antimolecules, antimolecule consists of antiatoms and antiatom consists of antielectrons, antiprotons and antineutrons. However, there are no such composition evidences unless one antimolecule, the antihydrogen $\overline{H}$, and all other composition matters are not found until today. In fact, such a composition mechanism only is a wishing thinking of humans with a priori hypothesis that all antigluons are attractive with the same color-charges (2.1) that of gluons, and the residual strong interaction within hadrons and antihadrons is attraction which forms the matter and antimatter. However, experimental evidences allude that the reality maybe not this case, resulting in the next assumption.

Repulsion Assumption. In this case, antigluons are all repulsive or interactions $\mathcal{F}_{\overline{g}^i}$ listed following

$$\begin{cases} \mathcal{F}_{\overline{g}^1} = -\mathcal{F}_{g^1} = -\mathcal{F}_{r\overline{g}}, \\ \mathcal{F}_{\overline{g}^5} = -\mathcal{F}_{g^5} = -\mathcal{F}_{g\overline{r}}, \\ \mathcal{F}_{\overline{g}^2} = -\mathcal{F}_{g^2} = -\mathcal{F}_{r\overline{b}}, \\ \mathcal{F}_{\overline{g}^6} = -\mathcal{F}_{g^6} = -\mathcal{F}_{b\overline{r}}, \\ \mathcal{F}_{\overline{g}^3} = -\mathcal{F}_{g^3} = -\mathcal{F}_{g\overline{b}}, \\ \mathcal{F}_{\overline{g}^7} = -\mathcal{F}_{g^7} = -\mathcal{F}_{b\overline{g}}, \\ \mathcal{F}_{\overline{g}^4} = -\mathcal{F}_{g^4} = -\mathcal{F}_{\frac{1}{\sqrt{2}}(r\overline{r}-b\overline{b})}, \\ \mathcal{F}_{\overline{g}^8} = -\mathcal{F}_{g^8} = -\mathcal{F}_{\sqrt{6}(r\overline{r}+b\overline{b}-2g\overline{g})}. \end{cases} \tag{2.2}$$

where $\mathcal{F}_{g^i}$ denotes interaction of gluon g^i for integers $1 \le i \le 8$. Notice that (2.2) will finally results in a repulsion of residual strong interaction within antiprotons and antineutrons such as those shown in Fig. 3.

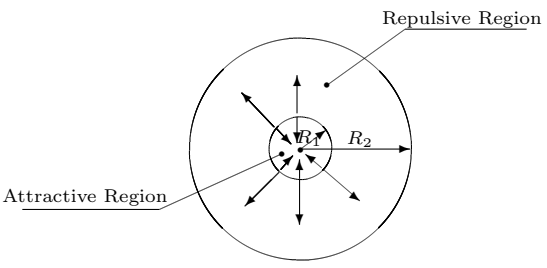

Fig. 3

Although we have also no experimental evidences on the repulsive behavior, likewise the attraction assumption on antigluons, we can explain the behavior of antimatters and the source of dark energy in the universe well by this assumption.

2.2 Antigluon's Repulsive Behavior

Let R_1, R_2 be the attractive, repulsive radius of a quark, respectively and let r be the distance to the center of a quark. We know the interaction behavior of gluons, antigluons $g^i, \overline{g}^i$, $1 \le i \le 8$ by Fig.2 and Fig.3 following.

Particle Name	$r < R_1$	$R_1 < r < R_2$	$r > R_2$
Gluon	Repulsion	Attraction	**0**
Antigluon	Attraction	Repulsion	**0**

Table 2.1

Whence, the residual strong interaction within an antiproton or an antineutron is repulsive, and an antiproton can not be bound with an antiproton, an antiproton can not be bound with an antineutron, and an antineutron can not also be bound with an antineutron in theory. We should discuss the residual strong interaction $\mathcal{F}$ combining with electromagnetism in detail. Let $D(p_1, p_2)$ be the minimum distance of 2 particles p_1, p_2. Then, by the ruler that like charges repel but unlike charges attract each other in nature, we easily know that

$$\begin{cases} D(\overline{p}_1, \overline{p}_2) > 0 & \text{if } p_1,\ p_2 \text{ both are antiproton;} \\ D(\overline{p}_1, \overline{p}_2) \ge 0 & \text{if one of } p_1,\ p_2 \text{ is antineutron,} \end{cases} \tag{2.3}$$

which implies that the minimum distance> 0 for 2 stable antiprotons, ≥ 0 for a stable antiproton with a stable antineutron or 2 stable antineutrons.

2.2.1 Antimatter's Combination Mechanism

Surely, the repulsive property of antigluons generates the antimatters following.

Antinucleon. We are easily know that there are no other stable antinucleon unless antiproton $\overline{P}$, antineutron $\overline{N}$ by the antigluon's behavior because the residual strong interaction of antiprotons, antineutron is repulsive, i.e., there are no stable antinucleon composed of more than 1 antiprotons or an antiproton with antineutrons.

Certainly, A.Zichichi et al at CERN of European and L.Redman et al at Brookhaven of USA artificially synthesized antideuterium $\overline{D}$ in 1965 which is consisted of an antiproton and an antineutron, and also followers such as those of antitritiu nucleon $\overline{T}$, antihelium nuclei $\overline{He}$, $\cdots$, etc. In fact, all of these antinucleons are made in laboratory with high energy but not stable, i.e., they

exist only a short time. *Why this happens*? It is subjectively explained by the notion that the antinucleon was finally annihilated with its nucleons counterpart. However, there are no experimental evidence for this explaining, and there are no such an annihilation observed but only the graspable feature of antinucleon disappeared from the eyes of humans.

This phenomenon can be explained naturally by the repulsive property of antigluons. Certainly, an antiproton can composed with antiprotons, antineutrons initially under the bombing of particle beam of high energy. However, as soon as an antinucleon forms, i.e., $D(p_1, p_2) < 0$ for antiparticles p_1, p_2 consisting of the antinucleon, the the residual strong interaction within the antinucleon acts on each antiparticle. It is repulsive. It will spontaneously separates antiparticles until $D(p_1, p_2) \geq 0$ for all of them, never needs the assumption that they are annihilated with their nucleon counterparts.

Antimolecule. A nucleon captures electrons to balance charges, and similarly, an antinucleon also captures positrons to make charge balance in theory, i.e. antimolecule. Thus, an antiproton $\overline{P}$, an antideuterium nucleus $\overline{D}$, an antitritiu nucleus $\overline{T}$ or generally, an antinucleon can be bound with one positron to produce antihydrogen $\overline{H}$, antideuterium $\overline{D}$, antitritiu $\overline{T}$, and generally, bound with positrons for balancing charges in the antinucleon to produce antimolecule $\overline{M}$ because the nuclear force between antinucleon and positrons is electromagnetism, an attractive force.

However, all of these antimolecules $\overline{M}$ are unstable unless the antihydrogen $\overline{H}$ because of the repulsive property of antigluons. Thus, even we can artificially synthesize antimolecules $\overline{M} \neq \overline{H}$ in high energy, $\overline{M}$ will spontaneously disintegrates to antihydrogen $\overline{H}$ or antineutrons one by one, such as those shown in Fig.4 for an antideuterium $\overline{D}$ in the universe.

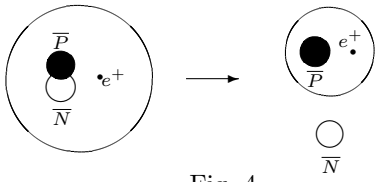

Fig. 4

Whence, an antimolecule $\overline{M}$ is unstable if $\overline{M} \neq \overline{H}$. It can only exists in high external pressure for resisting the repulsion of residual strong interaction. We summary the states of antimolecules Table 2.2.

$\overline{M}$	Existing	State	Synthesized
$\overline{M} \neq \overline{H}$	High energy	Unstable	No
$\overline{H}$	Usual condition	Stable	Yes

Table 2.2

Indeed, W.Oelert et al artificially synthesized a few antihydrogens at CERN in 1995 but these antihydrogens only exist in 4×10^{-8}s ([2]), seems likely to contradict the stable behavior of antihydrogen listed in Table 2.2. *How do we explain this case*? Notice that the experiment of W.Oelert et al verified that all antihydrogens are annihilated with hydrogens, not appearing of an unstable behavior, i.e.,

$$\overline{H} \ + \ H \rightarrow \text{ Engery}$$

because our earth is full of hydrogens, consistent with Table 2.2. Thus, we can classify known and unknown but maybe existing antimatters in Table 2.3.

$\overline{M}$	External Energy	State	Verified
e^+	Usual energy	Stable	Yes
$\overline{P}$	Usual energy	Stable	Yes
$\overline{N}$	Usual energy	Stable	Yes
$\overline{H}$	Usual energy	Stable	Yes
Antideuteron	High energy	Unstable	Yes
$\overline{M} \neq \overline{H}$	High energy	Unstable	No

Table 2.3

As is well-known, positron was found in constituents of cosmic rays, and we can imitate the Big Bang and get antimatters in high energy laboratory. However, they are unstable unless antiprotons, antineutrons and antihydrogens implied by Repulsion Assumption in Table 2.3. Then, *where are the hiding places of antimatters* $\overline{M} \neq \overline{H}$ *in the universe*? Theoretically, we are easily to get stable antimatters likewise to pick up a small stone on the earth but unstable antimatters can be only obtained in the situation of high energy, i.e., near or in fixed stars or high energy laboratory hold with

$$\mathcal{F}_{\text{epf}} \ > \ \mathcal{F}_{\text{rsa}}, \tag{2.4}$$

where $\mathcal{F}_{\text{epf}}$, $\mathcal{F}_{\text{rsa}}$ are respectively the external pressure force and the residual strong interaction within antiproton or antineutron of repulsion. Certainly, the equation (2.4) also explains the reason that why it is hard to get an antimatter $\overline{M} \neq \overline{H}$ in the laboratory of humans because it needs higher energy $\mathcal{F}_{\text{epf}}$ to bind antiprotons and antineutrons and we have no such a powerful laboratory until today. But, *why are we also hard to get antiprotons and antineutrons on the earth, both of them are stable*? It is because the earth is full of protons and neutrons, or matters, which results in the transiently existing of antiproton and antineutron after they come into beings in the laboratory.

Then, *where is the stable antimatter and why can we not find them outside laboratory unless the positron*? All

stable antimatters should be far away from galaxy. Otherwise, they will be annihilated with their counterparts matter. Thus, stable antimatters can be only existing in intergalactic spaces. There may be 2 existing forms of antimatters following:

C1. Free Antimatter. The free antimatter includes free positron, free antiproton, free antineutron and free antihydrogen. They are floating on space one by one, and if one of them collides with its matter counterpart it will annihilates into repulsive energy, which will further separates free antimatters to avoid collision again and finally, stable.

C2. Antimatter Star. The antimatter star includes antiproton star, antineutron star, antihydrogen star or their combination. As it is well-known, there are matters such as those of oxygen, nitrogen, argon, carbon dioxide, hydrogen and other matters in space but no proton stars, and an antimatter on the star may be collided with its matter star into annihilation. However, an antimatter star will be finally stable because if $D(\overline{p}_1, \overline{p}_2) \geq 0$, the residual strong interaction between antiparticles $\overline{p}_1$ and $\overline{p}_2$ is $\mathbf{0}$, i.e., stably existed. And *why can they not be annihilated with their counterparts matter completely*? Affirmatively, antimatters on surface of the star will be annihilated with their matter counterparts. But, as soon as the annihilation happens, a repulsion energy between the matter and antimatter star appears, which will finally pushes the matter and antimatter away until their distance $D(p, \overline{p}) > 0$ and forms a neutral space. A simple calculation enables us knowing respectively the upper density d_p, d_n and d_c of antiproton star, antineutron star and other antimatter stars as follows:

$$\begin{aligned} d_p &\leq \left(\frac{1}{16\times 10^{-16}}\right)^3 \times (1.6726231\times 10^{-27}) kg/m^3 \\ &= (2.44140625\times 10^{44}) \times (1.6726231\times 10^{-27}) kg/m^3 \\ &= 4.08355249\times 10^{17} kg/m^3, \\ d_n &\leq \left(\frac{1}{6.8\times 10^{-16}}\right)^3 \times 1.6749286\times 10^{-27} \\ &= (3.18033788\times 10^{45}) \times (1.6749286\times 10^{-27}) \\ &= 5.32683887\times 10^{18} kg/m^3, \\ d_c &< 5.32683887\times 10^{18} kg/m^3. \end{aligned}$$

3 Matter-Antimatter's Scenery Behind the Big Bang

Certainly, antimatter formed accompanying with matter after the Big Bang, i.e., the universe exploded into a seething fireball consisting of equal particles and antiparticles, and radiation. And then, the universe expanded rapidly, cooling in the process, and finally the matter and antimatter formed, which is in accordance with the sentence: *All things are known by their beings, and all beings come from non-beings* in Chapter 40 of TAO TEH KING, a well-known Chinese book written by Lao Zi, an ideologist in ancient China. We are able to build up a scenery of what happened, i.e., the forming of universe after the Big Bang ([16]) following.

STEP 1. Around 10^{-34} seconds, the universe burst its banks in a rush of expansion, growing at an exponential rate, i.e., inflation. During this period, energy, first repulsion and then, attraction were created to fill the expanding universe, which are the source of matter and antimatter in the universe.

STEP 2. Around 10^{-10} seconds, both of the strong repulsive and attractive force separated out. The pairs of quark and antiquark, the gluon and antigluon would have moved freely about in a very hot state called a quark-gluon or antiquark-gluon plasmas. By the hot pressure originated from the Big Bang, antimatter first come into being with a process that antiquark-gluon plasmas were composed to antiprotons, antineutrons and antiatoms as they captured positrons, and then antimolecules or antimatters one by one.

STEP 3. In about 10^{-7} seconds, the universe had cooled enough for the quark-gluon plasma to convert into the proton, neutron, and antimatter be spontaneously separated to antihydrogens, antiprotons, antineutrons under the residual strong interaction within an antiproton or an antineutron at the same time. All of them were freely floating.

STEP 4. Around 1 second, a few pair of matter and antimatter such as those of electron and positron, proton and antiproton, neutron and antineutron were annihilated into repulsive energy when they collided and then, pushed the matter and antimatter away until a neutral space appeared. Otherwise, the antimatter freely floated with its counterpart matter in the space.

STEP 5. Once the universe was a few seconds old, it became cool enough for the combination of protons and neutrons to form hydrogens, heliums, and antimatter were separated to antihydrogen, antiprotons, antineutrons, and positrons were thrown out from antimolecules. Certainly, it may be annihilated if the hydrogens, heliums collided with antihydrogen or antihelium existed in this time.

STEP 6. In about half an hour after the Big Bang, the amount of matter settled down but was constantly battered by the huge amount of light radiation, and in the meanwhile, antimatter stars were formed along with the cosmic inflation by their repulsion of interaction. Free antimatter also exists if they were not annihilated with its counterpart matter.

STEP 7. In about 3×10^5 years, the universe had become dilute and cool enough for light to go its own way unimpeded. More atoms and molecules started to form

by nuclei capturing electrons, and matter was born gradually, and antimatters were stable unless free positrons, which will annihilated if they collided with electrons.

STEP 8. In about 10^9 years, there began to form stars, fixed stars, planets, and appearing lives with existed stable antimatters in the universe. After 1.37×10^{10} years apart from the Big Bang, the universe evolves at its present visible and observable state, both including matters and stable antimatters.

Although antiproton or antineutron stars have not be determined by humans today, they are indeed existing and will be found in the universe someday.

4 Application's Preconditions

As we discussed, there are no antimatter likewise matters on the earth and there are no stable antimatter unless free antimatter such as those of positrons, free antiprotons, free antineutrons, free antihydrogens and antimatter stars, i.e., antiprotron star, antineutron star or their combination in universe. It is completely different from the normal matter's world. There are no possibility for the birth of living antibeings, no antipeoples, and it is only a symmetrical mirror of elementary particles but with a different mechanism on composing antimatters.

Certainly, the most interested character for humans today is that antimatter can be completely annihilated into clean energy if it collides with its counterpart matter, without any waste left over. However, where and how to extract it, and how to reserve it are 3 typical problems should be solved before its universal applied.

Problem 1. Antimatter Searching. By the repulsion assumption, one could find antimatter only in its 2 states following.

1. **High Energy.** In this case, there are 2 places maybe find antimatter, i.e., the place in or near fixed stars in universe and the high energy laboratory. As we known, all materials made by humans technology can not arrive at any fixed stars unless new high heat resistant material be created someday. Certainly, we can artificially synthesize antimatter in laboratory but only get very little used for scientific research, and the energy needed for synthesized antimatter is far exceeding the energy of annihilation, can not be universal applied for humans ([1], [2]).

2. **Stable.** The stable antimatter includes free antimatter and antimatter stars. The former is sloppy, freely floating without a fixed position in space. Thus, it is also difficult to collect a good supply of antimatter in this case. However, antiproton, antineutron or their combination star may be a good resource for getting plenty of antimatter in universe, extracted for application.

Problem 2. Antimatter Extracting. There are 2 preliminaries for extracting antimatter from an antimatter star. One is to determine its accurate position in space. Another is developed such a spaceship that can arrive at the antimatter star with mining tools. Notice that such a spaceship can not landed on and we can not excavate antimatter from such an antimatter star likewise mining in the earth. Otherwise, the repulsion of residual strong interaction within antiprotons and antineutrons will push it away from the star, i.e., a maybe extracting is the spaceship close to the antimatter star as possible and mines antimatter like scooping water in a pond by a spoon, on which there is a layer pushing away matter and antimatter on surface.

Problem 3. Antimatter Retaining. Clearly, it is difficult to retain antimatter in a container made by normal matter because antimatter will annihilates with the normal matter. Generally, the researchers construct an electromagnetic filed between antimatter and normal matter to separate them for retaining antimatter in laboratory, i.e., Penning trap. However, it only exists in a very short times in this way. For example, the antiproton only exists in less than 1 second in 2010, and 16 minutes in 2016 at CERN ([1]). There are no possible for applying antimatter to humans in such a retaining way.

Notice that an antiproton will annihilates and produces repulsive energy if it collides with a proton. We can construct a closed container filled with uncompressed hydrogens for retaining a mount of antiproton if its wall is strong enough to resist the repulsive energy produced in the annihilation of surface antiprotons with protons in all H's, where, it is assumed that the number of hydrogen is equal to that of antiprotons on the surface of extracted antiprotons.

Similarly, we can construct such a closed container for retaining antineutron if its wall material is stable without neutrons in theory. However, it is more difficult for retaining antineutron because of the β-Decay, i.e.,

$$n \to p + e^- + \overline{\nu}_e.$$

5 Further Discussions

There are a few topics related with antimatter further discussed following which are all important for understanding our universe.

Unmatter. By definition, unmatter is neither matter nor antimatter but something in between such as those of atoms of unmatter formed either by electrons, protons, and antineutrons, or by antielectrons, antiprotons and neutrons discussed in [19],[20]. However, there are no stable unmatter if the repulsion assumption on anigluon is true because there are no matters when antimatter appeared after the Big Bang, and as the matter

turned up, the repulsion forced antimatters to decompose into positrons, antiproton, antineutron, antihydrogen, blocked their combination naturally, and if they collided with their counterpart matter, they will annihilated into energy. Even if they combined on condition they are unstable and break down into elementary antiparticles and normal matter in a very short time. Whence, unmatter can be only found by artificially synthesized in high energy laboratory.

Gravitation. As it is well known by Newton, there exists universal gravitation $F = G\frac{m_1 m_2}{r^2}$ in 2 normal particles with masses m_1, m_2 respectively, where r is the distance of the 2 particles and G the constant of gravity, and Einstein understood it by space curvature ([7]). But, *what is it about antiparticles*? *Is it also attractive*? As we discussed, if the behavior of antigluons is repulsive, the residual strong interaction within hadrons is repulsive, and the gravitation between 2 antiparticles should be contrary to the attractive, i.e., the repulsive $F = -G\frac{m_1 m_2}{r^2}$ for 2 antiparticles with masses m_1, m_2 in distance r. We then have the behaviors of gravitation in particles and antiparticles following:

(1) **Attractive** in 2 normal particles;

(2) **Repulsive** in 2 antiparticles;

(3) **Equilibrium** in an antiparticle and its normal particle with an equilibrium distance in space.

Obviously, such gravitational behaviors can be also characterized by properties of space curvature.

Dark Energy. Clearly, the dark energy exists only in a repulsive behavior for the observed accelerating universe, without substantial evidence ([15]). *Where does it comes from*? And *what is its acting mechanism*? Why we can not hold on the dark energy is because we always understand the universe by its normal matter with an assumption that antimatter is only a mirror and follows the same rules of matter, only a partial view and results in the asymmetry of matter and antimatter. However, if we stand on a whole view, we can conclude that the dark energy naturally originates from antimatter's, i.e., antiproton's and antineutron's repulsion.

Conclusively, the Big Bang produced the equality of particles and antiparticles but different forming mechanisms, i.e., attractive and repulsive with the 4 known fundamental forces, respectively on matter and antimatter, which formed the universe, observable or unobservable by humans today.

Submitted on October 5, 2019

References

1. Andresen G.B. Confinement of antihydrogen for 1000 seconds. *Nature Phys.* 2011, v. 8, 558–564.
2. Close F. Antimatter. Oxford University Press Inc., New York, 2009.
3. Fraser G. Antimatter: the Ultimate Mirror. Cambridge University Press, 2000.
4. Ma T. View Physics by Mathematics – Elementary Particles and Unified Field Theory. Science Press, Beijing, 2014, (in Chinese).
5. Mao L. Combinatorial speculation and combinatorial conjecture for mathematics, *International J. Math. Combin.*, 2007, v. 1(1), 1–19.
6. Mao L. Combinatorial fields-an introduction, *International J. Mathematical Combinatorics*, 2009, v. 1(3), 1–22.
7. Mao L. Combinatorial Geometry with Applications to Field Theory. The Education Publisher Inc., USA, 2011.
8. Mao L. Mathematics on non-mathematics - A combinatorial contribution, *International J. Math. Combin.*, 2014, v. 3, 1–34.
9. Mao L. Extended Banach $\overrightarrow{G}$-flow spaces on differential equations with applications. *Electronic J. Mathematical Analysis and Applications*, 2015, v. 3(2), 59–91.
10. Mao L. A review on natural reality with physical equation. *Progress in Physics*, 2015, v. 11, 276–282.
11. Mao L. Mathematics with natural reality – Action flows, *Bull. Cal. Math. Soc.*, 2015, v. 107(6), 443–474.
12. Mao L. Complex system with flows and synchronization. *Bull. Cal. Math. Soc.*, 2017, v. 109(6), 461–484.
13. Mao L. Harmonic flow's dynamics on animals in microscopic level with balance recovery. *International J. Math. Combin.*, 2019, v. 1, 1–44.
14. Mao L. Science's dilemma – A review on science with applications, *Progress in Physics*, 2019, v. 15, 78–85.
15. Mazure A. and Vincent le Brun V. Matter, Dark Matter, and Anti-Matter. Springer-Verlag New York Inc., 2011.
16. Peacock O.A. Cosmological Physics. Cambridge University Press, 1999.
17. Phillips T.J. Antimatter may matter, *Nature*, 2016, v. 529, 294–295.
18. Ho-Kim Q, Yem P.X. Elementary Particles and Their Interactions. Springer-Verlag Berlin Heidelberg, 1998.
19. Smarandache F. A new form of matter – unmatter, composed of particles and anti-particles. *Progess in Physics*, 2005, v. 1, 9–11.
20. Smarandache F., Rabounski D. Unmatter entities inside nuclei, predicted by the Brightsen nucleon cluster model. *Progress in Physics*, 2006, v. 1, 14–18.

Unified Two Dimensional Spacetime for the River Model of Gravity and Cosmology

Alexander Kritov
E-mail: alex@kritov.ru

Within the proposed assumptions, including the existence of the discrete (minimally uncertain) volume of space, the possibility of mapping of Euclidean 3D to 1D space in the spherically symmetric case is considered. In introduced unified pseudo-Minkowski 2D spacetime (t,η) the river velocity for the Schwarzschild metric represents the uniform acceleration. The Rindler coordinate transforms in 2D spacetime lead to the Schwarzschild-de Sitter metric in static 4D coordinates and result in the scale factor that coincides with the one for cosmological expansion for the Universe with dark energy. The FLRW metric with such scale factor has the conformal form in unified 2D spacetime, and the varying Hubble parameter can be expressed with conformal time via the simple expression. The dynamic and continuity of the uniformly accelerated Rindler flow in unified 2D spacetime are reviewed.

The river model of gravity and the analog gravity is an alternative to the General Relativity (GR) approach to gravitation. The purpose of this article is to exhibit the analogy between the radial river velocity in three spatial dimensions with the motion along one spatial dimension. In the beginning, the three new physical parameters are to be introduced: the mass-radius, the discrete volume of space, and the new spatial coordinate η that is mapped to three spatial dimensions which allows introducing unified two-dimensional space-time (t, η). Note: Only the case of spherical symmetry is reviewed.

1 The river model of gravity and the equivalence principle

The river model of gravity [5] and the analog gravity [2] is the approach to gravity where the equivalence principle (EP) holds. But it is interpreted in such a way that instead of equivalence of gravity to the acceleration, it aligns gravity with non-uniform velocity $v(r)$ denoted as the river velocity. In the analog gravity models, the velocity $v(r)$ is considered to be a movement of some physical medium in flat background spacetime. The flow of the medium is considered to be stationary and irrotational. The use of non-uniform $v(r)$ instead of the acceleration provides the intuitively obvious connection to the metric in static coordinates

$$ds^2 = -c^2\left(1-\frac{v^2}{c^2}\right)dt'^2 + \left(1-\frac{v^2}{c^2}\right)^{-1}dr^2 + r^2 d\Omega^2 \quad (1)$$

where $d\Omega^2 = \sin^2\theta d\phi^2 + d\theta^2$ and coordinate time is denoted as t'. Contrary to that, attempts to embed the acceleration from the EP to a similar form of the metric are still highly disputable.

It was demonstrated in [8] using the coordinate transforms that the static metric (1) in the comoving reference frame has the following *equivalent* form

$$ds^2 = -c^2 d\tau^2 + a(\tau)^2\left(dR^2 + R^2 d\Omega^2\right) \quad (2)$$

which is the Robertson-Walker (FLRW) metric for the spatially flat case ($k = 0$) and $a(\tau)$ is the scale factor related to the river velocity as $v = R\dot{a}$, and v is the proper velocity of the comoving frame. Such equivalency of the static metric (1) to (2) is known for the de Sitter metric only (for example [16]), and the river velocity is associated with the Hubble flow. But the conformity between an arbitrary static metric and the comoving metric (2) in general case is missing or avoided in the literature. Recently, however, Mitra [10] proposed the clarifying view on this problem, which supports the presented approach.

2 The prerequisites of the model

Three postulates of the model are

1. The fundamental significance of the Hubble constant H_0*. The term "varying Hubble constant" can be misleading and is not applied to the approach. The constant is the fundamental value that does not vary with time. Instead it is proposed to use the varying parameter $\mathcal{H}(\tau) = \dot{a}/a$. The significance of it is distinguished from the Hubble constant. Further, the Hubble constant H_0 is denoted as H for shortness.

2. The incompressibility of the fluid and its constant density. It was given in [7], based on the conformal factor issue in the analog gravity and on the continuity equation. The significance of the moving fluid and moving space is the same in the presented approach which allows having aether overtones in the interpretation of such models.

3. The outward direction of the fluid from the center of mass. Czerniawski [4] pointed out that the Gullstrand-Painlevé metric can be written with negative and positive v equivalently. The same is given in [7, 8] for the analog gravity based on the fact that the river velocity comes to the static metric as squared value. If the river velocity depends on central mass then it hardly can be modeled by ingoing flow as the flow at a

*As an example, Dirac's large number coincidence can indirectly support this point or as it was conjectured in [9] $H_0 = m_e c^2/(2^{128}\hbar)$.

distance r somehow should "know" the value of mass located at the point $r = 0$, which intuitively would contradict to the sense of the short-range action of the hydrodynamics.

3 Mass-radius r_m and mass-volume V_m

Let m be a point mass of an elementary particle in the center of a sphere with radius r. Let's designate the certain radius r_m of the spherical volume V_m such as

$$m = \rho_0 \left(\frac{4}{3} \pi r_m^3 \right) \qquad \rho_0 = k\rho_c \tag{3}$$

denoting them respectively as mass-radius and the mass-volume. The value of the fluid density ρ_0 is expressed via the critical density ρ_c and k is some coefficient of order of unity and its estimates are given later. Then it can be also noted that

$$r_m = \left(\frac{3}{4\pi} \frac{m}{\rho_0} \right)^{1/3} = \left(\frac{2Gm}{kH^2} \right)^{1/3} . \tag{4}$$

As an example, for the river velocity in case of the Schwarzschild gravity [3, 5]

$$v(r) = \sqrt{\frac{2Gm}{r}} \tag{5}$$

the equation motion of a fluid (directed outwards as postulated) can be simplified as

$$r(t) = \left(\frac{3}{2} \sqrt{2Gm}\, t \right)^{2/3} = k^{1/3} r_m \left(\frac{3}{2} Ht \right)^{2/3} . \tag{6}$$

In such case the space is expanding in outwards direction and its spherical volume within the radius r denoted further as V increases with time as

$$V(t) = V_m k \left(\frac{3}{2} Ht \right)^2 \tag{7}$$

near the mass m. The definition of comoving distance R is $r = Ra$. Then one can note that particularly the scale factor can be represented as

$$r(t) = r_m k^{1/3} a(t) \qquad a(t) = \left[\frac{V(t)}{kV_m} \right]^{1/3} . \tag{8}$$

Importantly, the scale factor defined in such does not depend on the value of point mass. The reviewed case yields

$$a(t) = \left(\frac{3}{2} Ht \right)^{2/3} . \tag{9}$$

The expression describes the scale factor near the point mass m, for example, near the elementary particle that implies the spatial flow with river velocity (5) corresponding to the Schwarzschild space-time geometry. Further, it will be referred as the scale factor if one may still assume that it just coincidences with the cosmological scale factor.

4 The discrete volume of space V_0

The second parameter that has to be introduces is the minimal measurable volume of space V_0, the constant such as

$$V_0 = \frac{m_0}{\rho_0} \tag{10}$$

where m_0 is minimal mass quanta that is defined as

$$m_0 = \frac{\hbar}{c^2} \beta H \tag{11}$$

based on the uncertainty relation and where β is some coefficient of order of unity, which is determined later*. The existence of such volume implies the uncertainty to measure simultaneously three spatial coordinates as

$$\Delta x \, \Delta y \, \Delta y \geq V_0 . \tag{12}$$

The existence of a discrete value for the volume of space can be conjectured as its fundamental property. As the Heisenberg uncertainty principle governs the linear 1D coordinate measurement, the minimal 2D area that corresponds to one bit of the information is the Planck area, then V_0 represents 3D the volume of space with minimal entropy or unit of information that can be measured. The substitution of the value for ρ_0 into (10) leads to

$$V_0 = \left(\frac{2\beta}{3k} \frac{c}{H} \right) S_{Pl} \tag{13}$$

where S_{Pl} is the Planck area. In order to evaluate the volume V_0 as sphere the large number relations from [9, the expressions (1) and (2.3)] can be applied to obtain exactly

$$V_0 = \frac{4\pi}{3} \left(\frac{\beta}{k} \right) r_e \lambda_e \lambda_p \tag{14}$$

where λ_p and λ_e are the de Broglie wavelength of proton and electron and r_e is the classical electron radius†. Notably, the expression shows that V_0 can be expressed via the properties of fundamental particles and λ_p with the dimensionless coefficients, which are determined later.

The minimal volume V_0 can also signify one bit of information as in terms of the total entropy of the Universe within the Hubble volume as substitution leads to

$$I = \frac{V_H}{V_0} = \left(\frac{k}{2\beta} \right) \frac{S_H}{S_{Pl}} \tag{15}$$

where S_H is the area of the Hubble horizon, and the second equality represents the Holographic principle, which should have some the numerical factor here as the identity on the left-hand side represents the entropy of pure space only (without matter and energy). The expression to be used further for V_m via V_0 obviously can be obtained as

$$V_m = V_0 \frac{m}{m_0} = \frac{V_0}{\lambda_m} \frac{c}{\beta H} \tag{16}$$

where λ_m is the de Broglie wavelength of the mass m.

*So V_0 can be simply treated as the mass-volume of m_0.

†with factor of $3/10$, as per cited work.

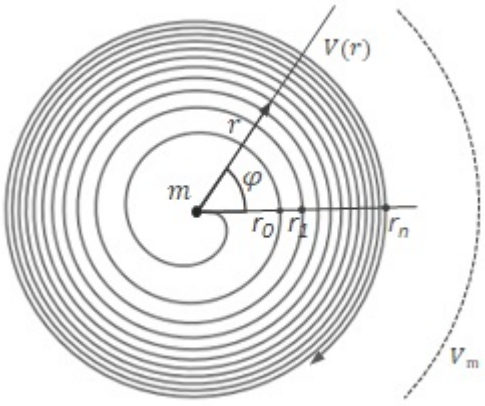

Fig. 1: The mapping of the spherical volume $V(r)$ to unified coordinate where $\eta = \phi\lambda_m/4\pi$ is represented by the angle ϕ. The spiral is given by the polar equation $r = a\phi^{1/3}$. Every turnover cycle corresponds to $dV = V_0$ and to the line segment with length λ_m in η coordinate.*

5 The unified coordinate η

The existence of discrete volumes leads to the proposition that 3D manifold may represent a countable set. Therefore all such V_0's within some spherical volume $V(r)$ can be mapped to fixed-line segments of one-dimensional coordinate. However, as V_0 is the quantity but is not an actual shape; therefore, such mapping is not uniquely defined. The new spatial-like coordinate η can be introduced† as following

$$\vec{\eta} = \lambda_m \frac{V(r)}{V_0} \vec{e_\eta} . \tag{17}$$

Such representation provides the mapping of the linear uncertainty relation for λ_m to the uncertainty for 3D volume V_0. The appearance of λ_m in the definition of η is motivated by its presence in (14), implying its fundamental significance as one of V_0's dimension. The coordinate can be understood as constituted of numbers of discrete deltas with the length of λ_m. Each of these deltas corresponds to *next in raw* V_0 within the spherical volume of $V(r)$.

The coordinate transformation likely represents the non-conformal mapping as it all angular information (ϕ,θ) of coordinates in 3D is lost as uses radial distance only. On another hand, the spherical shell with the volume $V_0 = 4\pi r^2 dr$ already does not have angular information due to the uncertainty of V_0. In such a way, the transformation is conformal. The definition can be also written in terms of differentials as

$$d\eta = dV \frac{\lambda_m}{V_0} . \tag{18}$$

*The spiral shows resemblance to the Theodorus spiral but constructed with the cubic roots instead of the square roots as $r_n = r_0[n^{1/3} - (n-1)^{1/3}]$.

†It can also be associated with the mass of space in spherical volume with postulated uniform density.

The ratio dV/V_0 corresponds to the natural number n (which is the number of spiral cycles as depicted in Fig. 1). In case if $V(r)$ as is not constant or there is a non-zero flux of the fluid, then it corresponds to the velocity

$$u = \frac{\partial\eta}{\partial t} = \frac{\lambda_m}{V_0}\left(\frac{\partial V}{\partial t}\right) . \tag{19}$$

The equation provides the direct correspondence between fluid flow in three-dimensional space and the velocity along the unified coordinate η. Then for the spherically symmetric case, the radial river velocity can be obtained as

$$v = \frac{V_0}{\lambda_m}\frac{u}{4\pi r^2} . \tag{20}$$

The meaning of the expression is evident with the help of Fig. 1, where the velocity u is angular velocity along the spiral line, and v is its projection to the radial direction. Substitution of (16) leads to

$$v = V_m \frac{\beta H}{c}\frac{u}{4\pi r^2} . \tag{21}$$

Also, the substitution of (16) into (17) provides the spherical volume expressed via η as

$$V = \eta\, V_m \frac{\beta H}{c} . \tag{22}$$

Noting the special point on η coordinate

$$\eta_m = \frac{c}{\beta H} \tag{23}$$

that corresponds to mass-radius r_m in 4D spacetime.

6 The motion along η in non-relativistic approximation

With the use of introduced coordinate, the space flow (7) can be represented as an equation of motion along η. The equation (19) for the Schwarzschild case above (7) (differentiating it with respect to time) gives

$$u = \frac{\lambda_m}{V_0}\left(V_m k \frac{9}{2} H^2 t\right) . \tag{24}$$

Applying (16)

$$u = \left(\frac{9k}{2\beta} Hc\right) t \tag{25}$$

which is the accelerated motion along coordinate η with constant acceleration‡

$$\alpha = \frac{9k}{2\beta} Hc . \tag{26}$$

Those, the Schwarzschild gravity with the river velocity (5) and for the scale factor $a(t)$ as in (9) represent *non-relativistic approximation* of motion with the constant acceleration (26) along coordinate η when $u \ll c$ or at near field of the point mass.

‡In the author's previous work [7] it was assumed that $k = 1$ and $\beta = \frac{3}{2}$ leading to $\alpha = 3Hc$ and (16) corresponds to the volume conversion relation.

7 The relativistic motion along η

It has to be considered now that unified coordinate η belongs to two dimensional Minkowski spacetime with the invariant line element

$$ds^2 = -c^2dt^2 + d\eta^2 \ . \tag{27}$$

The relativistic motion with the constant proper acceleration corresponds to the Rindler or also known as Kottler-Møller coordinates transforms [12, 13]

$$t = \frac{c}{\alpha}\sinh\left(\frac{\alpha}{c}\tau\right) \tag{28}$$

where τ is proper time and t is coordinate time and α is given by (26). The two-velocity is

$$u^i = c\left(\cosh\left(\frac{\alpha}{c}\tau\right), \sinh\left(\frac{\alpha}{c}\tau\right)\right) \tag{29}$$

where $i = 0, 1$. And the equation of motion along the coordinate is

$$\eta = \eta_0\cosh\left(\frac{\alpha}{c}\tau\right) - \eta_0 \tag{30}$$

where the initial conditions are set in such way that $\eta = 0$ at $t = 0$ (because of $V(0) = 0$ as (22)) and the Rindler horizon distance is

$$\eta_0 = \frac{c^2}{\alpha} = \left(\frac{2\beta}{9k}\right)\frac{c}{H}\,. \tag{31}$$

The significance of such distance is the fact that the moving object can not receive any information from the point of its origin anymore. Therefore, the dependency of gravitation from central mass should vanish*. The substitution of the equation of motion via η (30) to expression for spherical volume (22) leads to

$$V(\tau) = V_m\frac{\beta Hc}{\alpha}\left[\cosh\left(\frac{\alpha}{c}\tau\right) - 1\right]. \tag{32}$$

Expressing the hyperbolic cosine via half of argument of hyperbolic sine and using (8) the scale factor is

$$a(\tau) = \left(\frac{2\beta Hc}{k\alpha}\right)^{1/3}\left[\sinh\left(\frac{\alpha}{2c}\tau\right)\right]^{2/3} \tag{33}$$

where expression for α can be easily substituted from (26). The substitution of the proper velocity u^1 from (29) into (21), expressing the hyperbolic sine by the hyperbolic cosine from (32) with the use of $kr_m^3H^2 = 2Gm$ (4) lead to the solution for the radial river velocity for spherically symmetric gravitational field of point mass

$$v(r) = \left(\left[\frac{2\beta}{3k}\frac{\alpha}{3Hc}\right]\frac{2Gm}{r} + \left[\frac{\alpha}{3Hc}\right]^2H^2r^2\right)^{1/2} \tag{34}$$

which is the river velocity for the Schwarzschild-de Sitter (SdS) metric with the additional repulsive Λ-term.

*Starting from this distance the de Sitter model has to be valid, see Section 9.

The scale factor (33) coincidences with the one used in the standard cosmology for the current "dark energy dominated" epoch where it has the following form (see for example [15])

$$a(\tau) = \left(\frac{\Omega_m}{\Omega_\Lambda}\right)^{1/3}\left[\sinh\left(\sqrt{\Omega_\Lambda}\frac{3}{2}H\tau\right)\right]^{2/3} \ . \tag{35}$$

Matching the Ω's parameters with obtained result (33) leads to

$$\Omega_m = \left[\frac{2\beta}{3k}\frac{\alpha}{3Hc}\right] \qquad \Omega_\Lambda = \left[\frac{\alpha}{3Hc}\right]^2 . \tag{36}$$

Comparing this with two factors multiplying respectively the first and the second term in the expression (34) one can see that they are surprisingly *identical*.

The presented approach, however, attaches the different significance to these coefficients. The first one implies how the Newtonian gravity deviates from its usual law by simply multiplying the Newtonian potential. It should be set to unity, therefore, which is the condition explicitly equivalent to setting up the value of the acceleration α to (26). Then setting the first parameter to unity and the substitution of the value for α from (26)

$$v(r) = \left(\frac{2Gm}{r} + \left[\frac{3k}{2\beta}\right]^2H^2r^2\right)^{1/2} \ . \tag{37}$$

The second factor signifies how repulsive Λ-term differs from (H^2r^2), and it also consequently adds the pre-factor for H in the de Sitter metric and multiplies the cosmological horizon c/H with the same value (see also (13)).

Further, in the frame of this model, the second parameter is set to unity which equivalently implies the following

$$\frac{3k}{2\beta} = 1 \qquad \alpha = 3Hc \tag{38}$$

and the pre-factor in the expression for the scale factor (33) becomes unity. In such case, the Rindler horizon (23) as the radial distance from the center of mass

$$r_R = r_m\left(\frac{\beta}{3}\right)^{1/3} \tag{39}$$

and the distance where the SdS river velocity (37) as function of r approaches its minimum†

$$r(v_{min}) = r_m\left(\frac{k}{2}\right)^{1/3} \tag{40}$$

are both coincidences. The possible case can be considered if one also equates the Rindler horizon distance η_0 (23) with η_m (31) then it would lead to $\beta = 3$ and $k = 2$ then the both expressions above would have no prefactors.

†Equating the derivative to zero and using $kr_m^3H^2 = 2Gm$ as per (4). Another two extreme points of $v(r)$ where it approaches c are given in [6].

The substantial fact that the Rindler transforms in unified 2D spacetime of the form (28) results in the switch from the Schwarzschild river velocity to the SdS gravity with the repulsive Λ-term in 4D spacetime, by taking into account the relativistic consideration for the uniform acceleration along η. Importantly the obtained river velocity for the SdS metric corresponds to the proper velocity of u^1 in unified spacetime and rationale for it is given in Section 10.

8 The FLRW metric in 2D and the conformal form

As it was done for 4D in Section 2 the scale factor a' for 2D spacetime can be introduced in the same way as

$$\eta = k\,\eta_m\,a'(\tau)\,. \tag{41}$$

Using (30), (31) and (23) with determined coefficients (38) results in

$$a'(\tau) = \sinh^2\left(\frac{3}{2}\,H\tau\right) \tag{42}$$

that corresponds to the following 2D metric

$$ds^2 = -c^2d\tau^2 + \left[\sinh\left(\frac{3}{2}\,H\tau\right)\right]^4 dz^2 \tag{43}$$

where z is the comoving distance, $u^1 = z\,\dot{a}'$ and τ is the proper time in the comoving frame*. Such form is the mapping of the Robertson Walker (FLRW) metric with the scale factor (33) to 2D spacetime. The metric is written for the fluid while it moves in pseudo-Minkowski spacetime (27). Contrary to the FLRW metric with the scale factor (33), (35) this metric has the conformal form. The conformal time τ' such as $d\tau = d\tau' a'(\tau)$ is given by the transform

$$\tau' = \int \frac{d\tau}{a'(\tau)} = -\frac{2}{3H\tanh\left(\frac{3}{2}\,H\tau\right)} \tag{44}$$

where the integration constant can be set to zero. Notably, conformal time has reversed direction opposite to τ

$$\tau' \in \left(-\infty, -\frac{2}{3H}\right). \tag{45}$$

The metric (43) takes the following form

$$ds^2 = \sinh^4\left(\frac{3}{2}\,H\tau\right)\left(-c^2d\tau'^2 + dz^2\right). \tag{46}$$

Or using (44)

$$ds^2 = \left[1 - \left(\frac{3}{2}\,H\tau'\right)^2\right]^{-2}\left(-c^2d\tau'^2 + dz^2\right) \tag{47}$$

providing the conformal form of the FLRW metric in unified two dimensional spacetime.

On another hand, in four-dimensional spacetime, there is the parameter $\mathcal{H}$†

$$\mathcal{H}(\tau) = \frac{\dot{a}}{a} = \frac{v}{r} = \frac{\dot{V}}{4\pi r^3}\,. \tag{48}$$

Using (32) for $V(\tau)$ with the hyperbolic sine of half argument leads to

$$\mathcal{H}(\tau) = \frac{H}{\tanh\left(\frac{3}{2}\,H\tau\right)} \tag{49}$$

where the parameter belongs to the following interval

$$\mathcal{H}(\tau) \in (+\infty, H)\,. \tag{50}$$

Then the parameter can be written in terms of conformal time τ' as given by (44)

$$\mathcal{H}(\tau) = -\frac{3}{2}\,H^2\tau'\,. \tag{51}$$

This expression connects the "varying Hubble constant" with conformal time in unified 2D spacetime. The range of $\mathcal{H}(\tau)$ is from $+\infty$ to H and $\mathcal{H}(\tau)$ is the infinitely approaching value of H, as shown.

Interestingly that the metric (43) represents the embedding class two geometry, implying that the minimal number of dimensions of flat spacetime where it can be embedded is four. The reason why at least two additional dimensions are required is that the derivative $\dot{a}(\tau)$ has zero at $\tau = 0$, see [1, the Theorem 2.2].

9 The note on $3Hc$ and the number of spatial dimensions, the de Sitter metric

The appearance of the factor 3 in the value of the uniform acceleration (38) is closely related to the number of spatial dimensions. It can be demonstrated by the example of the de Sitter metric. Expressing the hyperbolic sine from the equation of motion (30) and substituting into the expression for proper velocity u^1 leads to

$$u(\eta) = c\,\frac{\eta}{\eta_0}\left(1 + \frac{2\eta_0}{\eta}\right)^{1/2}. \tag{52}$$

For far away distances when $\eta \gg \eta_0$ the second term in the equation can be neglected and using the value for η_0 from (31) it reduces to $u(\tau) = 3H\eta(\tau)$ with the solution

$$\eta(\tau) = a_1\exp(3H\tau) \tag{53}$$

where a_1 can be set to the Rindler horizon distance η_0 as per (39). Then it becomes

$$V = \left(\frac{\beta}{3}\right)V_m\exp(3H\tau)\,. \tag{54}$$

*The metric clearly differs from the known form in comoving Rindler frame $ds^2 = -c^2\left(1 + \alpha^2x^2\right)d\tau^2 + dx^2$ as the later uses different coordinate x that is defined locally in the observer's frame.

†Though the definition is the same as "varying Hubble constant" in the standard cosmology, their meanings have to be distinguished.

Using (8) and taking the cubic root result in

$$a(\tau) = \left(\frac{\beta}{3k}\right)^{1/3} \exp(H\tau) \tag{55}$$

which is the de Sitter metric where the factor 3 in the argument of the exponent disappears because of the cubic root. Interestingly pre-factor can not be unity in such way (the same can be shown by approximating (33)).

10 Coordinate time in 2D and in 4D spacetimes

Time is an arbitrary coordinate in gravitational theories including the GR [11] as it is not considered as absolute time. The model uses the proper time of the moving space τ that comes to the metric (2). The radial river velocity of the fluid / space v is the fluid's proper velocity in pseudo flat 4D Minkowski spacetime [3, 8] and v is the projection of proper velocity u_1 in 2D (t, η) as shown. However, the projection of coordinate velocity u_c in 2D (t, η) does not correspond to coordinate velocity of the fluid v_c in 4D because the Lorenz invariance in 2D cannot be applied to the Lorenz invariance is 4D. Therefore coordinate time in (t, η) is not synchronized with coordinate time in 4D (t', r, θ, ϕ). Such disagreement in coordinate times can be seen from the fact that time t in (t, η) implies how an observer residing at rest in $\eta = 0$ (so $r = 0$) measures its time. However, the coordinate time in 4D t' (that comes to the metric (1)) is time measured by static observer residing far away from the gravity $r = \infty$ (so $\eta = \infty$).

Whereas proper time τ of the comoving fluid in 2D is the same as proper time in 4D and such proper time invariance may imply invariance of the energy for coordinate transform from 2D to 4D but the topic requires further analysis. Coordinate time t' in four dimensional space time can be obtained from τ using the transform for the Gullstrand-Painlevé metric [3, 8]

$$d\tau = dt' - \frac{v}{c^2}\left(1 - \frac{v^2}{c^2}\right)^{-1} dr \tag{56}$$

where τ is also proper time in 2D. As v represents proper velocity $(dr/d\tau)$ then dividing both sides by $d\tau$ it takes following form

$$dt' = \frac{d\tau}{1 - \frac{v^2}{c^2}} \tag{57}$$

Then the transform from proper time to coordinate time in 4D is given by respective integral using $v(\tau)$.

11 The dynamic of the Rindler flow along η

One dimensional flow with constant acceleration and velocity u provides certain simplification of the case study on the one hand. The analogue of one dimensional density for example becomes $\rho_\eta = m_0/\lambda_m$. However, some of the parameters like pressure can not be defined. The constant two-force acting on a fluid element is

$$F^i = m_0\,\alpha\left(\sinh\left(\frac{\alpha}{c}\tau\right), \cosh\left(\frac{\alpha}{c}\tau\right)\right) \tag{58}$$

where $i = 0, 1$ and $\alpha = 3Hc$ as per (38). Using definition for m_0 (25) the norm of the constant force is

$$|F| = \frac{9k}{2c}\,\hbar H^2\,. \tag{59}$$

It is easy to see that work done by such force at distance from 0 to the Rindler horizon given by (31) is exactly

$$|F|\,\eta_0 = m_0\,c^2 \tag{60}$$

and does not depend on values of β and k. This expresses the significance of the Rindler horizon distance in the frame of the model. The relativistic energy density for such fluid is $e = \rho_\eta c^2\gamma = \rho_\eta u^0 c$. The integration yields the total energy within the line segment $(0, \eta)$ as

$$\begin{aligned} E &= \int_0^\eta e\,d\eta = \rho_\eta c \int_{\tau=0}^{\tau(\eta)} u^0 u^1 d\tau = \frac{m_0 c^4}{2\alpha\lambda_m}\cosh^2\left(\frac{\alpha}{c}\tau\right)\Big|_0^{\tau(\eta)} \\ &= \frac{m_0 c^4}{2\alpha\lambda_m}\left(\cosh^2\left(\frac{\alpha}{c}\tau\right) - 1\right) \end{aligned} \tag{61}$$

where in the last identity the value is taken at $\tau = 0$. Notable that the expression in brackets coincidences with $(u^1)^2$. Setting the hyperbolic cosine to 2 at distance η_0 as per (31) the total energy of the fluid from 0 to the Rindler horizon distance becomes

$$E(\eta_0) = \left(\frac{\beta}{2}\right)mc^2 \tag{62}$$

where $\alpha = 3Hc$ (38), (16) to express m and (31) were used. The energy invariance between 2D and 4D can be proposed based of the invariance for proper time τ between two spacetimes but it requires further analysis.

12 The continuity of the Rindler flow

The fluid flow with the relativistic uniform acceleration along η has many notable properties. As an example with the source placed at point $\eta = 0$ in case of incompressible fluid its strength is

$$\sigma = \frac{\partial m}{\partial t} = m_0\,\frac{\partial u}{\partial t} = 0\,. \tag{63}$$

However further along the coordinate such sink-source term is non-zero. It is easy to see using the equation of motion (30) for two points with initial distance λ_m (where we fix the initial line segment at $dt = \lambda_m/c$) then the distance between them increases with time as*

$$d\eta = \lambda_m \sinh\left(\frac{\alpha}{c}\tau\right). \tag{64}$$

In comoving frame of reference one can use proper velocity u^1 for the continuity equation. The divergence of proper velocity can be obtained as

$$\mathrm{div}(u^1) = \frac{\partial u^1}{\partial \eta} = \frac{\partial u^1}{\partial t}\,\frac{\partial t}{\partial \eta} = \frac{\alpha}{u_c} = \frac{\alpha}{c\tanh\left(\frac{\alpha}{c}\tau\right)}\,. \tag{65}$$

*Then the substitution of α from (38), using (17) leads to the element of the fluid growth in 3D as $V(\tau) = V_0 \sinh(3H\tau)$ which is exactly the same relation as suggested in [7] for the fluid parcel growth.

Lemma. The divergence of the proper velocity in 2D equals to divergence of the radial river velocity in 4D

$$\mathrm{div}(u^1) = \mathrm{div}(v)\,. \tag{66}$$

Proof. The radial velocity is irrotational as stated then

$$\mathrm{div}(v) = \frac{1}{r^2}\frac{\partial}{\partial r}\left(r^2 v\right) = \frac{2v}{r} + \frac{\partial v}{\partial r}\,. \tag{67}$$

Expressing v with u as given in (21)

$$\mathrm{div}(v) = \frac{V_m \beta H}{c}\frac{\partial u}{\partial r}\frac{1}{4\pi r^2} \tag{68}$$

where two identical terms dropped. As

$$\frac{\partial u}{\partial r} = \frac{\partial u}{\partial \eta}\frac{\partial \eta}{\partial r} = \frac{\partial u}{\partial \eta}\frac{c}{V_m \beta H}\,4\pi r^2 \tag{69}$$

where (22) was used the substitution into (68) proves the lemma.

Combining (65), (66) and (49), using the value for α (26) and the trigonometric identities the divergence of the river velocity becomes

$$\mathrm{div}(v) = \frac{3\dot{a}}{2a}\left[1 + \left(\frac{a}{\dot{a}}H\right)^2\right]. \tag{70}$$

The equation provides the correspondence of the parameter $\mathcal{H}(\tau) = \dot{a}/a$ to the sink-source strength of fluid with constant density.

13 The limitations of the model

The first limitation of the model is that it does not provide any feasible solution for the Kerr-Newman neither for the Reissner–Nordström metrics. In the presented model, the rotation of the in 3D can not be distinguished in η coordinate because of the uncertainty of the volume V_0 represented as the spherical shell, as depicted in Fig. 1. Though it does not create any issue for the model because the Kerr-Newman river velocity does not have any dependency on angular coordinates (ϕ, θ) but only on radial coordinate as shown in [5]

$$v(r) = \left[\frac{2Gmr - Q^2}{r^2 + A^2}\right]^{1/2} \tag{71}$$

where A is the angular momentum per unit mass of a rotating mass, and Q is its charge. The model has difficulties in obtaining the analytic expressions in the same way for such velocity. There are two arguments to support the model, particularly is that the Kerr-Newman metric is a pure theoretical consequence of the GR and is not anyhow verified experimentally. The second argument is that the model is not unique in the sense that the coordinate η can be introduced differently but in the same manner for example

$$\gamma d\eta = dV\,\frac{\lambda_m}{V_0} \tag{72}$$

where γ is u^0 in the unified 2D spacetime. In such case spatial 3D coordinates (dV at right hand side) have "mixed" projection to both η and t (contrary to reviewed case where $\eta \to dV$ directly). Introduced in such way the river velocity for the SdS metric would be simply

$$v_p = v_c\gamma = \left(\frac{r_m^3 H^2}{r}\right)^{1/2}\left(1 + \frac{r^3}{r_m^3}\right)^{1/2} \tag{73}$$

where $kr_m^3 H^2 = 2Gm$. So the coordinate velocity is the Schwarzschild river velocity. Such alternative definition of η aligns coordinate time t in 2D and t' in 4D. The case for the mixed projection can be elaborated in future work.

14 Free fall velocity and symmetries

In the frame of the presented approach, the acceleration α along η has a positive value. Its projection to 4D results in positive radial velocity v in an outward direction (that in the Schwarzschild case corresponds to the negative deceleration in outward direction). The free-fall velocity v_{ff} is connected to the river velocity as $v_{ff} = -v$. The changing of sign in the acceleration α corresponds to the transform of the river velocity to free-fall velocity as $\alpha \to -\alpha \quad v \to v_{ff}$ Alternatively, the transform of the river velocity to free-fall velocity can be given via the change of sign of proper time τ because time reversal changes a sign of u and therefore it changes a sign of the radial river velocity v as per (20) $\tau \to -\tau \quad v \to v_{ff}$. However, such time reversal does not change a sign of the acceleration α. If one would extend the direction of η coordinate to the negative values (understanding that it would correspond to negative volume or negative ρ_0) then mirroring the coordinate η (to opposite direction) means the equivalently the change of sign of the acceleration as per the equation of motion (30) $\eta \to -\eta \quad \alpha \to -\alpha$.

15 Conclusions

The proposed analogy of unified two-dimensional spacetime brought a few convenient advantages to study the cosmological metrics and gravitation via the simplification. From the perspective of unified 2D spacetime the Schwarzschild gravity can be viewed as a non-relativistic approximation of flow with the constant acceleration. Then the relativistic considerations of such movement in unified 2D spacetime lead to the appearance of the repulsive Λ-term corresponding to the SdS metric. And this is far from being analogy as the case is only possible if the unified 2D spacetime is considered as *physical* spacetime. It can be interpreted as the "internal" spacetime of the moving fluid of the analog gravity and the River model.

As shown, the FLRW metric in unified 2D spacetime has the conformal form. The conformal time is connected to the parameter $\mathcal{H}(\tau)$ that is usually associated with the "varying Hubble constant". The parameter $\mathcal{H}$ varies from the infinity in the past to the Hubble constant, which will be approaching infinite time (49). Therefore the model has no place for the

cosmological Big Crunch. The cosmological Big Bang is also absent. The model suggests that the Big Bang is going on continuously, equivalently signifying the emission of the fluid from the center of the point mass of every elementary particle where it is represented by the Rindler coordinate singularity at $\eta = 0$, $\tau = 0$. The Universe can be static as the equivalence of the metrics (1) and (2) is stressed.

The parallel of the model with the Conformal Quantum Mechanic that utilizes a 1D coordinate is yet to be analyzed. Possible outlook to the quantum properties of the Rindler fluid with constant force (59) (the linear potential) in unified 2D coordinates can be interesting. Embedding the electric charge to the metric in the frame of the model (where some of the parameters are to become imaginary) can be challenging.

Mathematical topics such as the topological coordinate transformation of 4D to 2D manifold and conformal mapping with the discrete maps in application to the presented model require further attention.

The exploration of additional coordinates is a strong trend since the foundation of Special Relativity. However, the opposite direction in the unification of known dimensions may also be surprisingly advantageous. The introduced unified 2D spacetime (t,η) via certain simplification offers a new perspective to look at gravitation and cosmology.

The presented intuitive approach reveals the significant parallel between gravity and motion in two-dimensional spacetime. As always, the analogy may be evidence of a hidden pattern in Nature; therefore, more thorough research and formal analysis are required.

Received on October 7, 2019

References

1. Akbar M. M. Embedding FLRW Geometries in Pseudo-Euclidian and Anti-de Sitter Spaces. arXiv: gr-qc/1702.00987v2.
2. Barcelo C., Liberati S., Visser M. Analogue Gravity. arXiv: gr-qc/0505065v3, 2011.
3. Czerniawski J. The possibility of a simple derivation of the Schwarzschild metric. arXiv: gr-qc/0611104.
4. Czerniawski J. What is wrong with Schwarzschild's coordinates? arXiv: gr-qc/0201037.
5. Hamilton A. J. S., Lisle J. P. The river model of black holes. *American Journal of Physics* 2008, v. 76, 519–532. arXiv: gr-qc/0411060.
6. Kritov A. Radiuses of Schwarzschild-de Sitter/AdS Black Holes. DOI: 10.13140/RG.2.2.14507.90406/2.
7. Kritov A. On the Fluid Model of the Spherically Symmetric Gravitational Field. *Progress in Physics*, 2019, v. 15 (2), 101–105.
8. Kritov A. From the FLRW to the Gravitational Dynamics. *Progress in Physics*, 2019, v. 15 (3), 145–147.
9. Kritov A. A new Large Number Numerical Coincidence. *Progress in Physics*, 2013, v. 2, 25–28.
10. Mitra A. Interpretational conflicts between the static and non-static forms of the de Sitter metric. *Scientific Reports*, 2012, v. 2, article 923.
11. Mitra A. Why the Big Bang Model Cannot Describe the Observed Universe Having Pressure and Radiation. *Journal of Modern Physics*, 2011, v. 2, 1436–1442
12. Møller C. The Theory of Relativity. Oxford Clarendon Press, 1955, p. 75.
13. Muñoz G., Jones P. The equivalence principle, uniformly accelerated reference frames, and the uniform gravitational field. arXiv: gr-qc /1003.3022v1.
14. Robertson H. P. On Relativistic Cosmology. *Phylosophy Magazin*, 1928, v. 5, 835–848.
15. Sazhin M. V., Sazhina O. S., Chadayammuri U. The Scale Factor in the Universe with Dark Energy. arXiv: astro-ph.CO, 1109.2258v1.
16. Tolman R. C. Relativity Thermodynamics and Cosmology. Oxford At the Clarenton Press, 1969, section 142.

A Simple Proof of the Second Law of Thermodynamics

G. G. Nyambuya

National University of Science and Technology, Faculty of Applied Sciences – Department of Applied Physics,
Fundamental Theoretical and Astrophysics Group, P. O. Box 939, Ascot, Bulawayo, Republic of Zimbabwe.
E-mail: physicist.ggn@gmail.com

By expressing the Boltzmann statistical weight function (W) in terms of the Boltzmann thermodynamic probabilities p_r, i.e. $\mathcal{W} = \mathcal{W}(p_1, p_2, \ldots, p_{r-1}, p_r, p_{r+1}, \ldots, p_m)$, and thereafter evoking the here set-forth Thermodynamic Probability Evolution Hypothesis – namely that, at the very least, a microstate can only evolve from a state of low thermodynamic probability to one of a higher thermodynamic probability, we demonstrate a simple and veritable proof of the Second Law of Thermodynamics (SLT), namely that the entropy of an isolated thermodynamic system always increases. Effectively and resultantly, this proof requires or points to the idea that the SLT holds not only statistically for an isolated system as currently understood, but must hold exactly for each of the microstates making up the system, hence, the restriction that the SLT holds only for an isolated thermodynamic system, may have to fall by the wayside.

The Law that entropy always increases – holds – I think, the supreme position among the Laws of Nature. If someone points out to you that your pet theory of the Universe is in disagreement with Maxwell's equations, then – so much the worse for Maxwell's equations. If it is found to be contradicted by observation[s], well – these experimentalists do bungle [up] things sometimes. But if your [pet] theory is found to be against the Second Law of Thermodynamics, I can give you no hope; there is nothing for it but to collapse in [the] deepest humiliation ... Sir Arthur Stanley Eddington (1882–1944), adapted from [1, pp. 37-38].

1 Introduction

The paramount *Second Law of Thermodynamics* (SLT) is one of the deepest, most profound and single-most important laws of physics. This seemingly sacrosanct law is born out of the solid and veritable soils of experimental philosophy. Be that as it may, this law has no corresponding fundamental theoretical justification except from the great Austrian theoretical physicist and philosopher – Ludwig Eduard Boltzmann (1844-1906)'s first (significant – albeit, failed) attempt at a proof via his all-famous and important *H-theorem* [2]. Boltzmann's attempt [2] was swiftly rejected (by Zermelo [3] and Leoschmidt [4]) as a complete proof and this is due to the assumptions made therein – i.e. critical assumptions which were rendered contrary to physical and natural reality as we know it, hence, to this day – despite the many spirited attempts at a proof, there is no accepted fundamental theoretical proof of the SLT; thus, it remains an open challenge to find a proof of the SLT. Herein, by way of writing down Boltzmann's *statistical weight function W*, as a function of the respective thermodynamic probabilities (p_r) of all the different microstates making up the given isolated thermodynamic system – i.e.:

$$\mathcal{W} = \mathcal{W}(p_1, p_2, \ldots p_{r-1}, p_r, p_{r+1}, \ldots p_{m-1}, p_m)\,, \qquad (1)$$

we humbly make an attempt at a proof that may shade some light on the very foundations and meaning of the SLT.

2 The four manifestations of entropy

Entropy manifests itself in four different forms. The first form is via Clausius' entropy, second is via Boltzmann's entropy, third is via Gibb's entropy and lastly is via the information theoretic entropy through Shannon's entropy. The main thrust of the present section is to try and link these four manifestations of entropy so that a proof of just one of them is sufficient proof for the rest of the entropies. Herein, we prove for the case of Boltzmann's entropy.

2.1 Clausius entropy

The great German physicist and mathematician – Rudolf Julius Emanuel Clausius (1822-1888), is – by and large – generally regarded as one of the central figures and founders of the science of *thermodynamics*. In his most important paper [5] entitled "*On the Moving Force of Heat*", Clausius first stated the basic ideas of the SLT and later, he introduced the concept of entropy (Clausius [6]). Further, in 1870, Clausius introduced the *Virial Theorem* which applies to heat [7]. Clausius' most famous statement of the SLT was published in both the German [8] and the English language [9]:

> Heat can never pass from a colder to a warmer body without some other change, connected therewith, occurring at the same time.

Further, in this famous paper [5], Clausius showed that there was a contradiction between Carnot's principle and the concept of conservation of energy and realising this, he restated

the two laws of thermodynamics to overcome this contradiction. For a system initially at temperature T_i and final temperature T_f and in-between these two temperature changes a net heat đQ takes place, for such a system, Clausius defined the entropy change, as:

$$\mathrm{d}\mathcal{S}_{\mathrm{C}} = \int_{T_i}^{T_f} \frac{đQ}{T}\,. \tag{2}$$

For an isolated thermodynamics system, the entropy always increases [6], and this is stated in the famous Clausius Law as:

$$\mathrm{d}\mathcal{S}_{\mathrm{C}} = \oint \frac{đQ}{T} \geq 0\,. \tag{3}$$

The landmark 1865 paper [6] in which he introduced the concept of entropy ends with the following summary of the *First* and *Second Laws of Thermodynamics*:

> The energy of the Universe is constant.
> The entropy of the Universe tends to a maximum.

2.2 Boltzmann entropy

Boltzmann's goal in his work [10] was to explain the behaviour of *macroscopic systems* in terms of the most fundamental *dynamical laws* governing their *microscopic constituents*. For example, consider clear and clean water in a container. In this container pour a drop of say potassium permanganate. If left to itself, the potassium permanganate will gradually spread in the water until the water is color blue i.e. the potassium permanganate is evenly spread throughout the water. Why does the water and potassium permanganate mixture prefer to be in the equilibrium macrostate where the potassium permanganate is evenly spread? Why?

To the mundane, the answer is that this is the way things are and to expect anything different is nothing short of asking for a miracle. The pedestrian mind will insatiably absorb this as an effect and consequence of the natural order of the world – not to Boltzmann. According to Boltzmann, this requires an answer that penetrates deep into the microscopic nature of reality at its most elementary and most fundamental level. That is, this has something to do with the evolution of the entropy of the system.

Boltzmann (1877) published his statistical interpretation of the SLT in response to objections from Loschmidt who had said that the *H-theorem* singled out the direction in time in which his H-function decreases, whereas the underlying mechanics was the same whether time flowed forward or backward. It is this paper that Boltzmann published his famous equation – where accordingly, at any give time – the Boltzmann entropy $\mathcal{S}_{\mathrm{B}}$ of this system is given by:

$$\mathcal{S}_{\mathrm{B}} = k_B \ln \mathcal{W}, \tag{4}$$

where k_{B} is the Boltzmann constant. Later, the reluctant German physicist [11], Max Karl Ernst Ludwig Planck (1858-1947), based the derivation of his black body radiation formula [12–14] on (4). Boltzmann's Eq. (4) has been successful in describing systems with minimal-most interactions in *Maxwell-Boltzmann*, *Fermi-Dirac* and *Bose-Einstein* statistics. For later instructive purposes, in the subsequent sections, we shall write down the corresponding thermodynamic weights ($\mathcal{W}$).

2.2.1 Maxwell-Boltzmann statistics

Maxwell–Boltzmann statistics (hereafter MB-statistics) describe the average distribution of non-interacting material particles over various energy states (microstates) in thermal equilibrium, and this kind of statistics is applicable in conditions where the temperature is high enough or where the particle density is low enough to render quantum effects negligible.

Suppose we have a gas of $\mathcal{N}$ identical point particles in a box of volume V. By "gas", we here-and-after mean that the particles are non-interacting with one another, or more realistically, the effects of the interactions are negligibly small. Suppose we know the single particle states in this gas. In MB-statistics, what we would like to know is what are the possible macrostates of the system as a whole. That is, how many ways are there of arranging the microstates? If n_r is the number of particles occupying the energy state ϵ_r, then, an appeal to statistics will tell us that the multiplicity W of different ways of arranging such a system is:

$$\mathcal{W}_{\mathrm{MB}} = \prod_{r=1}^{m} \frac{\mathcal{N}!}{n_r!}\,. \tag{5}$$

It was pointed out by Gibbs, that the above expression for $\mathcal{W}$ does not yield an *extensive entropy*, and as such – it must be faulty somehow. This problem is known as the *Gibbs paradox*. The problem is that the particles considered by the above equation are not indistinguishable. In other words, for two particles (A and B) in two energy sublevels the population represented by [A,B] is considered distinct from the population [B,A] while for indistinguishable particles, they are not.

2.2.2 Bose-Einstein statistics

If we carry out the same argument presented above in the MB-statistics – albeit, this time for indistinguishable particles, we are led to the Bose-Einstein (BE) multiplicity expression $\mathcal{W}_{\mathrm{BE}}$ i.e.:

$$\mathcal{W}_{\mathrm{BE}} = \prod_{r=1}^{m} \frac{(n_r + \mathrm{g}_r - 1)!}{n_r!(\mathrm{g}_r - 1)!}\,. \tag{6}$$

The MB-distribution follows from this BE-distribution for temperatures well above absolute zero, implying that $\mathrm{g}_r \lggg 1$. The MB-distribution also requires low density, implying that $\mathrm{g}_r \lggg n_r$. The BE-theory of was developed in 1924-5 by the Indian theoretical physicist Satyendra Nath Bose (1894-1974) and in full collaboration with Bose [15], the idea

was later adopted and extended by the great Albert Einstein (1879-1955). Due to Dirac [16, 17], particles that follow the BE-theory are called *bosons*.

2.2.3 Fermi-Dirac statistics

First derived in 1926 by the great Italian physicist – Enrico Fermi (1901-1954) [18, 19] and later in the same year by the finest and greatest English theoretical physicist of the modern age, Paul Adrian Maurice Dirac (1902-1984) [20], Fermi-Dirac statistics (here-and-after FD-statistics) describe a distribution of particles over energy states in systems consisting of many identical particles that obey the *Pauli Exclusion Principle*, where according no two particle can occupy the same quantum state and this has a considerable effect on the properties of the system. Further, FD-statistics apply to identical particles with half-integer spin (fermions) in a system in thermodynamic equilibrium. Additionally, the particles in this system are assumed to have negligible mutual interaction (gas) and this allows the many-particle system to be described in terms of single-particle energy states.

As is the case in the derivation of $\mathcal{W}_{\mathrm{BE}}$: suppose we have a number of energy levels, labelled by index i with each level having energy ϵ_r and containing a total of n_r particles. Further, suppose each level contains g_r (degeneracy) distinct sub-levels, all of which have the same energy, and which are distinguishable. The Pauli exclusion principle allows that only one fermion can occupy any such sub-level. The number w_r of ways of distributing n_r indistinguishable particles among the g_r sub-levels of an energy level, with a maximum of one particle per sub-level, is given by the binomial coefficient, using its combinatorial interpretation:

$$w_r = \frac{\mathrm{g}_r!}{n_r!(\mathrm{g}_r - n_r)!}\,. \tag{7}$$

The number of ways that a set of occupation numbers n_r can be realized is the product of the ways that each individual energy level can be populated, i.e.:

$$\mathcal{W}_{\mathrm{FD}} = \prod_{r=1}^{m} \frac{\mathrm{g}_r!}{n_r!(\mathrm{g}_r - n_r)!}\,. \tag{8}$$

2.3 Gibbs entropy

The great theoretician – Josiah Willard Gibbs (1839-1903), after whom the Gibbs entropy is named, was an American mathematician, chemist and physicist who made important and fundamental theoretical contributions to mathematics, chemistry and physics. Gibbs argued that for a thermodynamic system with W macrostates, if P_r is the thermodynamic probability of occurrence of the i^{th} macrostate, then the entropy $\mathcal{S}_{\mathrm{G}}$ of this system measured over all the macrostate $r = 1, 2, \ldots, m-1$, $\mathcal{W}$ is defined [21, 22]:

$$\mathcal{S}_{\mathrm{G}} = -k_B \sum_{r=1}^{\mathcal{W}} P_r \ln P_r\,, \tag{9}$$

where P_r is the probability of occurrence of the r^{th} macrostate. This definition, like Boltzmann's entropy, is a fundamental postulate whose ultimate justification is its ability to explain experimental facts, especially for systems of interacting particles.

The work of Gibbs on the applications of thermodynamics was instrumental in transforming physical chemistry into a rigorous inductive science. In *Statistical Mechanics* (a term coined by Gibbs himself), he combined the work of James Clerk Maxwell and Ludwig Boltzmann on the kinetic theory of gases, thus explaining the macroscopic laws of thermodynamics as a consequence of the underlying fundamental statistical properties of ensembles of the possible states of a physical system composed of many particles.

Gibbs' approach is very useful in the study of "equilibrium" statistical mechanics and solid state physics [22], whereas Boltzmann's approach is very useful in the study of gas-like systems such as electrons, photons, etc. However, Gibbs' approach in the treatment of nonequilibrium systems presents contentious problems [22, 23].

The American – Wayman Crow Distinguished Professor of Physics at Washington University in St. Louis – Edwin Thompson Jaynes (1922-1998), demonstrated [24] in 1965 that the Gibbs entropy is equal to the classical "*heat engine*" entropy of Clausius ($\mathrm{d}\mathcal{S} = \int_{T_i}^{T_f} \mathrm{d}Q/T$). Therefore, the Gibbs entropy is the same as the Clausius entropy, i.e.:

$$\mathcal{S}_{\mathrm{G}} = \mathcal{S}_{\mathrm{C}}\,, \tag{10}$$

hence, a proof that $\mathrm{d}\mathcal{S}_{\mathrm{G}} \geq 0$ is as well a proof that $\mathrm{d}\mathcal{S}_{\mathrm{C}} \geq 0$. Later in the paper, we will prove that $\mathrm{d}\mathcal{S}_{\mathrm{G}} \geq 0$, thus, accordingly, this proof is a proof of the Clausius entropy as well.

2.4 Shannon entropy

The concept of entropy in *Information Theory* describes how much information there is in a signal or event. The *Entropy Information Theory* was advanced by the American mathematician, electrical engineer, and cryptographer – Claude Elwood Shannon (1916 – 2001) in his now famous 1948 paper [25, 26] entitled "*A Mathematical Theory of Communication*". The Shannon entropy is a carefully constructed function of a set of probabilities that satisfies a number of constraints. These constraints are chosen such that entropy measures the uncertainty associated with a probability distribution.

An intuitive understanding of information entropy relates to the amount of uncertainty about an event associated with a given probability distribution. As an example, consider a box

containing many coloured balls. If the balls are all of different colours and no colour predominates, then our uncertainty about the colour of a randomly drawn ball is maximal. On the other hand, if the box contains more red balls than any other colour, then there is slightly less uncertainty about the result: the ball drawn from the box has more chances of being red (if we were forced to place a bet, we would bet on a red ball). Telling someone the colour of every new drawn ball provides them with more information in the first case than it does in the second case, because there is more uncertainty about what might happen in the first case than there is in the second. Intuitively, if we know the number of balls remaining, and they are all of one color, then there is no uncertainty about what the next ball drawn will be, and therefore there is no information content from drawing the ball. As a result, the entropy of the "signal" (the sequence of balls drawn, as calculated from the probability distribution) is higher in the first case than in the second.

Shannon, in fact, defined entropy as a measure of the average information content associated with a random outcome. Shannon's definition of information entropy makes this intuitive distinction mathematically precise. His definition satisfies these desiderata:

1. The measure should be continuous – i.e. changing the value of one of the probabilities by a very small amount should only change the entropy by a small amount.
2. If all the outcomes (ball colours in the example above) are equally likely, then entropy should be maximal. In this case, the entropy increases with the number of outcomes.
3. If the outcome is a certainty, then the entropy should be zero.
4. The amount of entropy should be the same independently of how the process is regarded as being divided into parts.

In his paper [25, 26], Shannon makes the claim that the only function satisfying the above requirement will be of the form:

$$\mathcal{S}_s = -k_s \sum_{r=1}^{m} p_r \log_2 p_r \tag{11}$$

where k_s is the Shannon constant. If the Shannon constant were to be set such that: $k_s = k_{\mathrm{B}} \ln 2$, then, the Shannon entropy will equal the Gibbs entropy, i.e.:

$$\mathcal{S}_s \equiv \mathcal{S}_{\mathrm{G}}. \tag{12}$$

Now, having discussed the four different manifestations of entropy, we shall proceed to describe our thermodynamic system.

3 Description of thermodynamic system

Key to our proof here is the clarity in the definition of what we here term the:

1. *Occupational Frequency of a Thermodynamic Microstate (OFTM).*
2. *Thermodynamic Probability (TP).*

As depicted in Table 1, we envisage a thermodynamic system to constitute discrete, finite and countable cells (microstates). These cells can each be numbered 1, 2, 3, ..., $r-1$, r, $r+1$, ..., $m-2$, $m-1$, m and in these cells we are to fit a total of $\mathcal{N}$ particles. The number of particles in each of these cells at a given material time is $n_1, n_2, n_3, \ldots, n_{r-1}, n_r, n_{r+1}, \ldots, \ldots, n_{m-2}, n_{m-1}, n_m$, respectively.

Now, the OFTM, f_r, of each of these microstates is such that:

$$f_r = \frac{n_r}{\mathcal{N}}, \tag{13}$$

where f_r is the total fraction of particles in the r^{th} cell at a given material time. We must note that:

$$\sum_{r=1}^{m} f_r = 1. \tag{14}$$

Now, to define the thermodynamic probability p_r, we need to introduce some new idea. This is the idea of the *potential holding capacity* of a given microstate. That is, take say the r^{th} microstate. This microstate has n_r particles occupying it, whereas the maximum possible number of particles that can occupy this microstate is q_r. What this means is that the microstate is not completely filled, but partially so. The tendency is to fill this microstate rather that empty it. The most probable state is that when this microstate is completely filled and the most unlikely is – likewise, when this microstate is empty.

Under such a setting, it follows that the ratio:

$$p_r = \frac{n_r}{q_r}, \tag{15}$$

must give the probability that the r^{th} microstate is occupied and f_r is simply the fraction of the number of particles occupying this microstate at a given material time relative to the total number of particles making up the entire system. Clearly:

$$0 \leq n_r \leq q_r, \tag{16}$$

hence:

$$0 \leq p_r \leq 1, \tag{17}$$

thus:

$$\left[\sum_{r=1}^{m} 0 \leq \sum_{r=1}^{m} p_r \leq \sum_{r=1}^{m} 1\right] \longrightarrow \left[0 \leq \sum_{r=1}^{m} p_r \leq m\right]. \tag{18}$$

Writing (18) in a more succinct manner, we will have:

$$0 \leq \frac{1}{m}\left(\sum_{r=1}^{m} p_r\right) \leq 1. \tag{19}$$

Now, having defined the occupational frequency of a thermodynamic microstate (f_r) and the thermodynamic probability (p_r), we shall proceed to lay bare the assumption or working hypothesis that will lead us to our desired proof of the SLT.

Table 1: **Arrangement of Particles in the Different Cells**

Parameter	**Cells**											
Cell Number	1	2	3	...	...	$r-1$	r	$r+1$	...	...	$m-2$	$m-1$	m
n_r	n_1	n_2	n_3	...	...	n_{r-1}	n_r	n_{r+1}	...	...	n_{m-2}	n_{m-1}	n_m
f_r	$\frac{n_1}{\mathcal{N}}$	$\frac{n_2}{\mathcal{N}}$	$\frac{n_3}{\mathcal{N}}$	...	...	$\frac{n_{r-1}}{\mathcal{N}}$	$\frac{n_r}{\mathcal{N}}$	$\frac{n_{r+1}}{\mathcal{N}}$	...	...	$\frac{n_{m-2}}{\mathcal{N}}$	$\frac{n_{m-1}}{\mathcal{N}}$	$\frac{n_m}{\mathcal{N}}$
q_r	q_1	q_2	q_3	...	...	q_{r-1}	q_r	q_{r+1}	...	...	q_{m-2}	q_{m-1}	q_m
p_r	$\frac{n_1}{q_1}$	$\frac{n_2}{q_2}$	$\frac{n_3}{q_3}$	...	...	$\frac{n_{j-1}}{q_{j-1}}$	$\frac{n_j}{q_j}$	$\frac{n_{j+1}}{q_{j+1}}$	...	...	$\frac{n_{m-2}}{q_{m-2}}$	$\frac{n_{m-1}}{q_{m-1}}$	$\frac{n_m}{q_m}$

4 Hypothesis (assumption)

We shall put forward our working hypothesis which we shall coin the name – *Thermodynamic Probability Evolution Hypothesis* (*TPE-hypothesis*), and this hypothesis states that:

> Thermodynamic probability changes are always positive, i.e. $\mathrm{d}p_r \geq 0$. That is to say, at time t_i, if the r^{th} state has energy $\epsilon_r(t_i)$, and if this energy state were to change to its next state $\epsilon_r(t_j)$, at a later time t_j $(i > j)$, then the accompanying thermodynamic probability changes $\mathrm{d}p_r$, from the state $\epsilon_r(t_i)$, to the state $\epsilon_r(t_j)$, are always such that: $\mathrm{d}p_r \geq 0$.

Given the above hypothesis (assumption), we shall now proceed to our most simple proof of the SLT from a Boltzmann entropy standpoint. But before that, we shall argue in the next section that a proof that the Boltzmann entropy always increases is sufficient proof that all the other three forms of entropy are bound by the same law, hence, a proof that the Boltzmann entropy always increases is a general proof of the SLT.

5 Boltzmann and Gibbs entropies

Our proof of the SLT to be presented in the next section makes use of the Boltzmann entropy. If we wanted a general proof that entropy always increases, this would mean we must prove the SLT for the four different manifestations of entropy. But, we do not need to do this because the Clausius and Shannon entropies are – one way or the other – equivalent to the Gibbs entropy, the meaning of which is that we would only need to prove for the two cases of the Gibbs and Boltzmann entropy. Again, because the Gibbs and Boltzmann entropy can be linked, it is sufficient to prove only for one of the two cases and in this paper, we prove for the case of the Boltzmann entropy.

To that end – i.e. in order to demonstrate this link between the Gibbs and Boltzmann entropy, we know that in the event that the probability of occurrence of all the $\mathcal{W}$ macrostate, the Gibbs entropy reduces to the Boltzmann entropy. To see this, we know that in this event where all the $\mathcal{W}$ macrostates are equally likely, we will have $P_r = 1/\mathcal{W}$, so that:

$$\mathcal{S}_{\mathrm{G}} = -k_B \sum_{r=1}^{\mathcal{W}} \left(\frac{1}{\mathcal{W}}\right) \ln\left(\frac{1}{\mathcal{W}}\right) = k_{\mathrm{B}} \ln \mathcal{W} = \mathcal{S}_{\mathrm{B}} \,. \tag{20}$$

In all other cases:

$$\mathcal{S}_{\mathrm{B}} < \mathcal{S}_{\mathrm{G}} \,, \tag{21}$$

hence, in general, we have that:

$$[\mathcal{S}_{\mathrm{B}} \leq \mathcal{S}_{\mathrm{G}}] \;\Rightarrow\; [\text{if } (\mathrm{d}\mathcal{S}_{\mathrm{B}} \geq 0), \quad \text{then}, \quad (\mathrm{d}\mathcal{S}_{\mathrm{G}} \geq 0)] \,, \tag{22}$$

hence, a proof that: $\mathrm{d}\mathcal{S}_{\mathrm{B}} \geq 0$, is also a proof that: $\mathrm{d}\mathcal{S}_{\mathrm{G}} \geq 0$. Consequently and according to the foregoing, a proof that: $\mathrm{d}\mathcal{S}_{\mathrm{B}} \geq 0$, is indeed a general proof of the SLT for all the four different manifestations of entropy.

6 Proof

As a starting point, we shall as has been done in (1), assume that the Boltzmann statistical weight function $\mathcal{W}$, of an arbitrary thermodynamic system is a function of the thermodynamic probabilities (p_r). With this assumption safely in place, we note that if we are to have:

$$\mathcal{W} = \mathcal{W}_0 \exp\left(\sum_{r=1}^{m} p_r - \sum_{r=1}^{m} p_r \ln p_r\right) , \tag{23}$$

where $\mathcal{W}_0$ is a constant for the given isolated thermodynamic system in question, then, we can very easily proffer a proof of the SLT on the basis of the TPE-hypothesis, because, from the Boltzmann Eq. (4), it follows from (1) that:

$$\mathcal{S}_{\mathrm{B}} = k_B \ln \mathcal{W}_0 + k_B \sum_{r=1}^{m} p_r - k_B \sum_{r=1}^{m} p_r \ln p_r \,, \tag{24}$$

hence, taking a differential of (24), one obtains that:

$$\mathrm{d}\mathcal{S}_{\mathrm{B}} = -k_B \sum_{r=1}^{m} \mathrm{d}p_r \ln p_r \,. \tag{25}$$

Now, since $0 < p_r \leq 1$, it follows from this – that $\ln p_r \leq 0$, and from the TPE-hypothesis where one is given that $\mathrm{d}p_r > 0$, it further follows that $\mathrm{d}p_r \ln p_r \leq 0$, hence:

$$\sum_{r=1}^{m} \mathrm{d}p_r \ln p_r \leq 0\,,$$

thus, inserting all these conditions into (25), we will have that:

$$\mathrm{d}\mathcal{S}_{\mathrm{B}} \geq 0\,, \tag{26}$$

hence result. Clearly, the SLT follows directly from a simple definition of W in terms of the thermodynamic probabilities of all the different microstates and as well as from the TPE-hypothesis.

7 General discussion

On the basis of the seemingly self-evident and reasonable *Thermodynamic Probability Evolution Hypothesis* here put forward, we have just "proved" (demonstrated) the SLT. If anything, the "proof" appears to us (and perhaps to the reader as well), to not only be very simple, but quite straight forward. Be that as it may – given the amount of effort that has gone into seeking a proof of the SLT, one can not help but wonder if this proof is really correct – are we not missing something here? How does it come about that such a very simple pedestrian proof has escaped the reach of those that have vigorously sought it? We do not know! All we can say is that, what we have before our eyes appears very strongly to be not only a veritable proof but a perdurable proof as well. We leave it up to the esteemed reader to be the judge on the validity or lack thereof the proof.

In addition, we do not know whether to call this a proof or a demonstration. The reason for this self-doubt is that, for a proof, the basis on which it stands must be firm – yet, in what we have presented, the basis is a mere hypothesis which we only evoked after we noted after a meticulous examination that if one were to express $\mathcal{S}_{\mathrm{B}}$, as function of p_r, i.e. $\mathcal{S}_{\mathrm{B}} = \mathcal{S}_{\mathrm{B}}(p_1, p_2, \ldots, p_r, \ldots p_m)$; the experimental result, $d\mathcal{S}_{\mathrm{B}} \geq 0$ can be deduced from a number-theoretic viewpoint provided that $dp_r > 0$. Realising this, we evoked this as our working hypothesis wherefrom the proof flowed smoothly. In this way, it would not appear – but strongly so that, what we have is a reverse engineered proof. In this way, it, ultimately, would mean that the SLT directly implies the TPE-hypothesis. Even if this were the case, it is still a great leap forward in our understanding of the SLT as this would mean the source of this law is the manner in which the thermodynamic probabilities evolve from one value-state to the next.

That is to say, the SLT holds because the dynamic thermodynamic probabilities $p_r(t)$, of the different microstates only change to attain at least higher values than their previous, that is, the given energy state only evolves (i.e. changes its state) to allow at least a greater thermodynamic probability. Thus, whether one decides that this is not a genuine proof because it has worked backwards from a experimental result ($\mathrm{d}\mathcal{S} \geq 0$) in which process the TPE-hypothesis is implied, one thing is pristine clear:

> It must be acknowledged that at the very least, the present demonstration (proof) has surely peered deeper into the nature of the SLT to unearth the TPE-hypothesis as a driver of this fundamental, paramount and sacrosanct law of Nature.

Hence, this paper may very well be a great – if not a giant leap forward, in humankind's endeavour to understand the mysterious and arcane foundations of the Second Law of Thermodynamics.

Entropy is (and has always been) one of those physics concepts that are difficult to define, let alone understand. Through his entropy function [Eq. (4)], Boltzmann defined it as a measure of the multiplicity of a thermodynamic system. Of the three definitions i.e. Boltzmann, Gibbs and Clausius entropy), the Clausius energy has been and is – the most difficult to define and understand. According to what we have presented herein, one can safely define entropy as:

> a measure of the probability of evolution of a thermodynamic system.

With entropy having been given this definition, it becomes much easier to understand the SLT as a simple statement about the dynamical evolution of the thermodynamic probability of the system.

Received on October 13, 2019

References

1. Eddington A. S. The Nature of the Physical World. Cambridge University Press, Cambridge and Bentley House, London Agents for Canada and India: Macmillan, 1^{st} edition, 1928.
2. Boltzmann L. E. Weitere Studien über das Wörmegleichgewicht unter Gasmolekülen. *Sitzungsberichte Akad. Wiss. (Vienna)*, 1872, v. 66 (Part II), 275–370.
3. Zermelo E. Ueber einen Satz der Dynamik und die mechanische Wärmetheorie. *Ann. der Phys.*, 1896, v. 293 (3), 485–494.
4. Loschmidt J. *Sitzungsber. Kais. Akad. Wiss. Wien, Math. Naturwiss. Classe*, 1876, v. 73, 128–142.
5. Clausius R. J. E. Ueber die bewegende Kraft der Wärme und die Gesetze, welche sich daraus für die Wärmelehre selbst ableiten lassen. *Ann. der Phys.*, 1850, v. 155 (4), 500–524.
6. Clausius R. J. E. Ueber verschiedene für die Anwendung bequeme Formen der Hauptgleichungen der mechanischen Wärmetheorie. *Ann. der Phys.*, 1865, v. 201 (7), 353–400.
7. Clausius R. J. E. On a Mechanical Theorem Applicable to Heat. *Phil. Mag. Ser. 4*, 1870, v. 40, 122–127.
8. Clausius R. J. E. Ueber eine veränderte Form des zweiten Hauptsatzes der mechanischen Wärmetheorie. *Ann. der Phys.*, 1854, v. 169 (12), 481–506.
9. Clausius R. J. E. On a Mechanical Theorem Applicable to Heat. *Phil. Mag. Ser. 4*, 1856, v. 12 (77), 81–98, .

10. Boltzmann L. E. Uber die Eigenschaften Monocyklischer und Anderer Damit Verwandter Systeme. *Crelles Journal*, 1874, v. 98, 68–94. (Also in Boltzmann L. *Wissenschaftliche Abhandlungen*, 1909, v. 3, 122–152; Hasenöhrl F. (Ed.). Leipzig. Reissued New York: Chelsea, 1969).
11. Kragh H. Max Planck: The Reluctant Revolutionary. *Physics World*, 2000, v. 13 (12), 31–36.
12. Planck M. K. E. L. Ueber das Gesetz der Energieverteilung im Normal Spectrum. *Ann. der Phys.*, 1901, v. 309 (3), 553–563.
13. Planck M. K. E. L. Entropie und Temperatur Strahlender Wärme. *Ann. der Phys.*, , 1900, v. 306 (4), 719–737.
14. Planck M. K. E. L. Ueber Irreversible Strahlungsvorgänge. *Ann. der Phys.*, 1900, v. 306 (1), 69–122.
15. Bose S. N. Plancks Gesetz und Lichtquantenhypothese. *Zeitschrift für Physik*, 1924, v. 26 (1), 178–181.
16. Miller S. Strung Together: The Cultural Currency of String Theory as a Scientific Imaginary. Univ. of Michigan Press, 2013.
17. Farmelo G. The Strangest Man: The Hidden Life of Paul Dirac, Quantum Genius. Faber & Faber, 2009.
18. Fermi E. On the Quantization of the Monoatomic Ideal Gas. *Rend. Lince*, 1926, v. 3, 145.
19. Fermi E. Zur Quantelung des Idealen Einatomigen Gases. *Zeitschrift für Physik*, 1926, v. 36 (11), 902–912.
20. Dirac P. A. M. On the Theory of Quantum Mechanics. *Proceedings of the Royal Society of London A: Mathematical, Physical and Engineering Sciences*, 1926, v. 112 (762), 661–677.
21. Riek R. A Derivation of a Microscopic Entropy and Time Irreversibility From the Discreteness of Time. *Entropy*, 2014, v. 16 (6), 3149–3172.
22. Lavis D. A. Boltzmann, Gibbs, and the Concept of Equilibrium. *Phil. Sci.*, 2008, v. 75 (5), 682–696.
23. Bishop R. C. Nonequilibrium statistical mechanics brussels–austin style. *Studies in History and Philosophy of Science Part B: Studies in History and Philosophy of Modern Physics*, 2004, v. 35 (1), 1–30.
24. Jaynes E. T. Gibbs vs Boltzmann entropies. *Am. J. Phys.*, 1965, v. 33 (5), 391–398.
25. Shannon C. E. A Mathematical Theory of Communication. *The Bell System Technical Journal*, 1948, v. 27 (3), 379–423.
26. Shannon C. E. A Mathematical Theory of Communication. *The Bell System Technical Journal*, 1948, v. 27 (4), 623–656.

Liouville's Theorem as a Subtle Statement of the First Law of Thermodynamics

G. G. Nyambuya

National University of Science and Technology, Faculty of Applied Sciences – Department of Applied Physics, Fundamental Theoretical and Astrophysics Group, P. O. Box 939, Ascot, Bulawayo, Republic of Zimbabwe.
E-mail: physicist.ggn@gmail.com

Just like the rest of the Laws of Thermodynamics, the First Law of Thermodynamics (FLT) is an empirical law firmly anchored on the unshakeable fertile soils of verifiable experimental philosophy. Be that as it may, this law (FLT) does not have a fundamental theoretical basis on which it is founded or rests upon. In the present paper, we demonstrate that Liouville's Theorem (in physics) can be cast or can be seen as an expression of the FLT. In this way, one can thus envisage Liouville's Theorem as a fundamental theoretical basis for the FLT.

A theory is the more impressive the greater the simplicity of its premises [are], the more different kinds of things it relates, and the more extended is its area of applicability ... Classical Thermodynamics ... is the only physical theory of universal content concerning which I am convinced that within the framework of the applicability of its basic concepts, it will never be overthrown ... Albert Einstein (1879-1955). Adapted from [1, p. 227].

1 Introduction

The *First Law of Thermodynamics* (FLT) is a version of the *General Empirical Law of Conservation of Energy* (GELCE) applicable to thermodynamic systems. The GELCE states that the total energy of an isolated system is a constant of time; energy can only be transformed from one form to another, but can never be created nor destroyed. The FLT is often stated as follows:

$$đQ = đU + đW\,, \tag{1}$$

where $đQ$, $đU$ and $đW$ are the change in the heat content of a thermodynamic system that accompanies a change in the internal energy $đU$ of the system, for an amount of work $đW$ performed on the system. Simple stated: the heat content of a thermodynamic system $đQ$, equals the change in the internal energy $đU$, plus the amount of work $đW$ done by the system on its surroundings. The FLT is an empirical law founded and strongly anchored on the fertile soils of experimental philosophy. There is no theoretical furnishment of this law. This paper makes an endeavour to proffer a theoretical justification of this law on the basis of Liouville's theorem [2], i.e. we demonstrate that Liouville's theorem can be viewed or can be seen as a statement of the FLT.

2 Liouville's theorem

In physics, Liouville's theorem [2], named after the great French mathematician Joseph Liouville (1809-1882), is a key theorem in classical statistical thermodynamics and in Hamiltonian mechanics*. The theorem asserts that the probability density function ϱ, is a time-constant along the trajectories describing the system – in other words, the *density of states* in an ensemble of many identical states with different initial conditions is constant along every trajectory in phase space. This time-independent density of states is in statistical mechanics known as the classical "*a priori probability*" where an "a priori probability" is a probability that is derived purely from deductive reasoning.

The probability density function (or phase space distribution function) ϱ is assumed to depend on position ($\vec{r} = \vec{r}(t)$) and momentum ($\vec{p} = \vec{p}(t)$), i.e. $\varrho = \varrho(\vec{r}, \vec{p})$, and this probability density function is constant along the trajectories of the system – i.e. the density of states of the *system points* in the vicinity of a given system point traversing through phase space remains constant through the passage of time. Liouville's theorem succinctly summarizes this through the equation:

$$\frac{d\varrho}{dt} = \frac{\partial\varrho}{\partial t} + \sum_{j=1}^{N} \dot{\vec{r}}_j \cdot \frac{\partial\varrho}{\partial\vec{r}_j} + \sum_{j=1}^{N} \dot{\vec{p}}_j \cdot \frac{\partial\varrho}{\partial\vec{p}_j} = 0\,. \tag{2}$$

Writing $\dot{\vec{r}}_j = \vec{v}_j$ and $\dot{\vec{p}}_j = \vec{F}_j$, the above can be written as:

$$\underbrace{-\frac{\partial\varrho}{\partial t}}_{\textbf{Term (I)}} = \underbrace{\sum_{j=1}^{N} \vec{v}_j \cdot \frac{\partial\varrho}{\partial\vec{r}_j}}_{\textbf{Term (II)}} + \underbrace{\sum_{j=1}^{N} \vec{F}_j \cdot \frac{\partial\varrho}{\partial\vec{p}_j}}_{\textbf{Term (III)}}\,, \tag{3}$$

where $\vec{v}_j$ and $\vec{F}_j$, are the velocity and resultant force acting on the j^{th} particle respectively. The task of the present paper is to identify Terms (I), (II) and (III) of (3) with $đQ$, $đU$ and $đW$, appearing in (1), respectively. In order for us to achieve this, it will require us to justly define – in an explicit manner – the

*There is also in complex analysis, Liouville's theorem, named after the same Joseph Liouville, and this theorem states that every bounded *entire function* (i.e., *integral function*) must be constant.

probability density function ϱ, thereby resulting in Liouville's theorem being nothing more (albeit – very insightful) than a statement of the FLT. Before we can do this, we need to set up in the next section, a theory that can explain or describe the evolution of thermodynamic fluctuations.

3 Theory of thermodynamic fluctuations

In our theory of thermodynamic fluctuations, we begin in Section 3.1 by defining what these fluctuations really are and having done that, we proceed in Section 3.2 to define the phase space on which the evolution of these thermodynamic fluctuations is defined.

3.1 Definition of thermodynamic fluctuations

That fluctuations are an intrinsic and inherent part and parcel of physical and natural reality is – indeed – common knowledge. Every observable (say, O) is – one way or the other – associated with some kind of random fluctuation (here-and-after denoted, δO). These fluctuations that we are talking about are different from the fluctuations in the measurement induced by random statistical human error. These are fluctuations that will manifest even when the impossible feat of reducing the intrinsic and inherent random statistical human error to zero.

In deeper terms, these fluctuations are no ordinary fluctuations encountered in statistics, but are intrinsic and inherent *Statistical Random Thermodynamic Fluctuations* (SRTF), they can not be eliminated even in the most idea of situations. These thermodynamic fluctuations are the quantum mechanical fluctuations that Niels Henrik David Bohr (1885-1962) and his followers in Copenhagen, Denmark envisaged (or dreamt of) in their historic, spirited and concerted effort to finding a meaningful, perdurable and lasting interpretation of Schrödinger's seemingly arcane quantum mechanical wavefunction Ψ.

About these thermodynamic fluctuations, we must hasten and categorically state that while there exists theories that attempt to explain the evolution of thermodynamic systems (in Γ-space), there does not exist similar attempts to describe the evolution of these SRTFs though some structured space as phase space. The present section makes an endeavour at such a feat.

3.2 Definition of the $\delta\Gamma$-space

Now, we shall promulgate three postulates that form the basis of our theory of thermodynamic fluctuations. In the first postulate, we shall set up an arena where these fluctuations are defined. In the second postulate, we shall propose a governing equation that describes the evolution of these fluctuations on the space on which they are defined, and lastly, in the third postulate, we set up some rules that define how changes in these fluctuations relate to changes in their corresponding canonical variables.

1. **Postulate (I):** Just as there exists the six-dimensional Γ-space ($\Gamma = \Gamma(x, y, z; p_x, p_y, p_z)$) on which the trajectory of a thermodynamic system can be traced via their evolution through this space as dictated to and governed by Liouville's theorem, there exists a corresponding six-dimensional space (which for our purposes, we shall call $\delta\Gamma$-space) on which the trajectory of the statistical random thermodynamic fluctuations $(\delta x, \delta y, \delta z; \delta p_x, \delta p_y, \delta p_z)$ can be traced.
2. **Postulate (II):** The dynamic and spatial evolution of these random statistical thermodynamic fluctuations $(\delta x, \delta y, \delta z; \delta p_x, \delta p_y, \delta p_z)$ on $\delta\Gamma$-space is governed by Liouville's equation $d(\delta\varrho)/d(\delta t) = 0$, i.e.:
$$\frac{\partial(\delta\varrho)}{\partial(\delta t)} + \sum_{j=1}^{N} \delta\vec{v}_j \cdot \frac{\partial(\delta\varrho)}{\partial\left(\delta\vec{r}_j\right)} + \sum_{j=1}^{N} \delta\dot{\vec{p}}_j \cdot \frac{\partial(\delta\varrho)}{\partial\left(\delta\vec{p}_j\right)} = 0 . \qquad (4)$$
3. **Postulate (III):** The partial differential elements of the canonical four-position $(\partial x, \partial y, \partial z, \partial t)$ and that of the canonical four-momentum $(\partial p_x, \partial p_y, \partial p_z, \partial E)$ are equal to the corresponding partial differential elements of the statistical random thermodynamic fluctuations $(\partial(\delta x), \partial(\delta y), \partial(\delta z), \partial(\delta t))$ for the four-position and $(\partial(\delta p_x), \partial\left(\delta p_y\right), \partial(\delta p_z), \partial(\delta E))$ for the four-momentum – i.e. written explicitly:
$$\begin{aligned} \partial t &= \partial(\delta t) \\ \partial x &= \partial(\delta x) \\ \partial y &= \partial(\delta y) \\ \partial z &= \partial(\delta z) \\ \partial E &= \partial(\delta E) \\ \partial p_x &= \partial(\delta p_x) \\ \partial p_y &= \partial\left(\delta p_y\right) \\ \partial p_z &= \partial(\delta p_z) . \end{aligned} \qquad (5)$$

With these three postulates (rules), we will go on to show that the Liouville Eq. (4) yields the FLT.

4 Derivation – First Law of Thermodynamics

With the theory governing the SRTFs having been set up in the previous section, we realise that if we are to set $\delta\varrho$ so that it is defined:
$$\delta\varrho = \exp\left(\frac{\delta\mathcal{S}_{\mathrm{TD}}}{\hbar}\right) , \qquad (6)$$
where $\hbar$ is Planck's normalized constant and:
$$\delta\mathcal{S}_{\mathrm{TD}} = \sum_{j=1}^{N} \left(\delta\vec{p}_j \cdot \delta\vec{r}_j - \delta E_j\, \delta t_j\right) , \qquad (7)$$
is the thermodynamic phase (or thermodynamic action) defined on $\delta\Gamma$-space, then one can very easily demonstrate that Liouville's theorem as defined in (4), is actually a subtle statement of the FLT. This thermodynamic phase has been defined along the lines of the space of a particle in the Hamilton–Jacobi theory (e.g. [3, pp. 490-491]) of particles where the energy E and momentum $\vec{p}$ of a partial are related to the particle's phase S (or action) via the equation $E = -\partial S/\partial t$ and $\vec{p} = \vec{\nabla} S$. These Hamilton–Jacobi definitions of E and $\vec{p}$

are the defining equations in the de Broglie-Bohm Pilot Wave Theory [4–7] of Quantum Mechanics (QM).

Now, with the idea in mind that $\delta\mathcal{S}_{\mathrm{TD}}$ is the thermodynamic phase (action) similar to a particle's phase (action) in the Hamilton–Jacobi theory, it is clear from the explicit definition of $\delta\mathcal{S}_{\mathrm{TD}}$ given in (7), that:

$$-\frac{\partial\left(\delta\varrho\right)}{\partial\left(\delta t\right)}=\sum_{j=1}^{N}\delta E_j=\delta E\,, \tag{8}$$

$$\frac{\partial\left(\delta\varrho\right)}{\partial\left(\delta\vec{r}_j\right)}=\delta\vec{p}_j\,, \tag{9}$$

$$\frac{\partial\left(\delta\varrho\right)}{\partial\left(\delta\vec{p}_j\right)}=\delta\vec{r}_j\,. \tag{10}$$

From these equations – i.e. (8), (9) and (10), it follows that*:

$$\sum_{j=1}^{N}\delta\vec{v}_j\cdot\frac{\partial\varrho}{\partial(\delta\vec{r}_j)}=\sum_{j=1}^{N}\vec{v}_j\cdot\frac{\partial\varrho}{\partial(\delta\vec{r}_j)}=\sum_{j=1}^{N}\vec{v}_j\cdot\delta\vec{p}_j\,. \tag{11}$$

At this point before we can proceed, we must ask the question: *What does the term $\vec{v}_j\cdot\delta\vec{p}_j$ represent?* For a clue, let us consider the classical expression for the kinetic energy of particle $K_j=p_j^2/2m$. Clearly $dK_j=p\,dp/m=v_j\,dp_j=\vec{v}_j\cdot d\vec{p}_j$. Therefore, the expression $\vec{v}_j\cdot\delta\vec{p}_j$ represents that thermodynamic induced fluctuations in the kinetic energy of the j^{th} particle constituting the thermodynamic system under consideration. These thermodynamic induced fluctuations in the kinetic energy $\vec{v}_j\cdot\delta\vec{p}_j$ constitute what we normally call or refer to as the internal energy δU of a thermodynamic system, hence:

$$\delta U=\sum_{j=1}^{N}\delta\vec{v}_j\cdot\frac{\partial\varrho}{\partial\vec{r}_j}=\sum_{j=1}^{N}\delta U_j\,. \tag{12}$$

Further, we have:

$$\sum_{j=1}^{N}\delta\vec{F}_j\cdot\frac{\partial\varrho}{\partial(\delta\vec{p}_j)}=\sum_{j=1}^{N}\delta\vec{F}_j\cdot\delta\vec{r}_j=\sum_{j=1}^{N}\vec{F}_j\cdot\delta\vec{r}_j\,. \tag{13}$$

Clearly, the expression† $\vec{F}_j\cdot\delta\vec{r}_j$, needs no explanation as it represents the work δW_j done on the j^{th} particle by the random thermodynamic fluctuations of position and forces, i.e.:

$$\delta W=\sum_{j=1}^{N}\delta\vec{F}_j\cdot\frac{\partial\varrho}{\partial\vec{p}_j}=\sum_{j=1}^{N}\delta W_j\,. \tag{14}$$

From all this, it follows that:

$$\delta E=\delta U+\delta W\,. \tag{15}$$

*The "δ" in $\delta\vec{v}_j$ in (11) is removed via the definitions given in (5).

†The "δ" in $\delta\vec{F}_j$ is removed via the definitions given in (5).

What (15) is telling us that while the fluctuations are random, they are correlated.

Now, for a system that moves from an initial state (i) to a final state (f), where the changes in the thermodynamic fluctuations ($\delta E,\delta U,\delta W$) are to be defined:

$$\begin{aligned}đQ &= \delta E_f - \delta E_i\\ đU &= \delta U_f - \delta U_i\\ đW &= \delta W_f - \delta W_i\,,\end{aligned} \tag{16}$$

where $đQ$, $đU$ and $đW$, are to have the same meaning as they have in (1), it follows from this that we will have the FLT, the meaning of which is that Liouville's theorem (4) is, in this way, a subtle expression of the FLT.

5 Discussion

As far as we can tell, the FLT is taken as an inviolable experimental fact. There has not been – at least in our survey of the literature, a similar attempt as that presented here where a fundamental theoretical basis is made to furnish the foundations of this law, hence, this work is without precedent insofar as its nature and goal is concerned. We believe the attempt presented herein is important for our deeper insight and understanding of the *Science of Thermodynamics*. The follow-up work (briefly discussed in Section 7) that we will present soon will attest to this.

For example, one may ask: *What drives thermodynamics, it is the direct changes in the canonical values of the internal energy U and the work W, or there – perhaps – is something else different from this?* If what we have presented is to be believed, then the answer is that thermodynamics is driven by the changes in the associated SRTFs in the canonical values of the internal energy U and the work W, that is to say, by $đ(\delta U)=\delta U_f-\delta U_i$ and $đ(\delta W)=\delta W_f-\delta W_i$. In a nutshell, it is the SRTFs that drive thermodynamics, and not the changes dU and dW.

6 Conclusion

Assuming the acceeptability of what has herein been presented, we hereby set the following as our conclusion:

1. From a fundamental theoretical standpoint, the First Law of Thermodynamics may very well be an expression to the effect that the Thermodynamic Evolution Probability Density Function $\delta\varrho$ is – in accordance with Liouville's theorem – an explicit time-constant along the phase-space trajectory for any thermodynamic system.
2. Liouville's Theorem can be viewed as (or may very well be) an expression of the First Law of Thermodynamics.

7 Follow-up work

In order for the effectiveness in its mission to deliver the core message it seeks to deliver, it is always prudent to keep a paper focused on the point on which it seeks to deliver – of which, the present has been to demonstrate that Liouville's

theorem can be shown to be a casting of the FLT. As always happens, there will always be follow-ups. At present, we have three immediate follow-up papers that we hope will be published in the present journal. These follow-up papers give further credence to the ideas that we have herein crafted and used to demonstrate that Liouville's theorem can be envisaged as a casting of the FLT.

1. In the first follow-up paper, we demonstrate that if $\delta\varrho$ is assumed to be a thermodynamic probability measure, then one can derive – with relative ease – Heisenberg (1927)'s quantum mechanical uncertainty principle [8].
2. In the second paper, which is a follow-up on our recent work presented in [9] on "A Simple Proof of the Second Law of Thermodynamics (SLT)", we demonstrate that – if $\delta\varrho$ is assumed to be the thermodynamic probability that derives entropy changes in thermodynamic systems, then for a Universe with a unidirectional forward arrow of time, the SLT directs that energy and time fluctuations $(\delta E, \delta t)$ are what derives thermodynamics.
3. Lastly, in the third paper, within the framework of the de Broglie-Bohm Pilot Wave Theory [4–7] of QM, commonly referred to as *Bohmian Mechanics* (BM), we set the square-root of the Schrödinger [10–12] quantum mechanical probability amplitude $\Psi^*\Psi = |\Psi|^2$ so that it equals $\delta\varrho$, i.e. $\delta\varrho = |\Psi|$, in which event, we demonstrate that all the criticism that has been levelled against BM – since its inception in 1952 – can easily be overcome. The importance of this is that it allows for a realistic interpretation of QM. This is good for the philosophy of QM.

We believe that all the above mentioned future works give *seminality* to the ideas here set forth.

Received on October 19, 2019

References

1. Holton G. and Elkana Y. Albert Einstein, Historical and Cultural Perspectives. Princeton University Press, Princeton, NJ, 2016. (ISBN 978-0-691-64026-6).
2. Liouville J. Sur la Théorie de la Variation des Constantes Arbitraires. *Journ. de Math.*, 1838, v. 3, 342–349.
3. Goldstein H. Classical Mechanics, 2nd edition. Addison-Wesley, Reading, MA, 1980. (ISBN: 978-0-201-02918-5).
4. de Broglie L. XXXV. A Tentative Theory of Light Quanta. *The London, Edinburgh, and Dublin Philosophical Magazine and Journal of Science*, 1924, v. 47 (278), 446–458.
5. Bohm D. J. A Suggested Interpretation of the Quantum Theory in Terms of "Hidden" Variables. I. *Phys. Rev.*, 1952, v. 85, 166–179.
6. Bohm D. J. A Suggested Interpretation of the Quantum Theory in Terms of "Hidden" Variables. II. *Phys. Rev.*, 1952, v. 85, 180–193.
7. Bohm D. J. Proof That Probability Density Approaches $|\psi|^2$ in Causal Interpretation of the Quantum Theory. *Phys. Rev.*, 1953, v. 89, 458–466.
8. Heisenberg W. K. Ueber den anschaulichen Inhalt der Quantentheoretischen Kinematik and Mechanik. *Zeitschrift für Physik*, 1927, v. 43 (3), 172–198. English Translation: Wheeler J. A. and Zurek W. H, eds. Quantum Theory and Measurement. Princeton University Press, Princeton, NJ, 1983, pp. 62–84.
9. Nyambuya G. G. A Simple Proof of the Second Law of Thermodynamics. *Progress in Physics*, 2019, v. 15 (3), 171–177.
10. Schrödinger E. An Undulatory Theory of the Mechanics of Atoms and Molecules. *Phys. Rev.*, 1926, v. 28, 1049–1070.
11. Schrödinger E. Quantisierung als Eigenwertproblem. *Annalen der Physik*, 1926, v. 384 (4), 361–376.
12. Schrödinger E. Quantisierung als Eigenwertproblem. *Annalen der Physik*, 1926, v. 385 (13), 437–490.

Resolution of the Smarandache Quantum Paradoxes

Robert Neil Boyd

Consulting physicist for Princeton Biotechnology Corporation, Dept. Information Physics Research, USA
E-mail: rnboydphd@comcast.net

In this paper we study the four Quantum Smarandache Paradoxes and try to explain and solve them.

1 Introduction

The **Quantum Smarandache Paradoxes** [1, 2, 3, 4, 5, 6] are enounced as follows:

- 1) Sorites Paradox (associated with Eubulides of Miletus (fourth century B.C.): Our visible world is composed of a totality of invisible particles.
- a) An invisible particle does not form a visible object, nor do two invisible particles, three invisible particles, etc. However, at some point, the collection of invisible particles becomes large enough to form a visible object, but there is apparently no definite point where this occurs.
- b) A similar paradox is developed in an opposite direction. It is always possible to remove a particle from an object in such a way that what is left is still a visible object. However, repeating and repeating this process, at some point, the visible object is decomposed so that the left part becomes invisible, but there is no definite point where this occurs. Generally, between <A> and <Non-A> there is no clear distinction, no exact frontier. Where does <A> really end and <Non-A> begin? One extends Zadeh's "fuzzy set" term to the "neutrosophic set" concept.
- 2) Uncertainty Paradox: Large matter, which is under the 'determinist principle', is formed by a totality of elementary particles, which are under Heisenberg's 'indeterminacy principle'.
- 3) Unstable Paradox: Stable matter is formed by unstable elementary particles.
- 4) Short Time Living Paradox: Long time living matter is formed by very short time living elementary particles.

2 Resolution of Smarandache Quantum Paradoxes

[R. N. Boyd]: I think some of the paradoxes may be resolved by a view that matter is infinitely subdivisible. See below:

[Paradox 1a]:
Sorites Paradox (associated with Eubulides of Miletus (fourth century B.C.): Our visible world is composed of a totality of invisible particles.
a) An invisible particle does not form a visible object, nor do two invisible particles, three invisible particles, etc. However, at some point, the collection of invisible particles becomes large enough to form a visible object, but there is apparently no definite point where this occurs.

[R. N. Boyd]: The statement was true in the 4th century BC, but it is not true now. We can now measure the masses of a vast array of elemental particles. And we now know that there are such ratios as "moles" in chemistry telling us how many atoms are involved in the situation. So today we can make such determinations. There are fabrication processes in the manufacture of integrated circuits that are capable of actually arranging very precisely, each atom in the fabrication. One example of these techniques is the use of epitaxal deposition, which is a one atom thick deposition of material. Screening and masking techniques allow atom-by-atom structuring to occur. These circuits can be small enough so that Cooper pairing is impossible and quantum phase-slips occur in the energized circuit. However, the problem has now shifted into the domains which are smaller than our present ability to perceive with our instrumentations. Typically colliders are used to attempt to make measurements of the elemental particles, and recent data seems to be pointing strongly to a realm of particles even smaller than quarks, which may indeed comprise quarks, if such creatures exist in the first place. (What we are calling quarks may be something else entirely, perhaps organizations of yet smaller particles.) I hold that there is a vast array of entities smaller than the Planck length, and have developed methods for imaging such entities.

I designed 6 methods for imaging SubQuantum particles (smaller than the Planck length). Valentini of Italy wrote a paper describing yet another way to accomplish SQ imaging. The easiest and cheapest to make SQ microscope of my design was publicized, and then tested for proof of principle by Dr. Bernd Binder of Germany. After a 2 years long effort, he verified proof of the principle of operation. The year after that, the design verified by Binder, was constructed at a university in Serbia. One of the Serbian professors sent me an email to inform me that the SQ microscope of my design has imaged entities as small as $10{\times}10^{-95}$ cm. The infinitely small is an unattainable goal in terms of technological approaches, but we know the infinitely small is there, by inferences.

It turns out, based on Kolmogorov's 5/3 law developed from studies of turbulence, that the smallest vortex resulting

from turbulence is an entity which lives at $10{\times}10^{-58}$ m, which we call a Kolmogorov Vortex. This is the smallest particle that is still influenced by gravitation. Entities smaller than this are the primary cause of gravitation.

Further on, there is a quantum coherence factor involved in palpable matter which has the quantum field communicating with all the parts of the automobile, for example, with further quantum communication occurring internal to the parts which make up the automobile. What we really need to be studying here is the coherence of objects, in the quantum field sense. What is the lower limit of quantum coherence? Is there a lower limit?

[Paradox 1b]:
b) A similar paradox is developed in an opposite direction. It is always possible to remove a particle from an object in such a way that what is left is still a visible object. However, repeating and repeating this process, at some point, the visible object is decomposed so that the left part becomes invisible, but there is no definite point where this occurs.

[R. N. Boyd]: There is, these days. But there may be a lower limit, which can be studied by quantum coherence of objects.

[Paradox 1b (continued)]:
Generally, between and there is no clear distinction, no exact frontier. Where does really end and begin? One extends Zadeh's "fuzzy set" term to the "neutrosophic set" concept.

[R. N. Boyd]: The boundary conditions are always very interesting. Those conditions which are both A and NOT A, yet neither A nor NOT A. Korzibski referred to these conditions as "NULL A". I call them boundary layers. They are a study in themselves, because boundary layers comprise a third state, and arise often.

[Paradox 2]:
2) Uncertainty Paradox: Large matter, which is under the 'determinist principle', is formed by a totality of elementary particles, which are under Heisenberg's 'indeterminacy principle'.

[R. N. Boyd]: Uncertainty does not apply to monochromatic coherent photons, nor indeed to any photonic system, by logical extension. See:
http://worlds-within-worlds.org/refutationofheisenberg.php

Indeterminacy only applies where there are elements of chance involved, most particularly involving systems of particles, which are quite susceptible to Zitterbewegung, while photons remain largely unaffected by it.

Hans Dehmelt of Germany was awarded the Nobel Prize in physics for keeping an electron pinned to one spot, so that its momentum and location could be known at the same time, for up to 3 months. Heisenburg uncertainty failed in those circumstances. This experiment is considered by many as evidence that the uncertainty principle fails, except under very limited circumstances.

It is easier to deal with this paradox when we consider that the uncertainty principle has failed, under many circumstance. A deterministic version of QM was developed based on experiential information factors, which imply an Intelligent Universe.

[Paradox 3]:
3) Unstable Paradox: Stable matter is formed by unstable elementary particles.

[R. N. Boyd]: The life time of the proton is calculated (not observed with instrumentation) to be on the order of $10{\times}10^{32}$ years. But this ignores plasma/aether factors, and more importantly, gamma ray dissociations of atoms, which cause protons to vanish back into the aether from whence they originated. Gamma ray dissociation of atoms also causes SQ particles (vortex lines, Bhutatmas) propagating with an infinite velocity, which are the cause of gravitation and are the cause of the development of new electrons, positrons, protons, neutrons, and atoms due to aether/plasma events on the surfaces of stars. Instrumented measurements have discovered that every atomic element is found streaming out from the sun in the "solar wind". SAFIRE has instrumented physical evidence that hydrogen and many other elements are created in plasma double layers (charge separation layers) verified by SEM (scanning electron microscopy) and optical correlation spectroscopy. The creation and dis-creation of elementary particles and atoms is a continuous cycle which occurs at all times in the infinite volume universe. The life span of a proton is much smaller than the calculated standard. The actual life span of the proton is determined by the number of gamma ray dissociation events passing through the given volume, per unit time. [Gustave Le Bon "Evolution of Matter" 1906]

[Paradox 4]:
4) Short Time Living Paradox: Long time living matter is formed by very short time living elementary particles. Consciousness and Experiencing informations are involved in all these processes. This information is the organization force which is responsible for many phenomena. The universe is constructed from Space, Time, matter, energy, and Experiencing. Consciousness is not limited to human beings. In fact, it has been demonstrated that all observables have some manner of consciousness, however rudimentary. Consciousness is a holographic energetic having soliton-like [coherent] properties. The best descriptions of the energetics of Consciousness arise from the works of V. Poponin (DNA Phantom Effect) and from a recent paper which shows that the radiation pattern of a symplectic E/M antenna is directly altered by the attention, intention, and emotional condition of the operators

of the transmission facility. This direct influence of the symplectic E/M also causes a divergence in the quantum field, and thus we have evidence that there is a direct relation between the quantum field and Consciousness. Let us never forget that there is a vast array of types of Consciousness, all of which will have some effect on the quantum field.

Also see the works of Andrej Detela. For example: http://www.zynet.co.uk/imprint/Tucson/4.htm#Physical.

Eventually holographic Artificial Intelligence such as HNeT (a variety of quantum computer), combined with Sub-Quantum Physics and Consciousness Physics will be able to map non-physical and dis-incarnate entities, as well as all the energetics of the commonly known life-forms. Eventually, communications will be established through this approach, with non-biological forms of Consciousness, such as rocks and stars.

Submitted on October 5, 2019

References

1. Editors, Quantum Smarandache Paradoxes, *Nature*, 2001, v. 413, no. 6854.
2. Smarandache F. Invisible Paradox, in "Neutrosophy. I Neutrosophic Probability, Set, and Logic", ProQuest & Information, Ann Arbor, MI, USA, 22–23, (1998).
3. Smarandache F. Sorites Paradoxes, in "Definitions, Solved and Unsolved Problems, Conjectures, and Theorems in Number Theory and Geometry", Xiquan Publ. House, Phoenix, 69-70, 2000.
4. Smarandache F. Quantum Quasi-Paradoxes and Quantum Sorites Paradoxes. *Progress in Physics*, 2005, v. 1, 7–8.
5. Smarandache F. Quantum Quasi-Paradoxes and Quantum Sorites Paradoxes. *Octogon*, 2005, v. 13, no. 1A, 232–235.
6. Smarandache F. Quantum Quasi-Paradoxes and Quantum Sorites Paradoxes [revisited]. *Infinite Energy*, 2006, v. 11, no. 66, 40–41.
7. Boyd R.N. Resolution of Smarandache Paradoxes, http://worlds-within-worlds.org/resolutionofsmarandache.php
8. Weisstein E.W. Smarandache Paradox. In: CRC Concise Encyclopedia of Mathematics, CRC Press, Boca Raton, Florida, p. 1661, (1998); http://mathworld.wolfram.com/SmarandacheParadox.html.

Generation of Baryons from Electromagnetic Instabilities of the Vacuum

Osvaldo F. Schilling

Departamento de Física, Universidade Federal de Santa Catarina, Campus, Trindade, 88040-900, Florianópolis, SC. Brazil.
E-mail: osvaldo.neto@ufsc.br

Baryons are generated from perturbations of magnetodynamic origin built upon a background sea of excitations at about 3.7 GeV adopting the proton state as a "substrate", as proposed by Barut. To simulate perturbations from such a state a sum over the energy spectrum of excitations is necessary. A Zeta-function regularization procedure previously adopted for the Casimir Effect is applied to eliminate divergences when the sum upon the energy spectrum states is carried out. States of negative energy compared to the background state are obtained and represent the baryons. The periodic behavior of the baryon masses with confined magnetic flux is reproduced with no further forms of energies required besides the magnetodynamic terms. This treatment implicitly supports the concept that quarks and leptons might be treated on similar theoretical grounds.

1 Introduction

In recent work [1] we have shown that through the imposition of gauge invariance conditions to the wavefunctions of a particle (represented in energy terms by a closed loop of current and performing zitterbewegung motion), it is possible to relate rest energy to magnetic energy for the baryons. Gauge covariance was imposed by making the magnetic flux linked through the region covered by the particle "orbit" quantized in units n of $\phi_0 = hc/e$, the flux quantum. We therefore *adopted* integer values of n (allowing also for half-integer values; which case depends upon the actual boundary conditions) in the analysis for the baryons, guided also by the criterion that n should be proportional to the magnetic moment (in n.m. units) in the classical limit of flux generated by self-fields.

Such model is essentially based upon heuristic arguments, and in particular the assumption that zitterbewegung currents flow inside complex particles like the baryons is the extension of a similar proposal made for the electron. The model predicts an inverse dependence of mass with the fine structure constant α, in agreement with experimental data analysis reported in the literature [1]. The model produces a reasonable agreement between the calculated magnetic (plus kinetic) energies and the rest energies, revealing also a clear dependence of rest mass upon the square root of the spin angular momentum, of the form predicted and observed in the literature. However, a noticeable scattering of data around the theoretical line still remained. The meaning of such scattering was not addressed in the previous work.

To better understand if such deviations might have a physical meaning rather than indicating possible limitations of the model, we decided that the data should be analyzed again in a slightly different way, by avoiding any previous assumption about the values of n. The number of flux quanta is now objectively determined through the model, from the product of the known values of mass and magnetic moment (through the same Eq. (3) of [1]; see below). The relation of mass with such "model-adapted" values of n, calculated from the available data, become the object of this new analysis.

To make the model expressions applicable to a sizeable number of particles, it is necessary to eliminate the effects on the rest energies of kinetic energy contributions specifically attributable to the "excess" spin angular momenta of decuplet particles (spin-3/2 particles) as compared to the spin-1/2 octet particles, which were evident in our previous paper [1]. Therefore, for the range of mass values covered by the decuplet particles, the elimination of such excess kinetic energy shall be made by subtracting from the masses of the decuplet particles the average difference between the actual masses of decuplet and octet particles, 244 Mev/c^2. The resulting "*transformed masses*" m_t of the decuplet thus have the same average as the masses of the octet particles, as shown in the Tables below.

This should eventually make all baryons fit the mass-energy expression derived for spin-1/2 in [1]. As expected, the new values of n are not substantially different from the ones adopted previously (see [1] for details in the Tables there). In this way, the margin of arbitrariness in the choice of n inherent to the previous criterion is eliminated and the determination of this parameter for each baryon becomes an objective for the model. From the new analysis, it should therefore be possible to better evaluate the internal consistency of the model itself, including the evaluation on whether the proposed interpretation of n as a true number (integer or not) of magnetic flux quanta is physically meaningful, as well as analysing how appropriate is the utilization of closed currents as a means of representing complex particles.

As shown in the following sections, the approach proved valuable. As far as results are concerned new important features have arisen from the analysis. By plotting against n both the octet baryon masses and the transformed rest masses m_t of the decuplet baryons, we obtain the novel result that a simple periodic function, with n in the argument, is capable of fitting the points. That is, the rest energy (given by magnetodynamic

Table 1: Data for the baryon octet (moments μ from [11]). According to Eq. (4) in gaussian units: $n = 1.16 \times 10^{47}\,\mu m$. The plot of m/m_{p} (m_{p} the proton mass) against n are shown in Fig. 2.

	abs μ (n.m.)	μ (erg/G)$\times 10^{23}$	m (Mev/c^2)	m(g)$\times 10^{24}$	n from Eq. (4)
p	2.79	1.41	939	1.67	2.73
n	1.91	0.965	939	1.67	1.9
$\sum^+$	2.46	1.24	1189	2.12	3
$\sum^0$	0.82 (theor.)	0.414	1192	2.12	1
$\sum^-$	1.16	0.586	1197	2.12	1.5
Ξ^0	1.25	0.631	1314	2.34	1.7
Ξ^-	0.65	0.328	1321	2.34	0.9
Λ	0.61	0.308	1116	1.98	0.7

terms) is periodic on magnetic flux.

Such result seems quite revealing since it has actually been repeatedly associated in the literature with the effect of confined flux upon the magnetic energies due to currents, flowing around multiply-connected paths, which is exactly what this research proposes to demonstrate happens inside particles. The Aharonov-Bohm effect of interfering electron beams surrounding a solenoid, as well as superconducting currents in rings [2, 3], charge density waves in dielectric structures [4], and even currents around normal metallic rings [5] (all surrounding confined magnetic flux) have been reported to display such periodic dependence of energy and current on magnetic flux.

Starting from a Lagrangian suitable to fermion fields [6], we obtain an energy spectrum for the possible current carrying states around the closed path confining magnetic flux. In order to simulate self-field perturbations involving pair creation/annihilation from vacuum, a sum over the states in the energy spectrum is necessary. An Epstein-Riemann zeta function regularization procedure previously adopted for the Casimir Effect is applied to eliminate divergences when the sum upon the energy spectrum states is carried out [7], and the periodic behavior of the baryon masses with magnetic flux is reproduced with no further forms of energies required besides the magnetodynamic terms.

It is a basic assumption of the model adopted in this treatment [1] that currents generate magnetic moments, which give rise to self-magnetic fields and flux within particles. An "anomalous" magnetodynamic energy is generated, which we identify with the additional rest energy of the "dressed" particles. It appears that the resulting trapped magnetic flux modulates the currents obtained from wavefunctions running around the closed path, through the imposition of a phase factor, and such phases vary from one baryon to another. The magnetic energy depends on such modulation, and thus also the mass along the baryon family. All these results are considered in detail in Section 2. A review of previous results of the model is also added for the sake of completeness of exposition.

2 Theory

2.1 Phenomenological determination of the parameter n

Isolated current-loops containing a single quantum of flux of value $\phi_0/2 = hc/2e$ are well known from type-II superconductivity. The formation of superconductor current loops is a many-body effect, though. In a series of papers we have investigated if there might exist single-particle systems confining flux in a similar manner [1]. It is essential that such proposal be quantitatively supported by experimental data. Let's consider the actual case of particles of the baryon octet. All the eight particles have well-established rest masses and magnetic moments. E. J. Post [8] considered how to write an energy-mass relation in a tentative model for the electron. Post showed that the magnetic moment for the electron could be obtained up to the first-order correction (from QED) with the equation:

$$mc^2 = \frac{\phi}{c}\, i + eV\,. \tag{1}$$

Here the left side is the rest energy of the electron, which from the right side is considered as fully describable by electromagnetic quantities. The first term on the right side is the energy of an equivalent current ring of value i linking an amount of flux ϕ, that should occur in a number n of flux quanta ϕ_0. In spite of the adopted parameters from electromagnetic theory, such term contains similar amounts of magnetic and kinetic energy contributions of moving charges, as discussed by London [9], and thus the kinetic effects are already included. The second (electrostatic energy) term is much smaller than the first (it will be neglected hereafter) and accounts for the radiation-reaction correction for the magnetic moment which is proportional to the fine structure constant α [8]. Post associates the current with the magnetic moment μ and the size R of the ring with the equation:

$$\mu = \frac{\pi R^2 i}{c}\,. \tag{2}$$

One then inserts (2) into (1) (without the electrostatic small term) and thus eliminates the current. The parameter R

Table 2: Data for the baryon decuplet (moments μ from ref. [11]). The average difference between the decuplet and octet particle masses is discounted as discussed in the text and the resulting mass is put in columns 4 and 5. According to Eq. (4) in gaussian units: $n = 1.16 \times 10^{47}\,\mu m$. The plot of m_t/m_p against n are shown in Fig. 2.

	abs μ (n.m.)	μ (erg/G)$\times 10^{23}$	$m_t = m - 244$ (Mev/c^2)	m_t(g)	n from (4)
Δ^{++}	4.52	2.28	986	1.75	4.64
Δ^{+}, Δ^{-}	2.81, 2.81	1.42	990	1.75	2.9, 2.9
$\sum^{+}$	3.09	1.56	1135	2.02	3.65
$\sum^{0}$	0.27	0.136	1136	2.02	0.32
$\sum^{-}$	2.54	1.28	1138	2.02	3
Ξ^{0}	0.55	0.28	1281	2.28	0.73
Ξ^{-}	2.25	1.14	1283	2.28	3
Ω^{-}	2.02	1.02	1428	2.54	3

has been calculated/measured for the nucleons only, but it remains part of the final expression for all baryons obtained after the combination of (1) and (2). We may conveniently eliminate R from this treatment by adopting for all baryons an expression which is valid for the leptons (assuming in that case $R = \lambda$, the Compton wavelength), and for the proton [1] (from experimental evidence), namely:

$$\mu = \frac{1}{2}\, e\, R\,. \tag{3}$$

In the present case we are interested in assessing a sufficiently large group of particles in order that the proposed association between mass and confined flux can be properly investigated, and the baryons form such a group.

The model by Post was devised to fit a single fundamental particle, the electron, and there was actually no discussion about the application to other particles. We are now able to justify (see Section 2.2) the proposal that the collective motion of constituents inside baryons can also be described in terms of currents, so that a similar model should apply.

The combination of equations (1) to (3) with $\phi = n\,(hc/e)$ can therefore be cast in the form (inserting $\alpha = e^2/\hbar c$):

$$n = \frac{2c^2\alpha}{e^3}\,\mu\, m\,. \tag{4}$$

Tables 1 and 2 bring the mass and magnetic moments data for all baryons of the octet and decuplet, alongside the values for n from (4). It should be noticed that according to the present treatment the proton corresponds to $n \approx 3$ (see Table 1). In a semiclassical treatment Barut [10] considered baryons and mesons as resulting from stabilized configurations of constituents linked together by dipolar magnetic forces. A quantum number is introduced and the rearrangement of parameters makes Barut's final formulas for mass quite similar to the ones obtained in [1]. In particular Barut obtains $n = 3$ for the proton, by associating one unit of angular momentum for each of three unit-charged constituents.

2.2 Heuristic model based upon field-theoretic concept

Eq. (4) stresses the fact that in this work, n is the parameter to be determined from the data available for mass and moment (note that it is the same as Eq. (3) of [1] written in another form). In addition, (4) can be rewritten in a useful form by isolating in it the expression for the nuclear magneton (n.m.), $e\hbar/2m_pc$, yielding $n = (m/m_p)\,\mu$ (n.m.). Here m_p is the proton mass and the magnetic moment is given in n.m. units.

All the parameters on the right side of (4) are known for the eight baryons of the octet, and are listed in Table 1 (data from [11]). Fig. 1 shows the plot of the calculated n against the magnetic moment for each particle, which mirrors the dependence of mass on magnetic properties for each octet baryon. Note the presence of a diagonal line. There is a tendency to form Shapiro-like steps at integer numbers of flux quanta, but the approach to the steps has an undulating shape rather than being sharply defined (note: such "Shapiro" steps for superconducting rings characterize the penetration of flux inside the ring in units of flux quanta).

The existence of a diagonal *baseline*, $n = \mu$ (n.m.) experimentally characterizes the presence of a *minimum* amount of mass in all baryons. From (4), it becomes clear that the proton mass would be this minimum mass. Barut in the 1970s proposed that the other baryons might be considered perturbations built upon a proton "fundamental state", thus providing a minimum amount of mass.

The undulations in the figure lie above the diagonal line since it characterizes a stable, fundamental-like state.

In fact the undulations can be thought as a consequence of the confinement of magnetic flux inside a multiply connected path described by each particle charge motion. Gauge covariance of a Lagrangian which describes such particle ends up imposing such periodic dependence on the magnetic properties of the particles. Similar problems have extensively been dealt with by condensed matter physics groups [2–6].

Let's consider a fermion field confined to a circular path of length L, enclosing an amount of self-induced magnetic flux ϕ in a potential A. We need to show that such a system

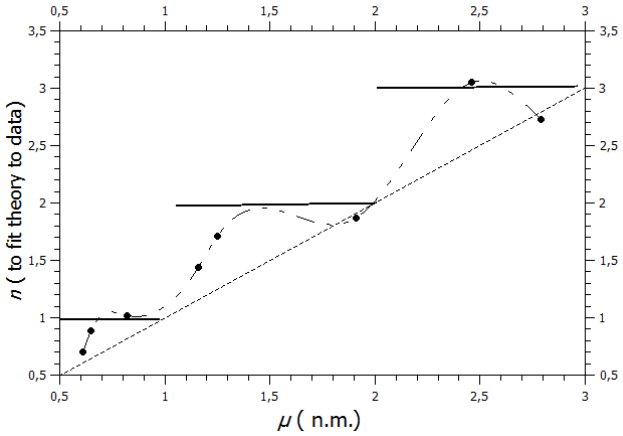

Fig. 1: Plot of n against the magnetic moment for the octet following Eq. (4) and Table 1. The diagonal line is the classical prediction of one flux quantum per nuclear magneton (n.m.). Nucleons are on the line. Horizontal (Shapiro-like) steps at integer values of n are shown. The data display undulations, and a tendency to reach for the steps (traced line as guide).

corresponds to a state detached from a higher state associated with a sea of excitations in equilibrium, and therefore might be used to represent a "quasiparticle". The relativistic Lagrangian for such a fermion can be modelled through the dressing of a proton of mass $m_{\rm p}$ in view of the presence of magnetodynamic terms [6]:

$$\mathcal{L} = \bar{\psi}\left\{i\alpha_\mu\left(\hbar\partial_\mu - i\,\frac{e}{c}\,A_\mu\right) - \alpha_4 m_{\rm p} c\right\}\psi\,, \qquad (5)$$

where the α_μ are Dirac matrices. This Lagrangian can readily be transformed into a Hamiltonian form. For A a constant around the ring path, the spectrum of possible energies for a confined fermion are obtained as:

$$\epsilon_{\rm k} = c\left\{\left(p_{\rm k} - \frac{eA}{c}\right)^2 + m_{\rm p}^2 c^2\right\}^{1/2} \qquad (6)$$

which comes straight from the orthonormalized definition of the Dirac matrices and diagonalization of the Hamiltonian. If one takes the Bohr-Sommerfeld quantization conditions, the momentum $p_{\rm k}$ (for integer k) is quantized in discrete values $2\pi\hbar k/L$. We start from this assumption but the true boundary conditions to close the wave loop might impose corrections to this rule in the form of a phase factor (see below). The potential A can be replaced by ϕ/L. Such charge motion is affected by vacuum polarization and the effects on the kinetic energy are accounted for in a way similar to that used in the analysis of the Casimir Effect, by summing over all possible integer values of k in (6) [6,7]. This summation diverges. According to the theory of functions of a complex variable the removal of such divergences requires that the analytic continuation of the terms be taken, which reveals the diverging parts which are thus considered as contributions from the infinite vacuum reservoir. A successful technique for this purpose begins with the rewriting of (6) in terms of Epstein-Riemann Zeta functions $Z(s)$ [7], including the summation over k from minus to plus infinity integers, and making a regularization (Reg) transformation. Here $M(\phi)$ is the flux-dependent dressed mass of a baryon, and $s \to -1$:

$$Mc^2 = U_0 + \mathrm{Reg}\sum_k c\left\{\left(p_{\rm k} - \frac{e\phi}{Lc}\right)^2\right\}^{-s/2} \qquad (7)$$

where we have allowed for the existence of a finite energy U_0 to represent an hypothetical state from which the individual baryons would condense, since they would correspond to lower energy states. Such particles should be characterized as states of energy Mc^2 lower than U_0. It is convenient to define from L a parameter with units of mass $m_0 = 2\pi\hbar/cL$, which will be used to define a scale in the fit to the data. We notice that m_0 is related to the parameter L in the same way field-theories regard mass as created from broken symmetries of fields, establishing a range for an otherwise boundless field distribution (e.g. as happens at the establishment of a superconductor state with the London wavelength related to an electromagnetic field "mass" by a similar expression). For convenience, we define the ratios $m' = m_{\rm p}/m_0$ and $u_0 = U_0/m_{\rm p}c^2$. For comparison with the data analysis in our previous work [1], we must introduce also the number of flux quanta n (integer or not) associated to ϕ, such that $n = \phi/\phi_0$. In terms of these parameters one may write (7) in the form:

$$\frac{M(n)}{m_{\rm p}} = u_0 + \frac{1}{m'}\,\mathrm{Reg}\sum_k\left\{(k-n)^2 + m'^2\right\}^{-s/2}\,. \qquad (8)$$

In the analysis of data, the experimental values of $M/m_{\rm p}$ for baryons will be plotted against n. The sum on the right side of (8) is a particular case of an Epstein Zeta function $Z(s)$, and becomes a Riemann Zeta function, since the summation is over one parameter k only. The summation diverges but it can be analytically continued over the entire complex plane, since the Epstein Zeta function displays the so-called reflection property. It has been shown that after the application of reflection the resulting sum is already regularized, with the divergences eliminated. The reflection formula is [7]:

$$\pi^{\frac{-s}{2}}\,\Gamma\left(\frac{s}{2}\right)Z(s) = \pi^{\frac{s-1}{2}}\,\Gamma\left(\frac{1-s}{2}\right)Z(1-s)\,. \qquad (9)$$

This replaces the diverging $Z(s)$ straight away by the regularized $Z(1-s)$, which converges (since $\Gamma(-1/2) = -2\sqrt{\pi}$, we see that the regularized sums are negative, like in the Casimir Effect solution).

For the sake of clarity we describe now the regularization of (8) below as (10), step by step (note that $s \to -1$, and the "reflected" exponent $-(1-s)/2$ replaces $-s/2$ of (8)).

In the first passage from the left, the entire summation argument is replaced by the Mellin integral which results into it. This creates a convenient exponential function to be integrated later. In the second passage, the Poisson summation formula is used, in which the summed exponential function is replaced by its Fourier Transform (note that the same notation k is used for the index to be summed in the Fourier transformed quantity). The objective is to replace the $k^2 t$ in the initial exponential by k^2/t. In this way, when the integration over t is carried out a modified Bessel function K is obtained. In the final line the $k = 0$ term in the sum is separately worked out and appears as the first term between brackets. The remaining summation in k therefore does not include 0 ("/0" as shown). The influence of the parameter n is, as we wanted to prove, to introduce a periodicity depending on the amount of flux confined by the current ring, and the regularized energy is therefore periodic in n. Therefore, $Z(1-s)$ is given as:

$$\sum_k \left\{(k-n)^2 + m'^2\right\}^{-(1-s)/2} =$$

$$= \frac{2}{\Gamma\left(\frac{1-s}{2}\right)} \int_0^\infty t^{\frac{1-s}{2}-1} \left(\sum_k e^{-(k-n)^2 t - m'^2 t} \right) \mathrm{d}t =$$

$$= \frac{2\sqrt{\pi}}{\Gamma\left(\frac{1-s}{2}\right)} \int_0^\infty t^{\frac{-s}{2}-1} \left(\sum_k e^{-2\pi i k n} \, e^{-\frac{\pi^2 k^2}{t} - m'^2 t} \right) \mathrm{d}t =$$

$$= \frac{2\sqrt{\pi}}{\Gamma\left(\frac{1-s}{2}\right)} \left(\frac{\Gamma\left(-\frac{s}{2}\right)}{m'^{-s}} + 2\pi^{\frac{-s}{2}} \sum_{k/0} \left(\frac{k}{m'}\right)^{\frac{-s}{2}} K_{\frac{s}{2}}(2\pi m' k) \, e^{-2\pi i k n} \right) \quad (10)$$

for $s \to -1$. From (9), the "Reg" summation in (8) becomes

$$\frac{\pi^{\frac{2s-1}{2}} Z(1-s)}{\Gamma\left(\frac{s}{2}\right) \Gamma\left(\frac{1-s}{2}\right)},$$

and the exponential produces a cosine term.

Since $\Gamma(-1/2) = -2\sqrt{\pi}$ we see that the regularized sum is negative, corresponding to energies lower than U_0. In the fitting to the data, we will admit that both m' and u_0 are adjustable parameters.

Fig. 2 shows the data for all baryons in Tables 1 and 2, and the plot of (8) regularized by (10), for $u_0 = 3.96$ and $m' = 0.347$ (corresponding to $m_0 = 2.88\, m_p$ and $U_0 = 3710$ MeV). The energy 3710 MeV would represent the sea of excitations from which the baryons would evolve.

Greulich [12] made a phenomenological analysis correlating the masses of all mesons and baryons with lifetimes greater than 10^{-24} s, to the electron mass and the constant α, obtaining that $m/m_e = N/2\alpha$. Such expression is consistent with our previous analysis in [1], as well as with the new results in the present work. Fig. 3 is a reproduction of Fig. 1 in his paper. We have added a traced line at 3710 MeV/c^2, which shows that such energy is in the correct range for a "parent" state from which all those particles below might evolve by symmetry breaking. There is no correction for spin in the masses of this plot and the points above the line belong to particles containing combinations of charmed, strange, and bottom quarks, which might not fit in the specific calculation considered in this paper.

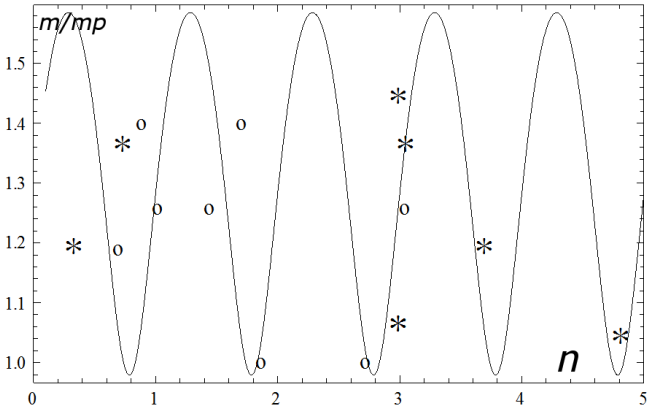

Fig. 2: Comparison of baryon masses calculated from Eq. (8) as a function of confined flux n, with data from Tables 1 and 2 for octet (open circles) and decuplet particles (m_t used, stars). The phenomenological Eq. (4) provides values for n as a function of mass and moment, and the relation between these quantities (data points) agrees quite well with the field-theoretical calculations (curve) of mass as function of n from Eq. (8). Nucleons are on the basis of the figure.

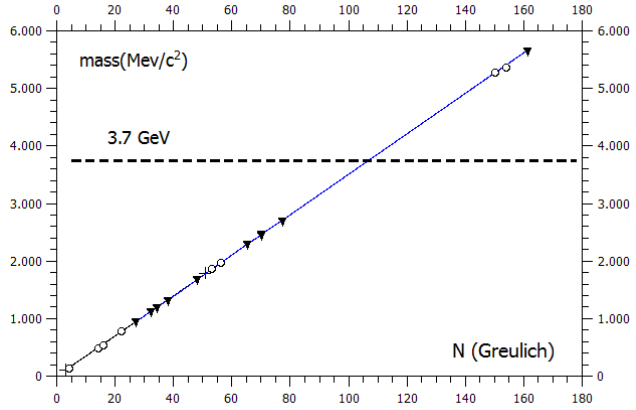

Fig. 3: This plot shows all baryons and mesons with lifetimes greater than 10^{-24} s [12] (see text for details). The traced line indicates the calculated 3710 Mev/c^2, which is in the expected range of energy for a parent-state for the particles below it.

3 Analysis and conclusions

The present paper provides a theoretical background for the phenomenological analysis of [1]. Such previous analysis has

been improved through the redefinition of the parameter n in terms of the experimental data on mass and magnetic moments for baryons. The basic idea has been the modeling of such particles by means of confined currents. The present work has shown that this is theoretically sensible. Closed currents are associated with confined magnetic flux. Since the represented particle is immersed in a sea of excitations, the energy spectrum of closed currents is summed up over all possible values of a Bohr-Sommerfeld kinetic quantum number, leaving the previously defined magnetic n as the parameter to dictate the mass differences among the baryons, in view of the fulfillment of gauge-covariance conditions. A regularization procedure is necessary since the original sums diverge. The model regards particles as the result of a type of condensation from a sea of excitations of top energy U_0, which is the accepted picture in field theories of the origin of mass (however no phase-transitions or broken symmetries are explicitly introduced in the present treatment). The lowest energy particles are the nucleons in this picture. The magnetic flux introduces a modulation of rest energy which is quite well reproduced and the parameter m' is defined with such a magnitude to cover all baryons up to the Ω^- particle. No other kinds of forces are necessary for such theoretical treatment to reproduce data, neither is necessary a detailed knowledge about inner constituents of baryons. As discussed in a previous paper [13], the good results obtained here support early treatments in which quarks and leptons are treated on the same theoretical framework. Such framework should essentially be based on quantum electrodynamics.

Received on November 8, 2019

References

1. Schilling O. F. A unified phenomenological description for the magnetodynamic origin of mass for leptons and for the complete baryon octet and decuplet. *Annales de la Fondation Louis de Broglie*, 2018, v. 43-1, 1.
2. Byers N. and Yang C. N. Theoretical considerations concerning quantized magnetic flux in superconducting cylinders. *Phys. Rev. Lett.*, 1961, v. 7, 46.
3. Parks R. D. Quantized magnetic flux in superconductors. *Science*, 1964, v. 146, 1429.
4. Kulik I. O., Roshavskii A. S., and Bogachek E. N./, Magnetic flux quantization in dielectrics. *J. Exp. Theor. Phys. Letters*, 1988, v. 47, 303.
5. Kulik I. O. Spontaneous and persistent currents in mesoscopic Aharonov-Bohm loops: static properties and coherent dynamic behavior in crossed electric and magnetic fields. *J. Exp. Theor. Phys.*, 2005, v. 101, 999 and references therein.
6. Bogachek E. N., Krive I. V., and Roshavskii A. S. Aharonov-Bohm oscillations in relativistic Fermi and Bose systems. *Theor. Math. Phys.*, 1990, v. 83, 419.
7. Lin R.-H. and Zhai X.-H. Equivalence of zeta function technique and Abel-Plana formula in regularizing the Casimir energy of hyperrectangular cavities. *Mod. Phys. Lett. A*, 2014, v. 29, 1450181.
8. Post E. J. Linking and enclosing magnetic flux. *Phys. Lett.*, 1986, v. 119A, 47.
9. London F. Superfluids, vol. I. Wiley, New York, 1950.
10. Barut A. O. Quantization of collective regular structures of particles. *Appl. Phys. (Lasers and Optics)*, 1995, v. B69, 123.
11. Simonov Y. A., Tjon J. A. and Weda J. Baryon magnetic moments in the effective quark lagrangian approach. *Phys.Rev. D*, 2002, v. 65, 094013.
12. Greulich K. O. Calculation of the masses of all elementary particles with an accuracy of approximately 1%. *J. Mod. Phys.*, 2010, v. 1, 300.
13. Schilling O. F. Heuristic methods for the calculation of mass for particles. viXra: quant/1807.0476 (http://vixra.org/abs/1807.0476).

Nuclear Fusion with Coulomb Barrier Lowered by Scalar Field

T. X. Zhang[1] and M. Y. Ye[2]

[1]Department of Physics, Chemistry, and Mathematics, Alabama A & M University, Normal, Alabama 35762, USA. E-mail: tianxi.zhang@aamu.edu
[2]School of Physical Science, University of Science and Technology of China, Hefei, Anhui 230088, China. E-mail: yemy@ustc.edu.cn

The multi-hundred keV electrostatic Coulomb barrier among light elemental positively charged nuclei is the critical issue for realizing the thermonuclear fusion in laboratories. Instead of conventionally energizing nuclei to the needed energy, we, in this paper, develop a new plasma fusion mechanism, in which the Coulomb barrier among light elemental positively charged nuclei is lowered by a scalar field. Through polarizing the free space, the scalar field that couples gravitation and electromagnetism in a five-dimensional (5D) gravity or that associates with Bose-Einstein condensates in the 4D particle physics increases the electric permittivity of the vacuum, so that reduces the Coulomb barrier and enhances the quantum tunneling probability and thus increases the plasma fusion reaction rate. With a significant reduction of the Coulomb barrier and enhancement of tunneling probability by a strong scalar field, nuclear fusion can occur in a plasma at a low and even room temperatures. This implies that the conventional fusion devices such as the National Ignition Facility and many other well-developed or under developing fusion tokamaks, when a strong scalar field is appropriately established, can achieve their goals and reach the energy breakevens only using low-techs.

1 Introdction

The development of human modern society is inseparable from energy. Since the fossil fuels are nearing exhaustion and renewable energy sources cannot be sufficient, the best choice to thoroughly solve the future energy problems must be the nuclear fusion power. The most critical issue in nuclear fusion is the extremely high Coulomb barrier between positively charged nuclei, usually over hundreds of keV or billions of Kelvins [1]. From the quantum tunneling effect, which is derived from Heisenberg's uncertainty principle and the particle-wave duality, nuclei with kinetic energy of around ten keV or hundred million Kelvins, which is about some tens times lower than the actual barrier, are energetic enough to penetrate the barrier and fuse one another with sufficient probabilities. There are in general three possible ways for nuclei to overcome the Coulomb barrier between them and hence achieve the thermonuclear fusion: (i) heating both species of nuclei (or the entire plasma including electrons) to the needed temperature, (ii) heating only the minor species of nuclei to the needed temperature, and (iii) lowing the Coulomb barrier to the needed level. Figure 1 sketches a schematic of the three approaches for nuclei to overcome their Coulomb barrier that blocks them from fusion. A combination of two or all of the three approaches will certainly work more efficiently.

Since the middle of the last century, fusion scientists have been focusing on the approach (i), i.e. study of how to efficiently heat the entire plasma for nuclei to have such high energies and how to effectively control and confine such extremely heated entire plasma. The major types of heating processes that have been applied so far include the Joule heating by driving electric currents, the injection heating by injecting energized neutral beams, and the radio frequency (rf) heating by resonating nuclei or electrons with antenna-generated radio-frequency waves. The magnetic and inertial confinements are two major types of confinements. Although having made great progresses in the development of various kinds of fusion devices or tokamaks, human beings are still not so sure how many difficulties to be overcome and how far need to go on the way of seeking this ultimate source of energy from the nuclear fusion [2].

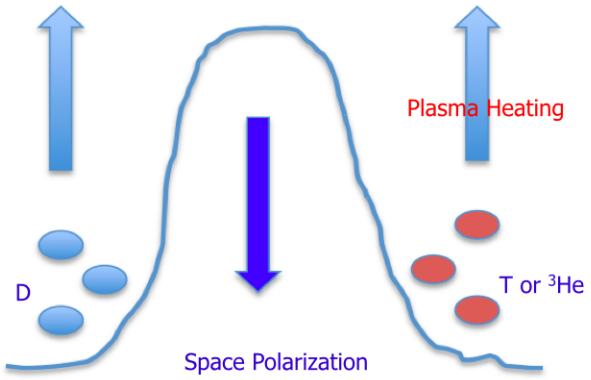

Fig. 1: A schematic of three ways for nuclei to overcome the Coulomb barrier. The first is the conventional approach that energizes both species of nuclei or the entire plasma including electrons to the needed energy for fusion. The second is the authors' recently developed approach that energizes the minor species of nuclei such as ^{3}He and T ions to the needed energy for fusion. And the third is the approach of this paper that lowers the Coulomb barrier to the needed level for fusion.

Recently, the authors innovatively proposed and further quantitatively developed the approach (ii), i.e. a new mechanism for plasma fusion at ten million Kelvins (MK) with extremely heated ^{3}He or tritium (T) ions [3–6]. This newly developed mechanism involves a two-stage heating process when an electric current is driven through a multi-ion plasma. The electric current first ohmically (or in the Joule heating process) heat the entire multi-ion plasma up to the order of 10 MK (or some keV), at which the electric resistivity in the plasma becomes too low for the electric current to be significantly dissipated further and the temperature of the entire plasma saturates at this level. When the electric current is continuously driven up to a critical point, the current-driven electrostatic H or D-cyclotron waves with frequency around twice as big as the ^{3}He or T-cyclotron frequency are excited, which can further heat ^{3}He or T ions via the second harmonic resonance to 100 MK and higher, at which the nuclear fusion between the extremely hot ^{3}He or T ions and the relative cold D ions (i.e. the D-^{3}He or D-T fusion) can occur. This new mechanism for plasma fusion at 10 MK with extremely heated ^{3}He or T ions can also greatly reduce the difficulty in controlling and confining of the plasma fusion.

In this study, we attempt to develop the approach (iii), i.e. to explore and find another new way towards this ultimate goal of using nuclear fusion energy through building an effective fusion reactor. Instead of only energizing the nuclei to the needed temperature, we lower the Coulomb barrier to the needed level. Towards this direction, there have been some analytical efforts done up-to-date by others for enhancing the quantum tunneling probability such as by catalyzing muons or antiprotons [7], driving cusps [8], spreading wave packets [9], forming coherent correlated states [10], screening with Bose-Einstein condensations [11], and so on. Rather than to catalyze the fusion, we will in this paper consider a scalar field to polarize the space or vacuum, in other words, to enhance the dielectric constant of the space or vacuum and hence reduce the electric potential energy or Coulomb barrier among nuclei. We will first calculate the effect of scalar field on the tunneling probability and the number of nuclei that can overcome the Coulomb barrier for fusion. We will then calculate the scalar field effect on the nuclear reaction rate of fusion. We will further investigate the physics and mechanism for a possible approach that generates a strong scalar field in labs to significantly lower the barrier and greatly enhance the quantum tunneling probability for nuclear fusion.

2 Lowering of the Coulomb Barrier by Scalar Field

Early studies have shown that the scalar field of a five-dimensional (5D) gravity can not only shallow the gravitational potential well by flattening the spacetime [12], or in other words, varying or decreasing the gravitational constant [13], but also lower the electric potential energy or Coulomb barrier among nuclei by polarizing the free space or vacuum [14, 15], or in other words, varying or increasing the dielectric constant [16]. From the exact field solution of 5D gravity [12, 17, 18], we can obtain the relative dielectric permittivity in the free space or vacuum polarized by a scalar field Φ as

$$\epsilon_r \equiv \frac{\epsilon}{\epsilon_0} = \frac{E_c}{E} = \Phi^3 \exp\left(\frac{\lambda - \nu}{2}\right), \tag{1}$$

where e^λ and e^ν are the $rr-$ and $tt-$ components of the 4D spacetime metric. This result implies that the electric potential energy or Coulomb barrier between nuclei is explicitly reduced by a factor of Φ^3. For a weak gravitational system such as in labs, because $e^\lambda \sim 1$, $e^\nu \sim 1$, we have $\epsilon_r = \Phi^3$. For a strong gravitational system such as nearby neutron stars or black boles, because $e^\nu \propto \Phi^{-2}$, we have $\epsilon_r \propto \Phi^4$. In quantum electrodynamics (QED) of particle physics, the vacuum polarization was calculated in accordance with the scalar Φ^3 theory [19]. The effect of scalar field vacuum polarization on homogeneous spaces with an invariant metric was obtained in [20].

The scalar field in the 5D gravity is a force field that associates with the mass and charge of a body and couples the gravitational and electromagnetic fields of the body. The scalar field associated with matter and charge in labs is negligible small, which may be able to be detected by the Laser Interferometer Gravitational-Wave Observatory (LIGO) that detected gravitational waves [21, 22]. For massive, compact, and, especially, high electrically charged objects such as neutron stars and black holes, we can have an extremely large scalar field. Although being one of the biggest unsolved mysteries in physics, the scalar field has been widely utilized to model and explain many physical phenomena such as Higgs particles, Bose-Einstein condensates, dark matter, dark energy, cosmic inflation, and so on.

Creatively, Wesson recently proposed a possible connection between the scalar field of 5D gravity and the Higgs scalar field of 4D particle physics [23]. The Higgs scalar field is an energy field that all particles in the universe interact with, and gain their masses through this interaction or Yukawa coupling [24, 25]. In the middle of 2013, CERN discovered the carrier of the Higgs scalar field, i.e. the Higgs boson, and thus confirmed the existence of the Higgs scalar field. On the other hand, according to the Ginzburg-Landau model of the Bose-Einstein condensates, the Higgs mechanism describes the superconductivity of vacuum. Therefore, the scalar field of the 5D gravity can be considered as a type of Higgs scalar field of 4D particle physics. The latter can be considered as a type of Ginzburg-Landau scalar field of Bose-Einstein condensates [26–28]. Then, that the scalar field of the 5D gravity can shield the gravitational field (or flatten the spacetime) and polarize the space or vacuum must imply that the Ginzburg-Landau scalar field of superconductors and superfluids in the state of Bose-Einstein condensates may also shield the gravitational field (or flatten the spacetime) and polarize the space or vacuum.

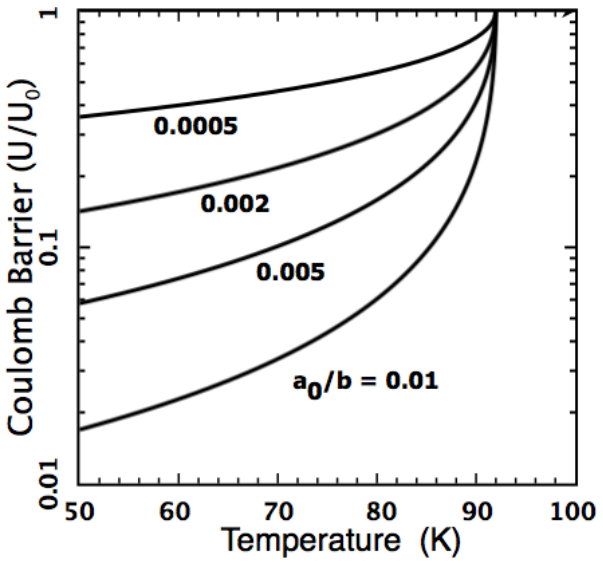

Fig. 2: The Coulomb barrier between two charges in the vacuum polarized by the Ginzburg-Landau scalar field of the Bose-Einstein condensate associated with the type II superconductor or superfluid, normalized by the barrier without the polarization, is plotted as a function of the temperature of the superconductor in the cases of different ratios of the two phenomenological constants a_0 and b.

In 1992, Podkletnov and Nieminen experimentally showed that a rotating disk of the type-II ceramic superconductor could shield Earth's gravity on a sample by a factor of $\sim 2-3\%$ [29]. If the disk is static, the shielding effect reduces $\sim 0.4\%$ [30]. Recently, we have explained these measurements as the gravitational field shielding by the Ginzburg-Landau scalar field of Bose-Einstein condensates associated with the type II ceramic superconductor disk [31], according to the 5D fully covariant gravity [12, 16, 18]. In the quantum field theory or quantum electrodynamics, many phenomena occurred or observed must be explained or described by relying on the physics of scalar field, for instances, the scalar field for cosmic inflation [32], the scalar field for dark matter or dark energy, and so on.

In the vacuum that is polarized by a Ginzburg-Landau scalar field of Bose-Einstein condensate associated with superconductor and superfluid, Φ_{GL}, the Coulomb barrier can be given by

$$U = \frac{U_0}{(1+\Phi_{GL})^3} \tag{2}$$

where

$$\Phi_{GL} = \sqrt{-\frac{a_0}{b}(T-T_c)} \tag{3}$$

with a_0 and b the two phenomenological constants, T and T_c the temperature and transition temperature of the condensate. For a quantitative study, we plot in Figure 2 the ratio of the Coulomb barrier in the vacuum that is polarized by the Ginzburg-Landau scalar field of Bose-Einstein condensates associated with a type II superconductor to that without polarization as a function of the temperature of the superconductor. In this plot, we have chosen the values $T_c = 92$ K and $a_0/b = 10^{-8}, 10^{-7}, 10^{-6}$ K^{-1} as done in [31, 33]. The vacuum polarization by a high magnetic field was measured by the Polarization of the Vacuum with Laser (PVLAS) using a superconducting dipole magnet of more than 8 Teslas magnetic field [34]. By a scalar field, a direct measurement of the vacuum polarization has not yet been conducted.

3 Penetrating of the Coulomb Barrier with Scalar Field

According to Gamow's tunneling probability [35] and Maxwell-Boltzmann's distribution function, one can find the relative number density of nuclei with energy from E to $E + dE$ in the plasma with temperature of T per unit energy that can penetrate the Coulomb barrier to be given by

$$\frac{dN}{dE} = \frac{2\pi}{(\pi kT)^{3/2}}\sqrt{E}\exp\left(-\frac{E}{kT}-\sqrt{\frac{E_g}{E}}\right), \tag{4}$$

where E_g is the Gamow energy determined by

$$E_g = 2m_r c^2(\pi\alpha Z_a Z_b)^2. \tag{5}$$

Here k is the Boltzmann constant, m_r is the reduced mass of nuclei, c is the light speed, Z_a and Z_b are the ionization states of nuclei, and $\alpha = e^2/(2\epsilon_0 hc)$ is the fine-structure constant. Considering the vacuum to be polarized by a scalar field (i.e. $\Phi > 1$), we modify the fine-structure constant by replacing ϵ_0 as $\epsilon = \Phi^3\epsilon_0$. It is seen that the scalar field can significantly reduce the Gamow energy and thus greatly increases the tunneling probability.

To see in more details for the increase of the tunneling probability, we plot in Figure 3 the Gamow peak in a D-T plasma first in the case of no scalar field (i.e. $\Phi = 1$). The plasma temperature has been chosen to be 10^7, 5×10^7, and 10^8 K, respectively. The result indicates, in a D-T plasma with density 2×10^{19} m^{-3} at 10^8 K, there are about two thousandth of total amount of nuclei to be able to tunnel through the barrier and participate in the fusion. Since the ion collision frequency in a fully ionized plasma can be estimated as $\nu_i = 4.8\times10^{-8} Z_i\sqrt{m_p/m_i}\ln\Lambda T_i^{-3/2} \sim 5$ Hz, for 10% of nuclei to react, the plasma must hold this temperature over 10 seconds. If the temperature is 5×10^7 or 10^7 K, then only around a few percent of or one in million nuclei can react within 10 seconds. Here we have used $\ln\Lambda = 6.8$ for ions.

With a scalar field, the tunneling probability will be significantly enhanced. Figure 4 plots the Gamow peak in a D-T plasma in the case of four different values of the scalar field (corresponding to the four lines in each panel, $\Phi = 1, 2, 10, 100$) and two different plasma temperatures of $T = 10^8$ K for the top panel and 10^7 K for the bottom panel. It is

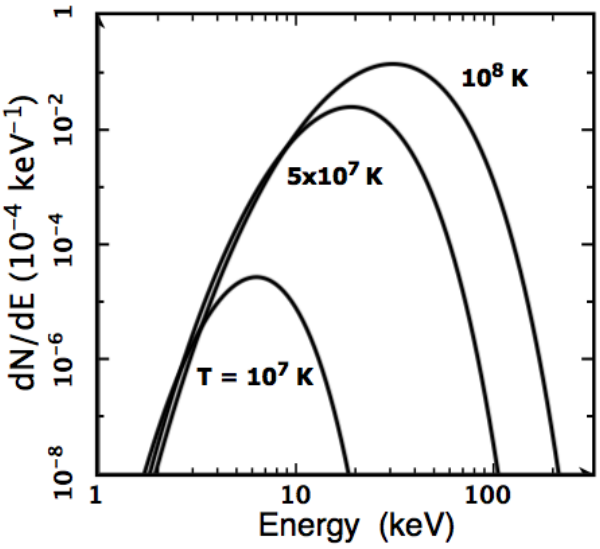

Fig. 3: The Gamow peak without a scalar field in a ^{2}H-^{3}H plasma with different temperatures or, in other words, the energy spectra of nuclei that are able to penetrate the Coulomb barrier for fusion. The relative number density of nuclei per unit energy with energy in the range from E to $E + dE$ is plotted as a function of the energy with temperature to be $T = 10^8, 5 \times 10^7, 10^7$ K, respectively. The maximum is usually called the Gamow peak [35].

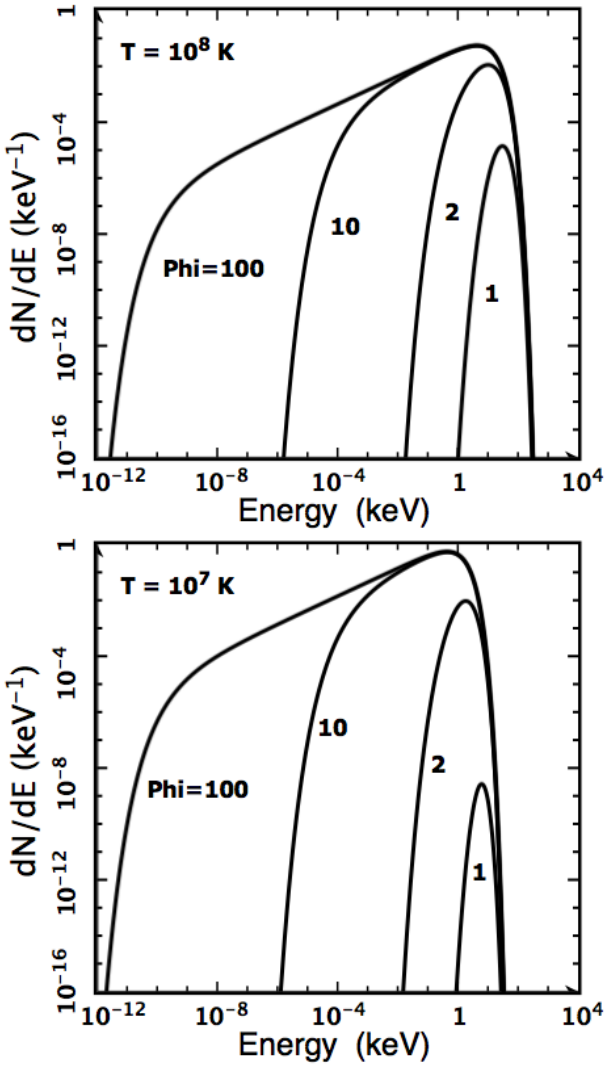

Fig. 4: The Gamow peak with a scalar field in a D-T plasma with different temperatures. This plots the energy spectra of nuclei that are able to penetrate the Coulomb barrier for fusion, i.e. the relative number density of nuclei per unit energy with energy in the range from E to $E + dE$ as a function of the energy with the scalar field $\Phi = 1, 2, 10, 100$ and temperatures to be $T = 10^8$ K for the top panel and 10^7 K for the bottom panel.

seen that when $\Phi > 2$ the number of nuclei that can tunnel through the barrier is enhanced by a factor of 1000 or greater at $T = 10^8$ K. At $T = 10^7$ K, the factor of enhancement can be 10^7 or greater. In addition, there are large amount of nuclei with extremely low energy can also tunnel through the barrier for fusion.

To see more details on the fusion of low energy nuclei, we plots the Gamow peak in Figure 5 for the D-T plasma with temperature equal to 10^6 K and 300K, respectively. In a 10^6 K plasma, the fusion can occur and be readily completed in seconds if $\Phi > 2$. At the room temperature, the nuclear fusion are also possible when $\Phi > 6$.

4 Fusion Rate

The fusion rate between two (i^{th} and j^{th}) species of ions, whose charge or ionization states are Z_i and Z_j, respectively, can be usually represented as [36–38]

$$R_{ij} = \frac{N_i N_j}{1 + \delta_{ij}} < \sigma v > \tag{6}$$

where N_i and N_j are the number densities of the two species of ions, δ_{ij} is the Kronecker symbol, which is equal to the unity if the two species of ions are identical, otherwise, it is zero, v is the relative velocity, and σ is the cross section, determined by

$$< \sigma v >= \frac{6.4 \times 10^{-18}}{A_r Z_1 Z_2} \Phi^3 S \xi^2 \exp(-3\xi) \quad \text{cm}^3/\text{s}, \tag{7}$$

with ξ to be defined as

$$\xi = 6.27 \Phi^{-2} (Z_i Z_j)^{2/3} A_r^{1/3} T^{-1/3}. \tag{8}$$

Here we have considered the effect of space polarization on both the Coulomb barrier and the Gamow factor, simply by replacing $Z_i Z_j$ into $Z_i Z_j / \epsilon_r$ with $\epsilon_r = \Phi^3$ due to the space

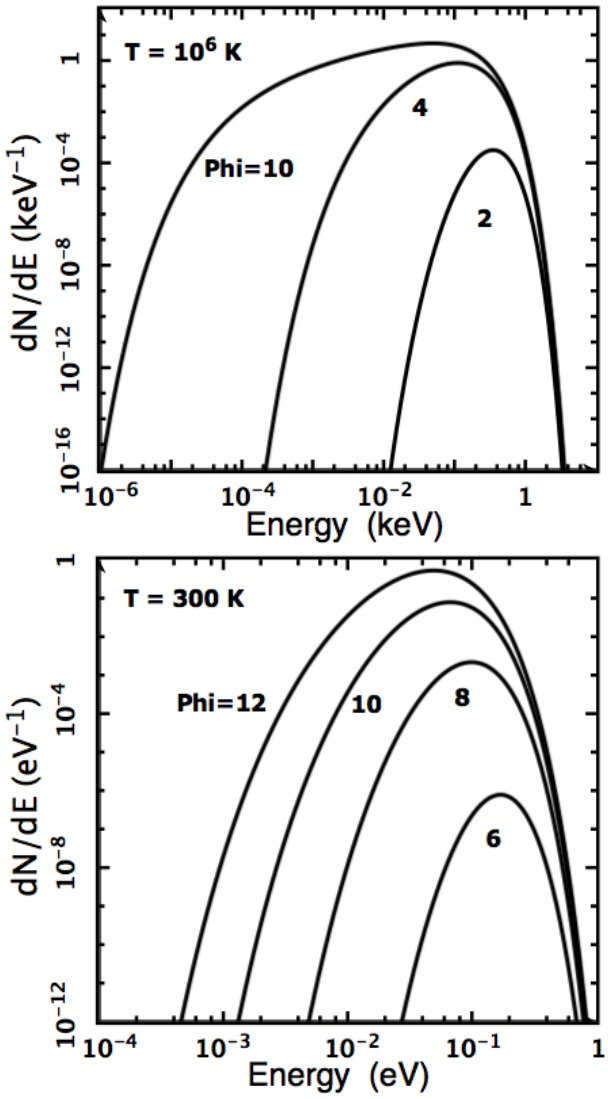

Fig. 5: The Gamow peak with a scalar field in a D-T plasma with different temperatures. This plots the energy spectra of nuclei that are able to penetrate the Coulomb barrier for fusion, i.e. the relative number density of nuclei per unit energy with energy in the range from E to $E + dE$ as a function of the energy with the scalar field $\Phi = 2, 4, 10$ and temperatures to be $T = 10^6$ K for the top panel. For the bottom panel, the scalar field is chosen to $\Phi = 6, 8, 10, 12$ and the temperature is chosen to be $T = 300$ K.

polarization by the scalar field Φ. In equations (7) and (8), the parameter S is the cross section factor, A_r is the reduced mass number, and T is the plasma temperature in keV. For the D-T fusion, we have $Z_i = Z_j = 1$, $A_r = 1.2$, and $S = 1.2 \times 10^4$ keV b.

To see how the scalar field to affect or enhance plasma fusion via the space polarization, we plot in Figure 6 the reaction rate of fusion as a function of the plasma temperature

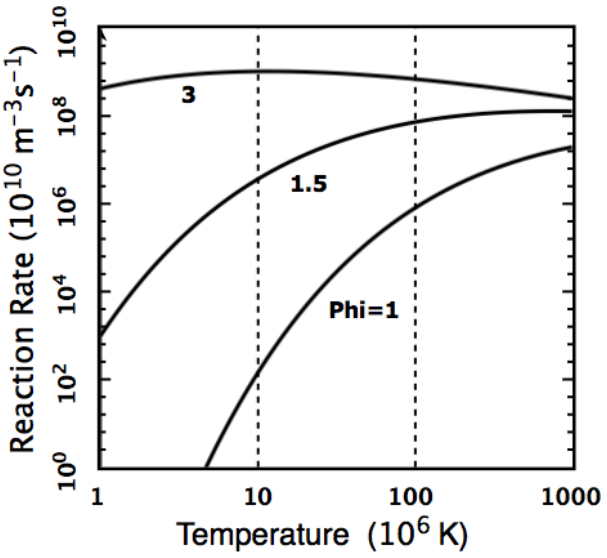

Fig. 6: The reaction rate of D-T fusion. The number of fusion reactions occurred in an unit volume (or m^3) of D-T plasma in one second is plotted as a function of the plasma temperature. Here the number densities of D and T nuclei are both chosen to 10^{19} m^{-3}, and the scalar field is chosen to 1, 1.5, and 3, respectively.

in the cases of the scalar field to be equal to $\Phi = 1, 1.5, 3$, respectively. It should be noted that the effect of scalar field comes from the difference of the scalar field from the unity or, in other words, there is no scalar field effect if $\Phi = 1$. The number densities of D and T nuclei are chosen to be $n_D = n_T = 10^{13}$ cm^{-3}. It is seen from the plot that the scalar field can significantly enhance the reaction rate of fusion. Without the effect of scalar field (i.e. $\Phi = 1$), the reaction rate of D-T fusion is about one thousandth m^{-3} s^{-1} (i.e. per cubic meters and per seconds) at temperature of about 10^8 K. With the effect of scalar field (i.e., $\Phi > 1$), the rate can be increased by 100 times to 10 percent m^{-3} s^{-1} when $\Phi = 1.5$ and by 1000 times to 100 percent m^{-3} s^{-1} when $\Phi = 3$.

5 Conclusion

We have developed a new mechanism for plasma fusion with the Coulomb barrier to be lowered by a scalar field. The result obtained from this study indicates, by polarizing the free space, a scalar field in associated with Bose-Einstein condensates can increase the electric permittivity of the vacuum and hence reduce the Coulomb barrier and enhance the tunneling probability. With a strong scalar field, nuclear fusion can occur in a plasma at a low and even room temperatures. Therefore, by appropriately generated a strong scalar field to polarize the space, we can make the conventional fusion devices to readily achieve their goals and reach the breakevens only using low-techs.

Acknowledgements

The authors thank reviewers for their scientific comments and editors for their great editions that significantly improve the manuscript qualities.

Submitted on November 18, 2019

References

1. Miyamoto K. Plasma Physics for Nuclear Fusion. Revised Edition, Cambridge, Masseschussetts, MIT Press, 1989.
2. Jassby D.L. Fusion reactors: Not what they are cracked up to be. *Bulletin of the Atomic Scientists of Chicago*, April 19, 2017.
3. Zhang T.X. Two-stage heating mechanism for plasma fusion at 10 MK, *Proceedings of IEEE 25th Symposium on Gusion Engineering (SOFE*, 2013, 978-1-4799-0171-5/13.
4. Zhang, T.X.,Ye M.Y. Plasma fusion at 10 MK with extremely heated ^{3}He ions. *IEEE Transactions on Plasma Science*, 2014, v. 42, 1430–1437.
5. Zhang T.X., Ye M.Y. Plasma fusion at ten million Kelvins with extremely heated tritium. *Physics of Plasmas*, 2017, Submitted.
6. Zhang T.X., Ye M.Y. Plasma fusion of deuterons at kiloelectron-volts with extremely heated tritons. *IEEE Trasaction on Plasma Science*, 2019, in reviewing.
7. Perkins L.J., Orth, C.D., Tabak, M. On the utility of antiprotons as drivers for inertial confinement fusion. *UCRL-ID-TR-200850*, 2003.
8. Ivlev B. Low-energy fusion caused by an interference. *Physical Review C*, 2013, v. 87, id. 034619.
9. Dodonov A.V. and Dodonov V.V. Tunneling of slow quantum packets through the high Coulomb barrier. *Physics Letters A*, 2014, v. 378, 1071–1073.
10. Vysotskii V.I. and Vysotskyy M.V. Formation of correlated states and tunneling for a low energy and controlled pulsed action on particles. *Journal of Experimental and Theoretical Physics*, 2017, v. 125, 195–209.
11. Premuda F. Coulomb barrier total screening by Bose-Einstein condensed deuterium in palladium blisters and reaction chains in high-density hysteresis. *Fusion Technology*, 1998, v. 33, 350–366.
12. Zhang T.X. Gravitational Field Shielding and Supernova Explosions. *The Astrophysical Journal Letters*, 2010, v. 725, L117–L121.
13. Dirac P.A.M. The electron wave equation in De-Sitter space. *Annasl of Mathematics*, 1935, v. 36, 657–669.
14. Nodvik J.S. Suppression of singularities by the g55 field with mass and classical vacuum polarization in classical Kaluza-Klein theory. *Physical Review Letters*, 1985, v. 55, L2519–L2522.
15. Dragilev V.M. Vacuum polarization of a scalar field in anisotropic multidimensional cosmology. *Theoretical Mathematics in Physics*, 1990, v. 84 887–893.
16. Zhang T.X. The 5D Fully-Covariant Theory of Gravitation and Its Physical Applications. *Galaxies*, 2015, v. 3, 18–51.
17. Chodos A., Detweiler S. Spherically-Symmetric Solutions in Five-Dimensional General Relativity. *General Relativity and Gravitation*, 1982, v. 14, 879–890.
18. Zhang T.X. Electric redshift and quasars. *Astrophysical Journal Letters*, 2006, v. 636, L61–L64.
19. Schwartz M. 2012 Quantum Field Theory and the Standard Model (Cambridge Univ. Press).
20. Breev A.I. Scalar field vacuum polarization on homogeneous spaces with an invariant metric. *Theoreticl and Mathematical Physics*, 2014, v. 178, 59–75.
21. Zhang T.X. Testing 5D Gravity with LIGO for Space Polarization by Scalar Field. *Progress in Physics*, 2017, v. 13, 180–186.
22. Abbort B.P. *et al.* Observation of Gravitational Waves from a Binary Black Hole Merger. *Physical Review Letters*, 2016, v. 116. 061102.
23. Wesson P.S. The Scalar Field of 5D Gravity and the Higgs Field of 4D Particle Physics: A Possible Connection. *arXiv: 1003.2476*, 2010.
24. Higgs P.W. Broken Symmetries and the Masses of Gauge Bosons. *Physical Review Letters*, 1964, v. 13, L508–L509.
25. Yukawa H. On the Interaction of Elementary Particles. *Proceedings of Physics and Mathematics Society of Japan*, 1935, v. 17, 48–57.
26. Ginzburg V.l., Landau L.D. On the theory of superconductivity. *Zh. Eksp. Teor. Fiz.*, 1950, v. 20, 1064–1082.
27. Castellanos E., Escamilla-Rivera C., Macias A., and Nunez D. Scalar field as a Bose-Einstein condensate? *Gen. Relat. Quant. Cosmol.*, 2014, DOI: 10.1088/1475-7516/2014/11/034.
28. Das S. Bose-Einstein condensation as an alternative to inflation, *Intern. J. of Mod. Phys.*, 2015, v. D24, 1544001.
29. Podkletnov E., Nieminen R.A. Possibility of gravitational force shielding by bulk $YBa_2Cu_3Q_{7-x}$. *Physica C*, 1992, v. 203, 441–444.
30. Li N., Noever D., Robertson T., Koczer R., Brantley W. Static test for a gravitational force coupled to type II YBCO superconductor. *Physica C*, 1997, v. 281, 260–267.
31. Zhang B.J., Zhang T.X., Guggilla P., Dohkanian M. Gravitational field shielding by scalar field and type II superconductors, *Progress in Physics*, 2013, v. 9, 69–75.
32. Guth A. Inflationary universe: A possible solution to the horizon and flatness problems. *Physical Review D*, 1981, v. 23, 347–356.
33. Zhang B.J., Zhang T.X. Vacuum polarization by scalar field of Bose-Einstein condensates and experimental design with laser interferences. *Progress in Physics*, 2017, v. 13, 210–214.
34. Bakalov D. *et al.* The measurement of vacuum polarization: The PVLAS experiment, *in Hyperfine Interactions*, 1998, v. 114, 103–113.
35. Gamow G. Quantum theory of the atomic nucleus. *Z. Phys.*, 1928, v. 51, 204.
36. Bahcall J.N.,, Ulrich R.K. Solar models, neutrino experiments, and helioseismology. *Review of Modern Physics*, 1988, v. 60, 297–372 .
37. Bahcall J.N. *et al.* Standard solar models and the uncertainties in predicted capture rates of solar neutrinos. Review of Modern Physics, 1982, v. 54, 767–799.
38. Ichimaru S. Nuclear fusion in dense plasma. *Review of Modern Physics*, 1993, v. 65, 255–299.

LETTERS TO PROGRESS IN PHYSICS

Instability of Protons Beyond 3 GeV Kinetic Energies Explains the Flux Profiles Observed in Cosmic Rays

Osvaldo F. Schilling

Departamento de Física, Universidade Federal de Santa Catarina, 88040-900, Florianópolis, SC. Brazil.
E-mail: osvaldo.neto@ufsc.br

We analyze available data for the flux of cosmic rays protons, and find evidence for instability of these particles as their kinetic energy increases beyond about 3 GeV. This is expected from our recent model [1] which proposes the existence of a parent state at 3.7 GeV, from which protons of about 1 GeV mass (as well as the other baryons) would condense in the form of flux-confining vortices. Therefore, this energy difference imposes that beyond 2.7 GeV kinetic energies such vortex states would become unstable compared to the parent, in agreement with the observation that highly energetic protons are rare in cosmic rays. The observation of protons of higher energies is attributed to cohesion provided, e.g. by strong forces, between proton constituents not considered in the vortex model.

We have recently developed a field-theoretical model for baryons in which such particles are modelled as vortices confining magnetic flux, which would "condense" from a parent state at 3.7 GeV, under the effect of electromagnetic instabilities of such a state [1,2]. This model has been shown to reproduce the relation of the masses of baryons with their magnetic moments (through an amount of confined magnetic flux) in a consistent, quantitative way. We here concentrate on the case of protons. Since the particles are assumed to be the result of the creation of states stabilized from a higher energy level, it should be expected that the number of protons will markedly decrease in cosmic rays for excessive kinetic energies. This is what we propose and actually verify in this Letter.

In Fig. 1, we show data for the number flux of protons plotted as $E\,(dN/dE)$ against kinetic energy E in GeV, for cosmic rays below 10 GeV kinetic energy, taken from the upper left corner of figure 1.1 of [3]. Below about 2 GeV kinetic energy there is an approximate plateau. From 2 GeV on, a marked decrease in the flux of protons is observed. The interpretation is that the number N of detected protons is reaching saturation above 2 GeV. To quantify such saturation, we have obtained the actual functional relations in the original double-log plot, to calculate the number N of particles in units of $(\mathrm{m}^2\ \mathrm{sr\ s})^{-1}$ for several energy intervals. Assuming from Fig. 2 below that the plateau in $E\,(dN/dE)$ would begin at about 0.1 GeV and goes up to 3 GeV, we obtain N=6800 by integration in this interval. Beyond 3 GeV the ordinate decays as $E^{-3/2}$. Therefore, one obtains by integration N=1100 between 3 and 10 GeV, and at last a very small N=204 between 10 and 100 GeV. That is, well over 80% of the protons in cosmic rays have energies below about 3 GeV, and the numbers beyond 10 GeV are negligible in absolute terms in spite of the great interest on them from the high-energy physics standpoint.

According to our model in [1], protons accelerated beyond 2.7 GeV kinetic energy (which comes from the difference between the parent level at 3.7 GeV and the proton rest mass of about 1 GeV, i.e. the "energy advantage") should become unstable since they lose the energy advantage acquired by settling in the lower energy vortex state. A related effect breaks Cooper pairs in superconductors if the energy associated with current becomes greater than the pairing interaction provided by phonon-intermediated coupling. Fig. 2 shows a plot of the estimated (from collected data) energy distribution for the interstellar flux of protons [3], which peaks exactly at 2.7 GeV. In view of the gigantic values of E beyond the peak one realizes the minute amount of very energetic particles to the right of the peak. That is, once more one concludes that protons are essentially unstable above 2.7 GeV kinetic energy.

In conclusion, this Letter analyzes data collected for the flow of protons in cosmic rays in the light of a recently proposed model in which protons are modelled as vortices in an energy state 2.7 GeV below a parent state from which they would have condensed [1]. We have indeed found evidence for a critical kinetic energy of 2.7 GeV in both the number distribution of protons and in their energy distribution. Although it is clear that 2.7 GeV represents a critical value for the energies of protons in cosmic rays, a very small ("tail") population of particles is detected at high energies. The expected question is: why do these particles still exist? In spite of providing a picture on how baryons condense from instabilities of the vacuum, the vortex model does not go as far as considering the internal structure of the baryons. The survival of some particles to high energies is certainly related to internal short-range strong forces between constituents, not considered in the model. The good results of the vortex model of [1] however suggest that the existence of the proton constituents cannot be neglected when dynamic effects take place at scales shorter than L/π with L the size of the current loop in [1], which is on the order of 10^{-16} m. It must be pointed out

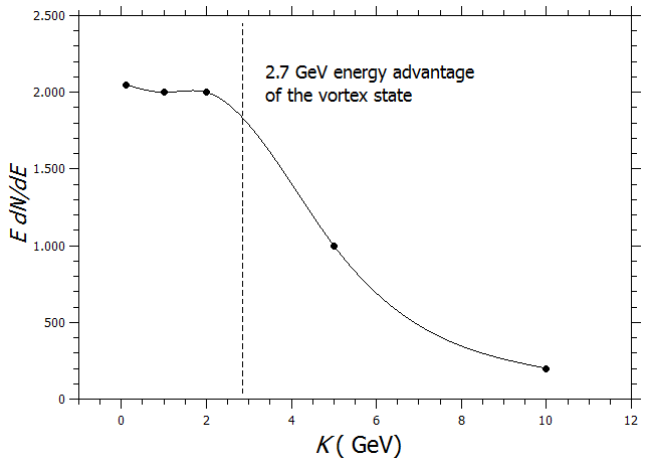

Fig. 1: Reproduction of the upper left part of the double-log plots in figure 1.1 of [3] (linearized scales are adopted here). The number flux of protons in 10^3 m^{-2} (sr. s)$^{-1}$ units is plotted against the protons kinetic energy in GeV. The vertical line is placed at the value of K that corresponds to total loss of the vortex energy advantage compared to the vacuum parent state (see [1]). Fast saturation in the detected N of protons is manifest in the drop of dN/dE as the energy increases. Integration shows that beyond 80% of N concentrates below 3 GeV energies. The solid line is a guide.

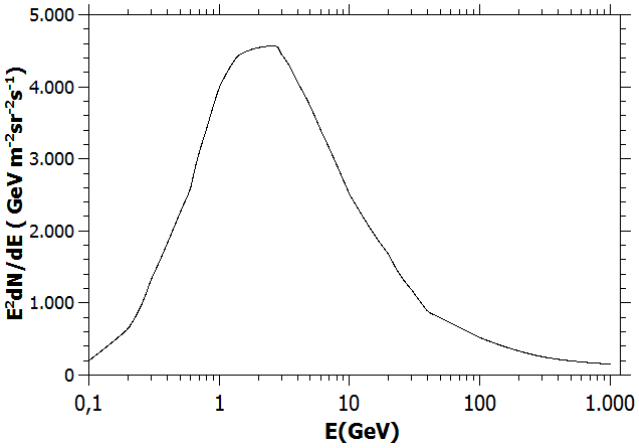

Fig. 2: Estimated energy flux distribution of interstellar protons in cosmic rays, which peaks at exactly K=2.7 GeV [3].

that [3] also displays data for the flux of electrons in cosmic rays in its Fig. 2.1. In this case there are few points in the plot but they peak at the expected range of about 3 GeV, and decay faster than the protons at higher energies. The electron is represented as the very first cross symbol to the left in figure 3 of our paper [1]. If the model applies also to leptons [2], the most energetic electrons might theoretically reach 3.7 GeV kinetic energies (although this requires acceleration to speeds quite close to the light speed). The fact that the electrons data peaks at lower energies and drops faster would be consistent with a greater instability of its structure as compared to the proton. Further investigations on this subject are clearly needed, mainly on the lower range of cosmic rays energies.

Received on December 6, 2019

References

1. Schilling O. F. Generation of Baryons from Electromagnetic Instabilities of the Vacuum. *Progress in Physics*, 2019, v. 15 (3), 185–190.
2. Schilling O. F. A unified phenomenological description for the magnetodynamic origin of mass for leptons and for the complete baryon octet and decuplet. *Annales de la Fondation Louis de Broglie*, 2018, v. 43-1, 1.
3. Gaisser T. K., Engel R. and Resconi E. Cosmic Rays and Particle Physics. Cambridge Universiy Press, Cambridge, 2016.

Progress in Physics is an American scientific journal on advanced studies in physics, registered with the Library of Congress (DC, USA): ISSN 1555-5534 (print version) and ISSN 1555-5615 (online version). The journal is peer reviewed and listed in the abstracting and indexing coverage of: Mathematical Reviews of the AMS (USA), DOAJ of Lund University (Sweden), Scientific Commons of the University of St.Gallen (Switzerland), Open-J-Gate (India), Referential Journal of VINITI (Russia), etc. Progress in Physics is an open-access journal published and distributed in accordance with the Budapest Open Initiative: this means that the electronic copies of both full-size version of the journal and the individual papers published therein will always be accessed for reading, download, and copying for any user free of charge.
The journal is issued quarterly (four volumes per year).

Electronic version of this journal: http://www.ptep-online.com

Postal address:
Department of Mathematics and Science, University of New Mexico,
705 Gurley Avenue, Gallup, NM 87301, USA